EVALUATING PHENOTYPIC EQUIVALENCE OF CULTURED CELLS IN THE CONTEXT OF THE FOREIGN BODY RESPONSE

by

Dolly Jeanne Holt

A dissertation submitted to the faculty of
The University of Utah
in partial fulfillment of the requirements for the degree of

Doctor of Philosophy

Department of Bioengineering

University of Utah

August 2012

The University of Utah Graduate School

STATEMENT OF DISSERTATION APPROVAL

The dissertation of Dolly Jeanne Holt

has been approved by the following supervisory committee members:

David W. Grainger	, Chair	06-14-2012 Date Approved
Christi M. Terry	, Member	06-14-2012 Date Approved
Robert Hitchcock	, Member	06-14-2012 Date Approved
Patrick A. Tresco	, Member	06-15-2012 Date Approved
Alana L. Welm	, Member	06-15-2012 Date Approved

and by Patrick A. Tresco , Chair of

the Department of Bioengineering

and by Charles A. Wight, Dean of The Graduate School.

ABSTRACT

The foreign body response (FBR) comprises a general, ubiquitous host tissue-based reaction to implanted materials, often resulting in device failure due to an aggressive host attack by immune cells, degrading materials, providing a toxic environment to nearby cells and stimulating a fibroproliferative response often resulting in subsequent encapsulation. The increasing use of implantable materials and devices necessitates an increased understanding of the body's response to implanted materials, and a better ability to screen the materials' behavior in vitro for predicting in vivo performance and designing more compatible materials. This work has focused on gaining a greater understanding of the in vitro behavior of both primary and secondary cells used to study the FBR and their respective ability to represent in vivo responses. We found that macrophages and fibroblasts in co-culture yielded more representative responses of in vivo signaling, than during mono-culture. We also identified fibroblasts that were capable of forming multinucleate giant cells in culture, and determined in vitro conditions in which macrophages senesce. Throughout these studies, we identified variations between primary- and secondary-derived macrophages and fibroblasts, and conclude that secondary cells in culture often have unrepresentative behavior of in vivo responses, and their use should be substantiated by primary-sourced cells. We further identified unique cell behavior in primary cultures that must be validated against in vivo cellular responses.

TABLE OF CONTENTS

ACKNOWLEDGEMENTS

I would like to thank Dr. David Grainger for his invaluable mentorship and guidance throughout my tenure at the University of Utah. I would also like to thank him for providing financial support including that for research and incredible travel opportunities. I would also like to thank him for his friendship and personal guidance during my time here. I would also like to thank the many advisors who helped tailor my research and encourage me to become a productive scientist including: Patrick Tresco, Robert Hitchcock, Christi Terry, Raymond Daynes, and Alana Welm. I would like to thank the Grainger lab members for all of their help and friendship during my dissertation work.

CHAPTER 1

INTRODUCTION[1]

Impact of the foreign body response

The use of biomedical implants, commonplace in current surgical practice to replace and repair tissue functions, is increasing with the aging population [1-3]. Though implants are successful in many cases and can improve the lives of those who receive them, they are notoriously plagued by insult from the host immune system and often fail. The failure rate of medical implants varies due to the type of implant, the material used, the age of the patient, as well as the genetics of the patient. For example, some implants such as silicone breast implants are prone to capsule contracture in greater than 50% of cases, and complications requiring repeat surgeries due to pain, contracture, rupture, infection, and implant migration are also as high as 50% after 10 years [4-6]. Hydrocephalus shunts have a failure rate of nearly 40% in pediatric patients within the first year [7-9]. Other implants such as total joint replacements have a far lower failure rate around 4% in total knee replacements (though that still accounts for over 22,000 failures annually) [10] and 6% in total hip replacements [11, 12]. Host attack can greatly impede sensing implants such as neural recording electrodes which fail during chronic implantation [13] and glucose sensors that suffer from progressive loss of signal [14]. Though glucose sensors have made recent improvements (the Dexcom® SEVEN® system is now FDA approved for 7 days compared to the previously approved 3 days for the Medtronic MiniMed Paradigm System), longer term implantation is still a goal scientists are working towards.

---

[1] This introduction has been adapted from the book chapter: Holt DJ, Grainger DW. Host Response to Biomaterials. Second Edition. An Introduction to Biomaterials and their Applications. Hollinger, JO.2011.ISBN-10:143981256X

Every material implanted in the body elicits some type of graded “foreign body response” (FBR), an abnormal, unresolved host healing response experienced over the life of the host, or a clinical nightmare if sufficiently adverse. Though improvements are continually being made and implants can succeed, the high failure rate of many implants requires increased focus. On-going efforts to improve biocompatible implant materials that reliably integrate with host tissue [15] without adverse events have not yet provided ideal materials performance, nor yielded design criteria for engineering this integration.

“Host response” refers to the sum total of molecular, cellular, organ, tissue and systemic consequences on host physiology as a result of device implantation. Though attempts have been made to fully characterize the FBR at the level of the complete human body, the organ, the specific tissue site, and the cell, it still remains an elusive phenomenon. The emerging picture is that the FBR is indeed a complex interaction of many cell types communicating back and forth with many different cell-cell and soluble protein-based signaling cues that elicit both normal and abnormal tissue-level responses. These signals are all elicited and processed by cells at the implant site to produce their global FBR response. This then compels further analysis at the cellular level to understand the basis for these processes and how they might relate to the concept of “implant biocompatibility”. Discrimination of events from tolerated versus failed implants at the cellular level could enable changes to molecular aspects of both materials and drugs that could modulate cell interactions in the FBR, and thus improve implant compatibility.

At the cellular level, the host macrophage cell is considered the primary modulator of the FBR, responding to early neutrophil activation from acute implantation trauma, invading and surveying the wound site and implant, and activating in situ by secreting cell signals (cytokines, enzymes and reactive oxygen species, ROS) attempting to orchestrate the resulting tissue response. This response in the absence of a biomaterial, typically produces normal healing. However, in the presence of a biomaterial, the healing response goes awry, producing the FBR.

This chapter describes aspects of the foreign body response to implanted materials, the role of in vitro models in understanding this response, and details regarding the roles of macrophages and fibroblasts, primary effector cells involved in this reaction.

The foreign body response

All medical device implantations into human hosts, even a syringe needle insertion into skin, create wounds. During normal wound repair, host tissue undergoes acute inflammation, scarring, tissue reconstruction, and remodeling [16]. Only in instances of unresolved infection in the wound will chronic inflammation recur. However, the presence of a foreign material interrupts the normal wound healing response, and the inflammatory phase persists in modified form, leading to a pathological condition at the implant site termed the "foreign body response" (FBR). The FBR is characterized by implant-associated cell activation, excessive fibrosis, inflammation, coagulation, possible infection and compromised healing. This is coupled with distinct cellular, histological, and biochemical events localized at the implant site. Upon implantation, initial blood- or extravascular fluid-material interactions coat the implant with a surface-bound protein layer composed of many different soluble proteins. The adsorbed protein matrix primarily governs in vivo cellular interactions (cells rarely, if ever, see a bare implant surface) and thus can determine host integration or rejection of the introduced biomaterial. The protein layer is a key event in the host response to implanted materials and how cells perceive this "invasion" but there are few methods known to actually control this layer adequately in vivo. Cell responses to this layer generally cause release of cell signaling factors to recruit additional cells and induce wound healing. Acute inflammatory responses produced early by infiltrating polymorphonuclear leukocytes (PMNs, including neutrophils) are generally resolved quickly (≤3 weeks [17]) and may appear normal. However, subsequent chronic inflammatory events persist at the implant site [18, 19] accompanying all implanted materials and eliciting an exaggerated and prolonged pathological response that counteracts normal healing processes. These unresolved events result in numerous complications, including compromised healing, fibrotic reactions, pain, tissue resorption, and increased infection rates [20]. The FBR is ostensibly involved in various implant complications [16] including necrosis of nearby cells due to the abnormal inflammatory and toxic environment [21], osteolysis and sepsis in total joint replacements [22], fibrous encapsulation of prosthetics [23] and sensors [24], stress cracking in pacemaker wires [25] and general materials degradation [26] and failure [27, 28] in vivo. Hallmark implant-associated events include:

- Phagocyte recruitment to the implant site via wound-induced chemotactic migration

- Cell interactions with adsorbed proteins on the implant surface
- Production of and response to cell cytokines both at and adjacent to the implant site
- Interaction with and activation of other cell types at the implant site
- Cellular oxidative and respiratory burst activity involving enzymes and reactive oxygen species
- Phagocyte differentiation to macrophage phenotype
- Formation and persistence of foreign body giant cells near the implant interface
- Fibrous encapsulation and excessive collagen production following fibroblast recruitment and proliferation
- Granulation tissue formation
- Chronic abnormalities eliciting unresolved wound healing

These adverse implant-associated events, their time course, and intensity all vary with tissue, anatomical location, and bulk implant material properties, as well as device design. Nonetheless, it is now clinically recognized that certain generic aspects of the FBR are common to all implanted materials and often preclude effective and complete wound healing. The concept of "biocompatibility" has therefore been modified from an absolute over-arching biomaterials criterion to an individualized relative performance-based criterion [29, 30]. Essentially, if the patient can live with it safely, it is "biocompatible". This result has few design specifications that inform the engineer or scientist about how to improve biomaterials.

Macrophages

The macrophage cell is a member of the mononuclear phagocyte family, a group of leukocytes, or white cells, originating in bone marrow as precursors and maturing in specific tissue sites to their terminal differentiated state [31]. Implant responses are thought to arise from both tissue-resident, mature macrophages, as well as blood-derived, recruited, newly differentiated macrophages. Macrophages are characterized by a spherical concentric nucleus containing several nucleoli, typically exhibiting a ruffled margin and many fine cytoplasmic granules. Macrophages are commonly considered to be central components of both the normal

healing and healthy immune response, capable of removal or destruction of deleterious materials, pathogens, or cells from the body. Macrophages are considered primary modulators of the FBR by altering the local inflammatory and wound healing cytokine levels to recruit cells acutely, degrade implants, and potentially inducing fibrosis and unresolved inflammation [32]. The FBR proceeds through a series of cellular stages, with macrophages central to each phase, specifically: 1) blood-derived monocyte wound site infiltration into the wound site in response to an acute wounding chemotactic cytokine gradient, 2) differentiation into macrophage phenotypes in situ, 3) adhesion to and activation at the implant surface, 4) fusion with resident cells to yield FBGCs at the implant surface [18, 19] and 5) interaction with invading fibroblasts to stimulate excessive collagen and proteoglycans by the fibroblasts.

Monocytes, as macrophage precursors, arise from bone marrow progenitor cells and are released regularly to travel the blood stream. Monocytes account for 1-6% of the circulating white blood cell population, remaining in circulation for 25 to 70 hours [33, 34]. Cues from the injured or traumatized tissue (i.e., surgical implantation) cause monocytes to extravasate from the blood and enter the tissue site. These monocytes then differentiate into tissue-resident macrophages, responding to both physical and chemical cues from tissue injury. Monocytes and macrophages have capabilities for excreting numerous pro- and anti-inflammatory cell signals. Macrophages also have the ability to produce pro-angiogenic and pro-healing signals. As phagocytes, both macrophages and neutrophils produce, excrete and use proteases, esterases, and highly oxidative chemicals to break down many types of foreign materials. Once degraded to pieces smaller than 6 microns, phagocytes attempt to ingest these materials for further intracellular neutralization and digest these materials in phagosomes, lysosomes and endosomes. This is routine for macrophage-based clearance of debris, both foreign and natural. However, biomaterials are often designed to be nondegradable and nonphagocytosable (e.g., as large ceramic, metal, and polymer devices). Nevertheless, macrophages will attempt to degrade all materials, continuously excreting their arsenal of chemicals as they seek to engulf the material. This metabolically exhausting situation in local phagocyte populations, constitutes “frustrated phagocytosis” – a syndrome characteristic of cells encountering most nondegrading biomaterials [35-38]. Ultimately, perhaps in response to a nonphagocytosable material much larger than their

cell size, macrophages can undergo fusion [39] to form foreign body giant cells (FBGCs), the histological hallmark of the FBR [18]. Macrophages undergoing frustrated phagocytosis often form a thin continuous cellular strata (up to two cell layers thick) directly adjacent to the material [35, 38]. The foreign body giant cell is generally considered a terminal stage for the phagocyte cell lineage in contact with macroscopic nondegrading materials [18, 27, 31], minimally containing three nuclei [40] though typically containing greater than twenty nuclei arranged in an irregular fashion [18]. FBGCs are not highly phagocytic, but they do exhibit increased lysosomal and respiratory enzyme activity [41], and are reported to exhibit fewer cell surface and complement receptors [42], suggesting a shift to a task-oriented phenotype directed to removing the insulting entity [18, 38].

As primary modulators of the FBR, macrophages are involved in many intercellular communication pathways between fibroblasts, lymphocytes, neutrophils and other macrophages [17, 38, 43] and are thought to stimulate angiogenesis (new vessel growth) at injury sites by secreting vascular endothelial growth factor (VEGF) [43]. During normal wound repair, the intensity of the signals secreted by macrophages typically allows for tissue repair, remodeling, and resolution. However in the presence of a foreign material, this signaling pathway diverges, often resulting in chronic inflammation, implant degradation, and fibrosis. Previous evidence [18, 19, 37, 44-52] suggests that localized, molecular events targeting macrophages from multiple implant site cues ultimately guide and promote abnormal host tissue response to implanted foreign bodies. Macrophages express surface receptors capable of sensing physical and chemical cues including mannose, deemed critical for FBGC fusion [18, 53, 54], and Fc [55], complement [56], lipoprotein, lectin-like, advanced glycosylation end-products (AGE), and adhesion and migration receptors. Additionally, macrophages respond to cues from the tissue milieu through molecular interactions with cytokine receptors including interleukin-4 (IL-4) [57], macrophage- and granulocyte macrophage-colony stimulating factor (M-CSF and GM-CSF) [58], and interferon-gamma (IFN-γ) [59] receptors among many others. Finally, macrophages coordinate the host tissue response to biomaterials by secreting a wide range (over 100) of substances varying in size (32-440,000 kD) and biological activity (from cell growth to cell death) [44, 59] including cytokines [46, 47, 60], enzymes such as lysozyme, proteases and lipases, as

well as enzyme inhibitors, complement components, reactive oxygen intermediates, and coagulation factors [31]. While many of the cellular and molecular players in the FBR have been identified, the precise mechanistic orchestration of these players in the host response to implants remains elusive. As a work in progress, therefore, the ability of the biomedical engineer to alter the FBR remains limited until specific cause-effect hypotheses allow new rational design criteria to be proposed regarding actual determinants of implant biocompatibility.

Macrophage senescence

Materials and devices are at risk for infection after implantation, even decades later [20, 22], despite high densities of macrophages localized to the surface throughout the duration of the implant [35, 38]. Over prolonged implant exposure, macrophages can become two-cell layers thick around monolithic implants [35, 38], completely infiltrate porous implants [61], and fuse to form FBGC at these surfaces [35-39]. That any of these commonly observed chronic responses result from macrophage in situ proliferation versus continual recruitment is not clear. Importantly, changes in their resident phenotypes, functional competence and capabilities to address infection risk over this implant duration, prompted by or correlated with their prolonged exposure and reaction to a foreign body (e.g., implant), are largely unknown.

This chronic infection risk may be due to the fact that unlike host tissue that is continuously renewed, limiting opportunities for bacterial colonization, tissue surrounding implanted materials remains relatively unchanged, encapsulated in fibrous scar tissue [17, 38, 62, 63]. The isolation of the implant from the host as a function of the FBR has been previously implicated in the susceptibility of the implant to infection via pathogen colonization [64-68]. Furthermore, while abundant macrophages are present, they may be transformed by the isolated environment or by their reactions to implants into states of relative inactivity, incapable of addressing microbial presence as effectively as during initial implant site recruitment. This could thus explain the risk of infection near implants even years after surgical placement of the implant.

Many cells in normal tissue are quiescent, a reversible nondividing state-of-rest. Importantly, quiescent cells can be stimulated to divide [69, 70]. Cells can also become senescent, a viable but irreversible nondividing state that cannot be overcome even with

mitogenic stimuli [71]. Senescent and quiescent cells are distinguished by altered patterns of gene expression [72, 73]. Senescent and quiescent transitions in macrophages at implant surfaces could explain their inability to adequately address bacterial infection in vivo in this context.

Previous studies have demonstrated a decreased phagocytic ability in aged macrophages [74] and a susceptibility of cells under oxidative stress to senesce [74, 75]. That macrophages demonstrate increased intracellular reactive oxygen species with age [76] and reside in high oxidative stress environments surrounding foreign bodies [17] could indicate their propensity to senesce and their subsequent incompetence to phagocytose pathogens at implant surfaces over time. Interestingly, foreign body giant cells, the chronic multinucleated macrophage-derived phenotypic hallmark surrounding implanted materials, also display decreased phagocytic ability [77], and increased lysosomal activity [41, 77], consistent with senescent cells [78] also known to multinucleate [79]. Macrophages have also been purported to undergo frustrated phagocytosis, an exhausting metabolic phenomenon that could compel macrophages to senesce around implants [35-38]. However, macrophage senescence around foreign bodies or in culture is not addressed in current literature.

Macrophages are commonly employed in in vitro assays seeking information on aspects of their involvement in pathologies such as cancer, autoimmune diseases, and the foreign body response [80-85]. As an immunomodulatory cell, macrophages are highly susceptible to telomere attrition [76]. Therefore, macrophage cultures may exhibit increased potential to senesce. However, they are not commonly assayed for this senescent phenotype. As both quiescence and senescence alter cell genetic profiles [72, 73], macrophage transitions to these states during in vitro culture likely influence assay outcomes. If the phenotypic state of the macrophage during culture is inconsistent with the in vivo phenotype it is intended to represent, it could lead to false conclusions, irreproducible results, and inconsistencies. Thus, maintenance of consistent macrophage phenotypes and activation states between in vivo and in vitro conditions is likely critical to ensuring proper in vitro model fidelity. Therefore understanding the possible consequences of macrophage senescent and quiescent transitions has important implications

both in vitro and in vivo. Chapter 4 therefore describes macrophage quiescence and senescence in various culture conditions.

Fibroblasts and the FBR

Fibroblasts are the most common connective tissue cell type in the body [86, 87] and are effector cells of the FBR responding to cytokines, from surrounding macrophages [38] and fibroblasts, such as transforming growth factor (TGFβ) and IL-1β [88] (shown to increase fibroblastic collagen production [89-93]). Fibroblasts are nearly universally associated with the foreign body response [51] as part of the normal wound stabilization, scarring and remodeling process. Correlated with their presence, and normal woundsite production of collagen and proteoglycan matrices, is often the presence of an abnormal avascular fibrotic tissue sheath (fibrous collagenous capsule) around foreign bodies [17, 38, 62, 63, 94-101]. This often impenetrable capsule forms a membrane many microns thick that physically encloses and surrounds many types of implants, especially those in soft tissue, in diverse physiological placements [19]. The host isolation of the implant from surrounding tissue and associated tissue transport systems produces transport and healing problems near implants and is responsible for many device failures, such as glucose sensors [102].

Fibroblasts can become altered in various pathologies such as fibrosis, cancer, aging, and the foreign body response (FBR) [38, 103-110]. One phenotypic alteration that is not widely acknowledged, but possible is fibroblast multinucleation [108-110]. Additionally, several other multinucleated cell types commonly derived from a macrophage cell origin are known including foreign body giant cells (FBGCs), Langhans' cells, and osteoclasts [18]. Significantly, FBGCs can form from the fusion of multiple monocytes/macrophages [39] during the FBR mounted by the host against implanted biomedical materials [17]. The FBR can cause device failure due to degradation by enzymes secreted by macrophages and abnormal collagen production by fibroblasts, resulting in an impeding collagen capsule [17, 38, 102]. Though macrophages and fibroblasts are both primary FBR effector cells [17, 38], fibroblasts, unlike macrophages, are not commonly considered to form multinucleated giant cells. In the context of the FBR, the foreign body giant cell (FBGC), derived from macrophages is presumed to be the only multinucleate cell

at the surface of an implant [18]. However, the milieu surrounding implants is abnormal, can be toxic to cells [21], and has been speculated to stimulate tumorigenesis [111, 112]. This unusual environment elicits the formation of FBGCs [113] and may also prompt fibroblasts to alter their phenotype and form multinucleated giant cells.

Previous studies have identified multinucleated cells in vivo ostensibly of fibroblast origin [108, 109], one describing cells appearing as "bizarre, atypical fibroblasts with hyperchromatic and large, pleomorphic nuclei and multinucleated floret-like giant cells"[110]. Several studies describe the presence of multinucleated fibroblasts in vitro [114-117] and in vivo in pathologies such as fibrosis and cancer and in aged tissue [103-110]. However, whether these cells multinucleate in vitro and in vivo via fusion similar to FBGCs [39] or through nuclear division without cytokinesis [114] is unclear. Chapter 3 of this work identifies multinucleate fibroblasts, both from primary and secondary cells and their mechanism for formation.

In vitro models of the FBR

Though the FBR is a nearly universal response to implanted materials of widely varying properties and has been studied for decades, the precise mechanisms by which it is manifested are largely unknown. The consequence of not fully understanding this process impedes the development of more successful longterm indwelling devices such as glucose sensors, neural recorders, orthopedic implants and many other longterm devices [22-24, 27, 28]. A greater understanding of the FBR will enable better development of materials and therapies to combat its deleterious effects against implanted material. In vitro models are commonly employed to study various mechanistic aspects of the FBR.

In contrast to complex in vivo models, cell culture in various forms provides a simplified, more cost-effective and focused analysis, utilizing fewer animals and enabling higher throughput of biomaterials assays. However, as a reductionist approach, these cell culture systems are perhaps overly simplified and inaccurate, examining only limited numbers and/or types of cells and their responses, and missing much of the essential positive and negative feedback signals from key cells necessary to faithfully duplicate in vivo aspects of the FBR. Consequently, in vitro models may be largely incapable of predicting and correlating in vivo phenotypes.

One important use of in vitro models is for regulatory approval of materials designed for in vivo use. The food and drug administration (FDA) requires ISO 10993 biocompatibility testing [118] that is often performed by the use of L-929 secondary mouse fibroblasts. Common assays include direct contact, where the implant is placed directly on a confluent layer of cells, and the cells are subsequently tested for toxicity, changes in gene expression, changes in phenotype, upregulation of inflammatory markers, etc. Agar diffusion is also used, where the media is removed from a confluent layer of cells and a culture medium containing 2% agar is added above the cells. Material and device samples are then placed over the surface and incubated for 24 hours. After this time, the cells are analyzed for viability and other changes listed above. Another common method is minimal essential medium (MEM) elution, where an extracted solution from the material is placed on cells to determine if any leachables are harmful to the cells [119-121]. These are standard practices for assessing the biocompatibility of a material or a device, but due to the simplicity of the in vitro model, these assays may be completely nonrepresentative of the response that would be elicited in vivo.

Understanding the differences between in vivo and current in vitro models, and providing some basis for improvements is described in Chapter 2. This study analyzed and compared extended duration in vitro co-cultures of primary and secondary macrophages and fibroblasts, two primary effector cells of the FBR [38, 93]. The premise of this study was to elucidate and distinguish signaling patterns between these cell types and determine relevant feedback systems that may enable more representative in vitro cellular responses to in vivo models, or provide evidence for confounding in vitro cell behavior.

Primary versus secondary cells in culture

Primary cells derived from living tissue can be close representations of in vivo cells, in respect to select responses, especially if used immediately postharvest [122]. However, after being removed from their extracellular niche and consequently missing integral adhesion proteins and dynamic signaling from their host, these cells may lose critical characteristics and behavior possessed by their in vivo counterparts. A prime example of this is decreased collagen production from primary cells in culture versus in vivo [123]. Also, where these cells require a living host

source, their isolation and purification can be expensive and time consuming. Additionally, imperfect purification methods often result in unwanted contaminating cells in primary cell cultures [124]. Isolation and purification of primary cells often require steps including mechanical and enzymatic breakdown, centrifugation, labeling, and fluorescence activated cell sorting (FACS) that often result in low yields and decreased viability [125]. Primary cells also possess limited passaging capacity (i.e., Hayflick limit [126]), and therefore must be isolated frequently.

Secondary cells or cell lines on the other hand are immortalized, do not undergo replicative senescence, and can be passaged and stored theoretically indefinitely. These cells are often highly proliferative and can be readily expanded, making their cost trivial in comparison to primary cells. These cells are easily obtained from commercial and private sources and are presumed to be 100% pure. Though not commonly known, secondary cells are frequently contaminated with other more aggressive but irrelevant cell types such as HeLa and K562, which can obscure assay results [127]. Additionally, their immortalization is often due to upregulation of oncogenes and through genetic transformation. This inherently changes their phenotypes compared to the noncancerous in vivo cells they represent and can result in inaccurate models. For example, murine RAW 264.7 macrophages are immortalized, transformed monocyte/macrophage-like cells frequently utilized in inflammatory assays [128-130]. However, these secondary derived immortalized cells are poorly validated and display cellular responses distinct from primary cells, such as types and levels of external receptor upregulation, excessive internalization rates, rapid proliferation with lack of contact inhibition, and distinct cytokine production dynamics [84, 122].

Though primary and secondary cells are frequently used in assays, they are not commonly substantiated for accuracy. Therefore primary and secondary sourced cells have been implemented in each study presented in this body of work in order to further elucidate discrepancies between these cell types and their fidelity to in vivo systems.

Introduction to this dissertation

The foreign body response is a ubiquitous in vivo series of events that often results in implant failure. Due to their cost effectiveness and simplicity, in vitro models are commonly employed to study this phenomenon, but are often unable to recapitulate integral aspects of this reaction and may yield inaccurate cellular behaviors and phenotypic responses. This dissertation sought to address the hypothesis that cultured cell phenotypes are not representative of in vivo cell behavior around implants and these differences are exacerbated in immortalized cell lines compared to primary cells. The objective of this body of work was to understand the in vitro behavior of both primary and secondary derived cells used to study the foreign body response and their respective ability cultured together or alone to represent in vivo responses. This has been addressed in the form of several in vitro systems.

Due to the inability of in vitro models to sufficiently recreate in vivo events, Chapter 2 aimed to develop a more representative in vitro model and identify feedback mechanisms that may be necessary to recapitulate in vivo signaling. Data presented there demonstrated that: coculture of macrophages with fibroblasts is more representative of in vivo conditions than monocultures of either macrophages or fibroblasts based on cytokine signaling dynamics seen during coculture that are also seen in vivo but absent from monoculture; primary macrophages demonstrate endotoxin tolerance with repeated exposure to LPS in culture -- more representative of in vivo responses than secondary macrophages that did not exhibit this tolerance; and primary and secondary macrophages are not equivalent in in vitro culture as shown by disparate responses to LPS exposure, cultured morphology, and cytokine production. This work was published in Holt DJ, Chamberlain LM, Grainger DW. Cell-cell signaling in co-cultures of macrophages and fibroblasts. *Biomaterials* 2010;31:9382-94. Chapter 5 continues work from Chapter 2 in a new preliminary study aiming to develop a more representative in vitro model to address multiple aspects of the FBR, including fibrosis, cell migration, and cytokine gradients seen in response to an implant. However because this work is incomplete, it has been placed into the future work section as a reasonable initiating project.

Multinucleated giant cells are considered the hallmark of the foreign body response, but are only presumed to be of macrophage origin both in vivo and in vitro, Chapter 3 aimed to

establish the existence and mechanism for formation of multinucleated fibroblasts in culture. Data presented there demonstrated that fibroblasts, like cultured macrophages, can form multinucleated cells in culture; secondary fibroblasts can form multinucleate via fusion with other fibroblasts in the presence of secondary macrophage cultures; primary fibroblasts can multinucleate in culture with or without the presence of primary or secondary macrophages, but not due to fusion, but rather senescence-associated nuclear division without cytokinesis; and primary multinucleated fibroblasts stain positive for replicative senescence. This work is published in Holt DJ, Grainger DW. Multinucleated giant cells from fibroblast cultures. *Biomaterials* 2011;32:3977-87.

Implants have a propensity for infection even years after implantation, despite being ostensibly covered in hundreds of macrophages, potentially due to a decreased state of action that macrophages may be in. The response of macrophages to bacterial challenge and stimuli may be affected by quiescence and senescence both in vivo and in vitro. Therefore, Chapter 4 aimed to determine the potential macrophages have to senesce in culture. Data presented there demonstrated that: primary macrophages undergo quiescence during high confluence cultures and senesce during longterm culture; secondary macrophages undergo quiescence during high confluence cultures and longterm culture, but do not senesce; senescence is delayed in primary macrophages, and quiescence is ameliorated in secondary macrophages in the presence of lipopolysaccharide stimulation. This work has been submitted to *Biomaterials* (December 2011).

Chapter 5 contains a summary of the accomplishments identified along each aim, plus a set of future experiments that I have proposed based on my analysis of strengths and weaknesses in my dissertation effort. This future work is focused on substantiating the in vitro findings presented here with in vivo models and developing more representative in vitro models of the FBR.

Throughout this work I have attempted to establish high fidelity in vitro models of the foreign body response and identify phenotypic behavior of macrophages and fibroblasts in culture and where this behavior deviates from in vivo systems.

References

1. Freedonia. Implantable Medical Devices; 2007 October 1. Report No.: FG1585840.

2. Branemark R, Branemark PI, Rydevik B, Myers RR. Osseointegration in skeletal reconstruction and rehabilitation: a review. J Rehabil Res Dev 2001 Mar-Apr;38(2):175-181.

3. Gunterberg B, Branemark P-I, Branemark R, Bergh P, Rydevik B. Osseointegrated prosthesis in lower limb amputation. The development of a new concept. In: Soede M, editor. Conference Book of IXth World Congress ISPO; 1998 June 28-July 3; Amsterdam, The Netherlands: ISPO; 1998. p. 137-139.

4. Asplund O. Capsular contracture in silicone gel and saline-filled breast implants after reconstruction. Plast Reconstr Surg 1984 Feb;73(2):270-275.

5. Venus MR, Prinsloo DJ. Immediate breast reconstruction with latissimus dorsi flap and implant: audit of outcomes and patient satisfaction survey. J Plast Reconstr Aesthet Surg 2010 Jan;63(1):101-105.

6. McCraw JB, Maxwell GP. Early and late capsular "deformation" as a cause of unsatisfactory results in the latissimus dorsi breast reconstruction. Clin Plast Surg 1988 Oct;15(4):717-726.

7. Albright AL, Haines SJ, Taylor FH. Function of parietal and frontal shunts in childhood hydrocephalus. J Neurosurg 1988 Dec;69(6):883-886.

8. Griebel R, Khan M, Tan L. CSF shunt complications: an analysis of contributory factors. Childs Nerv Syst 1985;1(2):77-80.

9. Villavicencio AT, Leveque JC, McGirt MJ, Hopkins JS, Fuchs HE, George TM. Comparison of revision rates following endoscopically versus nonendoscopically placed ventricular shunt catheters. Surg Neurol 2003 May;59(5):375-379; discussion 379-380.

10. Sharkey PF, Hozack WJ, Rothman RH, Shastri S, Jacoby SM. Insall Award paper. Why are total knee arthroplasties failing today? Clin Orthop Relat Res 2002 Nov(404):7-13.

11. Langton DJ, Jameson SS, Joyce TJ, Gandhi JN, Sidaginamale R, Mereddy P, et al. Accelerating failure rate of the ASR total hip replacement. J Bone Joint Surg Br 2011 Aug;93(8):1011-1016.

12. Barrack RL, Mulroy RD, Jr., Harris WH. Improved cementing techniques and femoral component loosening in young patients with hip arthroplasty. A 12-year radiographic review. J Bone Joint Surg Br 1992 May;74(3):385-389.

13. Biran R, Martin DC, Tresco PA. Neuronal cell loss accompanies the brain tissue response to chronically implanted silicon microelectrode arrays. Exp Neurol 2005 Sep;195(1):115-126.

14. Gerritsen M, Kros A, Sprakel V, Lutterman JA, Nolte RJ, Jansen JA. Biocompatibility evaluation of sol-gel coatings for subcutaneously implantable glucose sensors. Biomaterials 2000 Jan;21(1):71-78.

15. Williams DF. A model for biocompatibility and its evaluation. J Biomed Eng 1989 May;11(3):185-191.

16. Ratner BD. Biomaterials Science: An Introduction to Materials in Medicine. 1st ed. San Diego: Acedemic Press, 1996.

17. Anderson JM, Rodriguez A, Chang DT. Foreign body reaction to biomaterials. Semin Immunol 2008 Apr;20(2):86-100.

18. Anderson JM. Multinucleated giant cells. Curr Opin Hematol 2000 Jan;7(1):40-47.

19. Tang L, Eaton JW. Natural responses to unnatural materials: A molecular mechanism for foreign body reactions. Mol Med 1999 Jun;5(6):351-358.

20. Darouiche RO. Device-associated infections: a macroproblem that starts with microadherence. Clin Infect Dis 2001 Nov 1;33(9):1567-1572.

21. Moilanen E, Moilanen T, Knowles R, Charles I, Kadoya Y, al-Saffar N, et al. Nitric oxide synthase is expressed in human macrophages during foreign body inflammation. Am J Pathol 1997 Mar;150(3):881-887.

22. Murray DW, Rushton N. Macrophages stimulate bone resorption when they phagocytose particles. J Bone Joint Surg Br 1990 Nov;72(6):988-992.

23. Stark GB, Gobel M, Jaeger K. Intraluminal cyclosporine A reduces capsular thickness around silicone implants in rats. Ann Plast Surg 1990 Feb;24(2):156-161.

24. Wisniewski N, Moussy F, Reichert WM. Characterization of implantable biosensor membrane biofouling. Fresenius J Anal Chem 2000 Mar-Apr;366(6-7):611-621.

25. Zhao Q, Topham N, Anderson JM, Hiltner A, Lodoen G, Payet CR. Foreign-body giant cells and polyurethane biostability: in vivo correlation of cell adhesion and surface cracking. J Biomed Mater Res 1991 Feb;25(2):177-183.

26. Picha GJ, Goldstein JA, Stohr E. Natural-Y Meme polyurethane versus smooth silicone: analysis of the soft-tissue interaction from 3 days to 1 year in the rat animal model. Plast Reconstr Surg 1990 Jun;85(6):903-916.

27. Anderson JM. Mechanisms of inflammation and infection with implanted devices. Cardiovas Path 1993;2(3):33S-41S.

28. McNally AK, Anderson JM. Interleukin-4 induces foreign body giant cells from human monocytes/macrophages. Differential lymphokine regulation of macrophage fusion leads to morphological variants of multinucleated giant cells. Am J Pathol 1995 Nov;147(5):1487-1499.

29. Williams D. The Williams Dictionary of Biomaterials. Liverpool, UK: Liverpool University Press, 1999.

30. Williams DF. Definitions in Biomaterials. Progress in Biomedical Engineering. Amsterdam: Elsevier, 1987.

31. Auger MJ, Ross JA. Chapter 1: The biology of the macrophage. In: Lewis CE, McGee JOD, editors. The Macrophage. Oxford: Oxford University Press, 1992.

32. Ratner BD HA, Scoen FJ, Lemons JE. Biomaterials science: an introduction to materials in medicine. 2nd ed. Amsterdam: Elsevier, 2004.

33. van Furth R, Cohn ZA. The origin and kinetics of mononuclear phagocytes. J Exp Med 1968 Sep 1;128(3):415-435.

34. Whitelaw DM. The intravascular lifespan of monocytes. Blood 1966 Sep;28(3):455-464.

35. Bernatchez SF, Parks PJ, Gibbons DF. Interaction of macrophages with fibrous materials in vitro. Biomaterials 1996 Nov;17(21):2077-2086.

36. Cannon GJ, Swanson JA. The macrophage capacity for phagocytosis. J Cell Sci 1992 Apr;101(Pt 4):907-913.

37. Anderson JM, Defife K, McNally A, Collier T, Jenney C. Monocyte, macrophage and foreign body giant cell interactions with molecularly engineered surfaces. J Mater Sci Mater Med 1999 Oct-Nov;10(10/11):579-588.

38. Anderson JM. Chapter 4 Mechanisms of inflammation and infection with implanted devices. Cardiovasc Pathol 1993;2(3):33S-41S.

39. Helming L, Gordon S. Macrophage fusion induced by IL-4 alternative activation is a multistage process involving multiple target molecules. Eur J Immunol 2007 Jan;37(1):33-42.

40. Kao WJ, Hubbell JA. Murine macrophage behavior on peptide-grafted polyethyleneglycol-containing networks. Biotechnol Bioeng 1998 Jul 5;59(1):2-9.

41. Williams GT, Williams WJ. Granulomatous inflammation--a review. J Clin Pathol 1983 Jul;36(7):723-733.

42. Papadimitriou JM, van Bruggen I. Evidence that multinucleate giant cells are examples of mononuclear phagocytic differentiation. J Pathol 1986 Feb;148(2):149-157.

43. Luttikhuizen DT, Harmsen MC, Van Luyn MJ. Cellular and molecular dynamics in the foreign body reaction. Tissue Eng 2006 Jul;12(7):1955-1970.

44. Barth S, Kleinhappl B, Gutschi A, Jelovcan S, Marth E. In vitro cytokine mRNA expression in normal human peripheral blood mononuclear cells. Inflamm Res 2000 Jun;49(6):266-274.

45. Brodbeck WG, Shive MS, Colton E, Ziats NP, Anderson JM. Interleukin-4 inhibits tumor necrosis factor-alpha-induced and spontaneous apoptosis of biomaterial-adherent macrophages. J Lab Clin Med 2002 Feb;139(2):90-100.

46. DeFife KM, Hagen KM, Clapper DL, Anderson JM. Photochemically immobilized polymer coatings: effects on protein adsorption, cell adhesion, and leukocyte activation. J Biomater Sci Polym Ed 1999;10(10):1063-1074.

47. DeFife KM, Yun JK, Azeez A, Stack S, Ishihara K, Nakabayashi N, et al. Adhesion and cytokine production by monocytes on poly(2-methacryloyloxyethyl phosphorylcholine-co-alkyl methacrylate)-coated polymers. J Biomed Mater Res 1995 Apr;29(4):431-439.

48. Groth T, Zlatanov I, Altankov G. Adhesion of human peripheral lymphocytes on biomaterials preadsorbed with fibronectin and vitronectin. J Biomater Sci Polym Ed 1994;6(8):729-739.

49. Jenney CR, Anderson JM. Adsorbed serum proteins responsible for surface dependent human macrophage behavior. J Biomed Mater Res 2000 Mar 15;49(4):435-447.

50. Kao WJ, McNally AK, Hiltner A, Anderson JM. Role for interleukin-4 in foreign-body giant cell formation on a poly(etherurethane urea) in vivo. J Biomed Mater Res 1995 Oct;29(10):1267-1275.

51. Tang L, Eaton JW. Inflammatory responses to biomaterials. Am J Clin Pathol 1995 Apr;103(4):466-471.

52. Tang L, Jennings TA, Eaton JW. Mast cells mediate acute inflammatory responses to implanted biomaterials. Proc Natl Acad Sci U S A 1998 Jul 21;95(15):8841-8846.

53. DeFife KM, Jenney CR, McNally AK, Colton E, Anderson JM. Interleukin-13 induces human monocyte/macrophage fusion and macrophage mannose receptor expression. J Immunol 1997 Apr 1;158(7):3385-3390.

54. McNally AK, DeFife KM, Anderson JM. Interleukin-4-induced macrophage fusion is prevented by inhibitors of mannose receptor activity. Am J Pathol 1996 Sep;149(3):975-985.

55. Berken A, Benacerraf B. Properties of antibodies cytophilic for macrophages. J Exp Med 1966 Jan 1;123(1):119-144.

56. Lay WH, Nussenzweig V. Receptors for complement of leukocytes. J Exp Med 1968 Nov 1;128(5):991-1009.

57. Paul WE, Ohara J. B-cell stimulatory factor-1/interleukin 4. Annu Rev Immunol 1987;5:429-459.

58. Gonwa TA, Frost JP, Karr RW. All human monocytes have the capability of expressing HLA-DQ and HLA-DP molecules upon stimulation with interferon-gamma. J Immunol 1986 Jul 15;137(2):519-524.

59. Nathan CF. Secretory products of macrophages. J Clin Invest 1998;79:319-326.

60. DeFife KM, Colton E, Nakayama Y, Matsuda T, Anderson JM. Spatial regulation and surface chemistry control of monocyte/macrophage adhesion and foreign body giant cell formation by photochemically micropatterned surfaces. J Biomed Mater Res 1999 May;45(2):148-154.

61. Rosengren A, Bjursten LM. Pore size in implanted polypropylene filters is critical for tissue organization. J Biomed Mater Res A 2003 Dec 1;67(3):918-926.

62. Williams C, Aston S, Rees TD. The effect of hematoma on the thickness of pseudosheaths around silicone implants. Plast Reconstr Surg 1975 Aug;56(2):194-198.

63. Higgins DM, Basaraba RJ, Hohnbaum AC, Lee EJ, Grainger DW, Gonzalez-Juarrero M. Localized immunosuppressive environment in the foreign body response to implanted biomaterials. Am J Pathol 2009 Jul;175(1):161-170.

64. Henninger N, Woderer S, Kloetzer HM, Staib A, Gillen R, Li L, et al. Tissue response to subcutaneous implantation of glucose-oxidase-based glucose sensors in rats. Biosens Bioelectron 2007 Aug 30;23(1):26-34.

65. Henriksen TF, Holmich LR, Fryzek JP, Friis S, McLaughlin JK, Hoyer AP, et al. Incidence and severity of short-term complications after breast augmentation: results from a nationwide breast implant registry. Ann Plast Surg 2003 Dec;51(6):531-539.

66. Reynolds AF, Shetter AG. Scarring around cervical epidural stimulating electrode. Neurosurgery 1983 Jul;13(1):63-65.

67. Turner JN, Shain W, Szarowski DH, Andersen M, Martins S, Isaacson M, et al. Cerebral astrocyte response to micromachined silicon implants. Exp Neurol 1999 Mar;156(1):33-49.

68. Robertson LT, Dow RS, Cooper IS, Levy LF. Morphological changes associated with chronic cerebellar stimulation in the human. J Neurosurg 1979 Oct;51(4):510-520.

69. Litovchick L, Florens LA, Swanson SK, Washburn MP, DeCaprio JA. DYRK1A protein kinase promotes quiescence and senescence through DREAM complex assembly. Genes Dev 2011 Apr 15;25(8):801-813.

70. Korotchkina LG, Leontieva OV, Bukreeva EI, Demidenko ZN, Gudkov AV, Blagosklonny MV. The choice between p53-induced senescence and quiescence is determined in part by the mTOR pathway. Aging 2010 Jun;2(6):344-352.

71. Gary RK, Kindell SM. Quantitative assay of senescence-associated beta-galactosidase activity in mammalian cell extracts. Anal Biochem 2005 Aug 15;343(2):329-334.

72. Cristofalo VJ, Volker C, Francis MK, Tresini M. Age-dependent modifications of gene expression in human fibroblasts. Crit Rev Eukaryot Gene Expr 1998;8(1):43-80.

73. Linskens MH, Feng J, Andrews WH, Enlow BE, Saati SM, Tonkin LA, et al. Cataloging altered gene expression in young and senescent cells using enhanced differential display. Nucleic Acids Res 1995 Aug 25;23(16):3244-3251.

74. Guayerbas N, Catalan M, Victor VM, Miquel J, De la Fuente M. Relation of behaviour and macrophage function to life span in a murine model of premature immunosenescence. Behav Brain Res 2002 Aug 21;134(1-2):41-48.

75. Severino J, Allen RG, Balin S, Balin A, Cristofalo VJ. Is beta-galactosidase staining a marker of senescence in vitro and in vivo? Exp Cell Res 2000 May 25;257(1):162-171.

76. Sebastian C, Herrero C, Serra M, Lloberas J, Blasco MA, Celada A. Telomere shortening and oxidative stress in aged macrophages results in impaired STAT5a phosphorylation. J Immunol 2009 Aug 15;183(4):2356-2364.

77. Papadimitriou JM, Robertson TA, Walters MN. An analysis of the Phagocytic potential of multinucleate foreign body giant cells. Am J Pathol 1975 Feb;78(2):343-358.

78. Kurz DJ, Decary S, Hong Y, Erusalimsky JD. Senescence-associated (beta)-galactosidase reflects an increase in lysosomal mass during replicative ageing of human endothelial cells. J Cell Sci 2000 Oct;113 (Pt 20):3613-3622.

79. Holt DJ, Grainger DW. Multinucleated giant cells from fibroblast cultures. Biomaterials 2011 Jun;32(16):3977-3987.

80. Lawrence T. Macrophages and NF-kappaB in cancer. Curr Top Microbiol Immunol 2011;349:171-184.

81. Deane S, Selmi C, Teuber SS, Gershwin ME. Macrophage activation syndrome in autoimmune disease. Int Arch Allergy Immunol 2010;153(2):109-120.

82. Lynn AD, Kyriakides TR, Bryant SJ. Characterization of the in vitro macrophage response and in vivo host response to poly(ethylene glycol)-based hydrogels. J Biomed Mater Res A 2009 Aug 25.

83. McInnes A, Rennick DM. Interleukin 4 induces cultured monocytes/macrophages to form giant multinucleated cells. J Exp Med 1988 Feb 1;167(2):598-611.

84. Chamberlain LM, Godek ML, Gonzalez-Juarrero M, Grainger DW. Phenotypic non-equivalence of murine (monocyte-) macrophage cells in biomaterial and inflammatory models. J Biomed Mater Res A 2009 Mar 15;88(4):858-871.

85. Jay SM, Skokos E, Laiwalla F, Krady MM, Kyriakides TR. Foreign body giant cell formation is preceded by lamellipodia formation and can be attenuated by inhibition of Rac1 activation. Am J Pathol 2007 Aug;171(2):632-640.

86. Kovacs EJ, DiPietro LA. Fibrogenic cytokines and connective tissue production. Faseb J 1994 Aug;8(11):854-861.

87. Ross R. The fibroblast and wound repair. Biol Rev Camb Philos Soc 1968 Feb;43(1):51-96.

88. Rodriguez A, Meyerson H, Anderson JM. Quantitative in vivo cytokine analysis at synthetic biomaterial implant sites. J Biomed Mater Res A 2009 Apr;89(1):152-159.

89. Bonniaud P, Margetts PJ, Ask K, Flanders K, Gauldie J, Kolb M. TGF-beta and Smad3 signaling link inflammation to chronic fibrogenesis. J Immunol 2005 Oct 15;175(8):5390-5395.

90. Gauldie J, Kolb M, Ask K, Martin G, Bonniaud P, Warburton D. Smad3 signaling involved in pulmonary fibrosis and emphysema. Proc Am Thorac Soc 2006 Nov;3(8):696-702.

91. Gauldie J, Bonniaud P, Sime P, Ask K, Kolb M. TGF-beta, Smad3 and the process of progressive fibrosis. Biochem Soc Trans 2007 Aug;35(Pt 4):661-664.

92. Ask K, Bonniaud P, Maass K, Eickelberg O, Margetts PJ, Warburton D, et al. Progressive pulmonary fibrosis is mediated by TGF-beta isoform 1 but not TGF-beta3. Int J Biochem Cell Biol 2008;40(3):484-495.

93. Kelly M, Kolb M, Bonniaud P, Gauldie J. Re-evaluation of fibrogenic cytokines in lung fibrosis. Curr Pharm Des 2003;9(1):39-49.

94. Christenson L, Aebischer P, McMillan P, Galletti PM. Tissue reaction to intraperitoneal polymer implants: species difference and effects of corticoid and doxorubicin. J Biomed Mater Res 1989 Jul;23(7):705-718.

95. Desai NP, Hubbell JA. Tissue response to intraperitoneal implants of polyethylene oxide-modified polyethylene terephthalate. Biomaterials 1992;13(8):505-510.

96. Kellar RS, Kleinert LB, Williams SK. Characterization of angiogenesis and inflammation surrounding ePTFE implanted on the epicardium. J Biomed Mater Res 2002 Aug;61(2):226-233.

97. Zachariou Z. Amniotic membranes as prosthetic material: experimental utilization data of a rat model. J Pediatr Surg 1997 Oct;32(10):1458-1463.

98. Ward WK, Slobodzian EP, Tiekotter KL, Wood MD. The effect of microgeometry, implant thickness and polyurethane chemistry on the foreign body response to subcutaneous implants. Biomaterials 2002 Nov;23(21):4185-4192.

99. Brauker JH, Carr-Brendel VE, Martinson LA, Crudele J, Johnston WD, Johnson RC. Neovascularization of synthetic membranes directed by membrane microarchitecture. J Biomed Mater Res 1995 Dec;29(12):1517-1524.

100. Kyriakides TR, Leach KJ, Hoffman AS, Ratner BD, Bornstein P. Mice that lack the angiogenesis inhibitor, thrombospondin 2, mount an altered foreign body reaction characterized by increased vascularity. Proc Natl Acad Sci U S A 1999 Apr 13;96(8):4449-4454.

101. Sharkawy AA, Klitzman B, Truskey GA, Reichert WM. Engineering the tissue which encapsulates subcutaneous implants. I. Diffusion properties. J Biomed Mater Res 1997 Dec 5;37(3):401-412.

102. Wisniewski N, Reichert M. Methods for reducing biosensor membrane biofouling. Colloids Surf B Biointerfaces 2000 Oct 1;18(3-4):197-219.

103. Powell CM, Cranor ML, Rosen PP. Multinucleated stromal giant cells in mammary fibroepithelial neoplasms. A study of 11 patients. Arch Pathol Lab Med 1994 Sep;118(9):912-916.

104. Ryska A, Reynolds C, Keeney GL. Benign tumors of the breast with multinucleated stromal giant cells. Immunohistochemical analysis of six cases and review of the literature. Virchows Arch 2001 Dec;439(6):768-775.

105. Tse GM, Law BK, Chan KF, Mas TK. Multinucleated stromal giant cells in mammary phyllodes tumours. Pathology 2001 May;33(2):153-156.

106. El-Labban NG, Lee KW. Myofibroblasts in central giant cell granuloma of the jaws: an ultrastructural study. Histopathology 1983 Nov;7(6):907-918.

107. Min KW, Gillies E. Multinucleated giant stromal tumor of the omentum: report of a case with immunohistochemical and ultrastructural investigation. Ultrastruct Pathol 1996 Jan-Feb;20(1):89-99.

108. Regezi JA, Courtney RM, Kerr DA. Fibrous lesions of the skin and mucous membranes which contain stellate and multinucleated cells. Oral Surg Oral Med Oral Pathol 1975 Apr;39(4):605-614.

109. Cho MI, Garant PR. Formation of multinucleated fibroblasts in the periodontal ligaments of old mice. Anat Rec 1984 Feb;208(2):185-196.

110. Hassanein A, Telang G, Benedetto E, Spielvogel R. Subungual myxoid pleomorphic fibroma. Am J Dermatopathol 1998 Oct;20(5):502-505.

111. Brand KG, Buoen LC, Johnson KH, Brand I. Etiological factors, stages, and the role of the foreign body in foreign body tumorigenesis: a review. Cancer Res 1975 Feb;35(2):279-286.

112. Tazawa H, Tatemichi M, Sawa T, Gilibert I, Ma N, Hiraku Y, et al. Oxidative and nitrative stress caused by subcutaneous implantation of a foreign body accelerates sarcoma development in Trp53+/- mice. Carcinogenesis 2007 Jan;28(1):191-198.

113. DeFife KM, Jenney CR, Colton E, Anderson JM. Cytoskeletal and adhesive structural polarizations accompany IL-13-induced human macrophage fusion. J Histochem Cytochem 1999 Jan;47(1):65-74.

114. Walen KH. Human diploid fibroblast cells in senescence; cycling through polyploidy to mitotic cells. In Vitro Cell Dev Biol Anim 2006 Jul-Aug;42(7):216-224.

115. Ohshima S. Abnormal mitosis in hypertetraploid cells causes aberrant nuclear morphology in association with H2O2-induced premature senescence. Cytometry A 2008 Sep;73(9):808-815.

116. Sundaram M, Guernsey DL, Rajaraman MM, Rajaraman R. Neosis: a novel type of cell division in cancer. Cancer Biol Ther 2004 Feb;3(2):207-218.

117. Walen KH. Budded karyoplasts from multinucleated fibroblast cells contain centrosomes and change their morphology to mitotic cells. Cell Biol Int 2005 Dec;29(12):1057-1065.

118. Guidance documents. [cited 2012 February 28]; Available from: http://www.fda.gov/MedicalDevices/DeviceRegulationandGuidance/GuidanceDocuments/

119. Nelson Laboratories Price Guide. 2012 [cited 2012 February 28]; Available from: http://www.nelsonlabs.com/Files/PDF/PriceBook.aspx

120. ASSESSING BIOCOMPATIBILITY: Biological Test Methods. [cited 2012 February 28]; Available from: http://www.pacificbiolabs.com/bio_methods.asp

121. Testing of Biocompatibility on Medical Device – Cytotoxicity (ISO 10993-5). 2008 [cited February 28]; Available from: http://www.hk.sgs.com/testing_of_biocompatibility_on_medical_device_cytotoxicity_iso_10993_5_news_hk?viewId=5847

122. Holt DJ, Chamberlain LM, Grainger DW. Cell-cell signaling in co-cultures of macrophages and fibroblasts. Biomaterials 2010;31(36):9382-9394.

123. Chen CZ, Peng YX, Wang ZB, Fish PV, Kaar JL, Koepsel RR, et al. The Scar-in-a-Jar: studying potential antifibrotic compounds from the epigenetic to extracellular level in a single well. Br J Pharmacol 2009 Nov;158(5):1196-1209.

124. Sreejit P, Kumar S, Verma RS. An improved protocol for primary culture of cardiomyocyte from neonatal mice. In Vitro Cell Dev Biol Anim 2008 Mar-Apr;44(3-4):45-50.

125. Boyum A. Isolation of lymphocytes, granulocytes and macrophages. Scand J Immunol 1976 Jun;Suppl 5:9-15.

126. Hayflick L, Moorhead PS. The serial cultivation of human diploid cell strains. Exp Cell Res 1961 Dec;25:585-621.

127. Hughes P, Marshall D, Reid Y, Parkes H, Gelber C. The costs of using unauthenticated, over-passaged cell lines: how much more data do we need? Biotechniques 2007 Nov;43(5):575, 577-578, 581-572 passim.

128. Sandeep Varma R, Ashok G, Vidyashankar S, Patki P, Nandakumar KS. Anti-inflammatory properties of Septilin in lipopolysaccharide activated monocytes and macrophage. Immunopharmacol Immunotoxicol 2011 Apr 12;33(1):55-63.

129. Lin NJ, Hu H, Sung L, Lin-Gibson S. Quantification of cell response to polymeric composites using a two-dimensional gradient platform. Comb Chem High Throughput Screen 2009 Jul;12(6):619-625.

130. Yoon WJ, Ham YM, Yoo BS, Moon JY, Koh J, Hyun CG. Oenothera laciniata inhibits lipopolysaccharide induced production of nitric oxide, prostaglandin E2, and proinflammatory cytokines in RAW264.7 macrophages. J Biosci Bioeng 2009 Apr;107(4):429-438.

CHAPTER 2

CELL–CELL SIGNALING IN CO-CULTURES OF MACROPHAGES AND FIBROBLASTS

Reprinted with permission from: Holt DJ, Chamberlain LM, Grainger DW. Cell-cell signaling in co-cultures of macrophages and fibroblasts. *Biomaterials* 2010;31:9382-94.

Biomaterials 31 (2010) 9382–9394

Contents lists available at ScienceDirect

Biomaterials

journal homepage: www.elsevier.com/locate/biomaterials

Cell–cell signaling in co-cultures of macrophages and fibroblasts

Dolly J. Holt [a], Lisa M. Chamberlain [b,1], David W. Grainger [a,b,*]

[a] Department of Bioengineering, University of Utah, Salt Lake City, UT 84112-5820, USA
[b] Department of Pharmaceutics and Pharmaceutical Chemistry, University of Utah, Salt Lake City, UT 84112-5820, USA

ARTICLE INFO

Article history:
Received 9 July 2010
Accepted 28 July 2010
Available online 6 October 2010

Keywords:
Foreign body response
Co-culture
In vitro signaling
Cytokines
Fibroblast
Macrophage

ABSTRACT

The foreign body response (FBR) comprises a general, ubiquitous host tissue-based reaction to implanted materials. *In vitro* cell-based models are frequently employed to study FBR mechanisms involving cell signaling responses to materials. However, these models often study only one cell type, identify only limited signals, and cannot accurately represent the complexity of *in vivo* inflammatory signaling. To address this issue, a cell co-culture system involving two primary effector cells of the FBR, macrophages and fibroblasts, was employed. Cell–cell signaling systems were monitored between these cell types, including long-term 1) culture of one cell type in conditioned media from the other cell type, 2) non-contacting cell co-cultures (paracrine signaling), and 3) contact co-cultures (juxtacrine signaling) of primary- and secondary-derived cells. Cell culture media and cell images were collected on Days 1, 2, 3, 7, 14, and 21 and changes in soluble protein secretion, cellular behavior, and morphology were assessed. Primary- and secondary-derived cells responded uniquely during each signaling scenario and to one another. In general higher *in vitro* fidelity to FBR-like responses was found in primary cell co-cultures compared to their mono-cultures and all secondary cell cultures.

1. Introduction

Implantation of any foreign material into living tissue evokes a host inflammatory response generally described as the foreign body response (FBR). The FBR – a cascade of cell-based soluble signaling events – reacts to and modulates the interface between an implanted device and the host tissue. This host response is associated with numerous complications including fibrosis, bone resorption, implant degradation, increased infection rates, delayed healing, pain, and general device failure [1–3].

In vitro models are commonly employed to study various mechanistic aspects of the FBR. In contrast to complex *in vivo* models, cell culture in various forms provides a simplified, more cost-effective and focused analysis, utilizing fewer animals and enabling higher throughput of biomaterials assays. However, as a reductionist approach, these cell culture systems are perhaps overly simplified and inaccurate, examining only limited numbers and/or types of cells and their responses, and missing much of the essential positive and negative feedback signals from key cells necessary to faithfully duplicate *in vivo* aspects of the FBR. Consequently, *in vitro* models may be largely incapable of predicting and correlating *in vivo* phenotypes. For example, a significant inconsistency between *in vitro* and *in vivo* models is the observed lack of inflammatory cell (e.g., macrophage) activation *in vitro* [4–6]. This has prompted the standard practice of adding lipopolysaccharide (LPS) [7] or other exogenous activating agents such as IFN-γ [8] or phorbol esters [9] to replicate cell activation seen *in vivo* [10] around implants. It has been suggested that the mere presence of a material *in vitro* in cell culture may be insufficient to mount a meaningful cell inflammatory response without the use of LPS [5]. However, even LPS stimulation *in vitro* produces an attenuated response compared to *in vivo* LPS activation. Reichert and co-workers showed that *in vitro* production of the inflammatory cytokine, IL-6, by secondary macrophages after LPS stimulation appeared to be non-responsive compared to untreated groups [6]. Their subsequent study showed that *in vivo* stimulation with LPS produced a drastic increase in IL-6 production compared to the non-stimulated group, supporting the contention that *in vitro* and *in vivo* responses were inconsistent [11]. Similarly, Roumestan *et. al.* showed that after LPS stimulation, *in vivo* production of inflammatory cytokine, TNFα, was nearly double that secreted by *in vitro* primary monocytes, underscoring the inconsistency between *in vivo* and *in vitro* models [12]. Understanding the differences between *in vivo* and current *in vitro* models, and providing some basis for improvements serve as motivation for this study.

* Corresponding author. Department of Pharmaceutics and Pharmaceutical Chemistry, University of Utah, Salt Lake City, UT 84112-5820, USA. Tel.: +1 801 581 3715; fax: +1 801 581 3674.
E-mail address: david.grainger@utah.edu (D.W. Grainger).
[1] Present address: Departments of Bioengineering, and Materials Science & Engineering, University of California at San Diego, La Jolla, CA 92093 USA.

0142-9612/$ – see front matter © 2010 Elsevier Ltd. All rights reserved.
doi:10.1016/j.biomaterials.2010.07.101

Further compounding translation between *in vitro* and *in vivo* models are variations seen *in vitro* between primary- and secondary-derived cells used almost interchangeably in literature reports for decades. Primary cells are derived from living tissue possess limited passaging capacity (i.e., Hayflick limit [13]), and are therefore best used almost immediately and for limited proliferative cycles. Secondary cells (cell lines) on the other hand are immortalized (often through genetic transformation), can be passaged and stored theoretically indefinitely, are frequently contaminated with other more aggressive but irrelevant cell types such as HeLa and K562 [14], and often lack much phenotypic semblance to their primary-derived counterparts. For example, murine RAW 264.7 macrophages are immortalized, transformed monocyte/macrophage-like cells frequently utilized in inflammatory assays [15–17]. However, these secondary-derived immortalized cells are poorly validated and display cellular responses distinct from primary cells, such as types and levels of external receptor upregulation, excessive internalization rates, rapid proliferation with lack of contact inhibition, and distinct cytokine production dynamics [4].

Macrophages and fibroblasts are primary FBR effector cells acting in concert in local implant-associated inflammation, cell recruitment, implant degradation, fibrosis, and chronic unresolved healing [1,18]. Pro-inflammatory cytokines secreted by both macrophages and fibroblasts are immediately upregulated post-injury and remain upregulated in the presence of a foreign material [5,11]. These soluble signals are recognized by the same cell in autocrine, and neighboring cells in paracrine, responses [19]. Macrophages and fibroblasts in the FBR communicate via soluble autocrine and paracrine signals as well as juxtacrine signals associated with direct cell–cell contacts. Hence, both chemical and physical cues exchanged between macrophages and fibroblasts at the implant site modulate cell migration, proliferation, protein synthesis, and enzymatic function associated with the FBR [1,5,18,20]. Fibroblasts, acting on cues from both recruited and tissue-resident macrophages, are thought to synthesize extracellular matrix, specifically collagens and keratins, resulting ultimately in implant fibrosis [1,18,20–22]. However, the precise mutual influences of these two cell types in the FBR are currently unknown.

This study analyzes and compares extended-duration *in vitro* co-cultures of primary and secondary macrophages and fibroblasts to elucidate and distinguish signaling patterns between these cell types and determine relevant feedback systems that may enable more representative *in vitro* cellular responses to *in vivo* models, or provide evidence for confounding *in vitro* cell behavior.

2. Methods and materials

2.1. In vitro secondary cell culture

Transformed murine secondary monocyte/macrophage-like cell line RAW 264.7 and fibroblast-like cell line NIH 3T3 were purchased from the American Type Culture Collection (TIB-71 for RAW and CRL-1658 for 3T3 ATCC, Manassas, USA). Frozen stocks were suspended in 20 ml of pre-warmed secondary cell control media (Dulbecco's modified eagle medium (DMEM) with 10% fetal bovine serum (FBS), 1% antibiotic/antimycotic, and 1% 4-(2-hydroxyethyl)-1-piperazineethanesulfonic acid (HEPES), all sourced from Invitrogen, Carlsbad, USA) and cultured in T75 flasks (BD Falcon, San Jose, USA) at 37 °C with 5% supplemental CO_2 until 80% confluency before passaging. RAW cells were passaged by scraping with a rubber policeman and used below passage 10. 3T3 fibroblasts were passaged in control media using bovine trypsin (Invitrogen) and used below passage 20. For all studies, cells were seeded into 12-well tissue culture-treated polystyrene plates (BD Falcon, San Jose, USA) and cultured for a period of 21 days in a serum-containing media as specified at 37 °C with 5% supplemental CO_2. Mono-cultures in control media, mono-cultures treated with pre-conditioned media (see below), mono-cultures stimulated with LPS (see below), non-contact co-culture (paracrine), and contact-culture (juxtacrine) conditions were designed for two-dimensional (2-D) adherent cell cultures on rigid materials, see Fig. 1A. Transwell® Permeable Supports (3-μm porous plasma-treated polycarbonate inserts) (Corning, Corning, USA) were utilized for paracrine non-contact cell co-cultures. Fibroblasts (1.2×10^5 per well) were added to mono-culture wells, juxtacrine co-cultures, and in the Transwell® inserts of paracrine co-cultures. Macrophage-like cells (3.1×10^5) were added to mono-culture wells, juxtacrine culture wells, and paracrine co-culture wells beneath the Transwell® inserts containing fibroblasts. Cell seeding concentrations were selected in order for wells to reach confluency by Day 1 of the experiment.

Mono-cultured cells (negative controls) and paracrine and juxtacrine co-cultures were grown in control media (Fig. 1B). Conditioned FBS-supplemented media (20 ml) was harvested from RAW cell cultures 3 days past confluency and from 3T3 cell cultures 7 days past confluency in T75 flasks. These times were the longest periods the cells could grow before requiring a media change and were thus selected to maximize cell-produced cytokine concentrations. These time points also

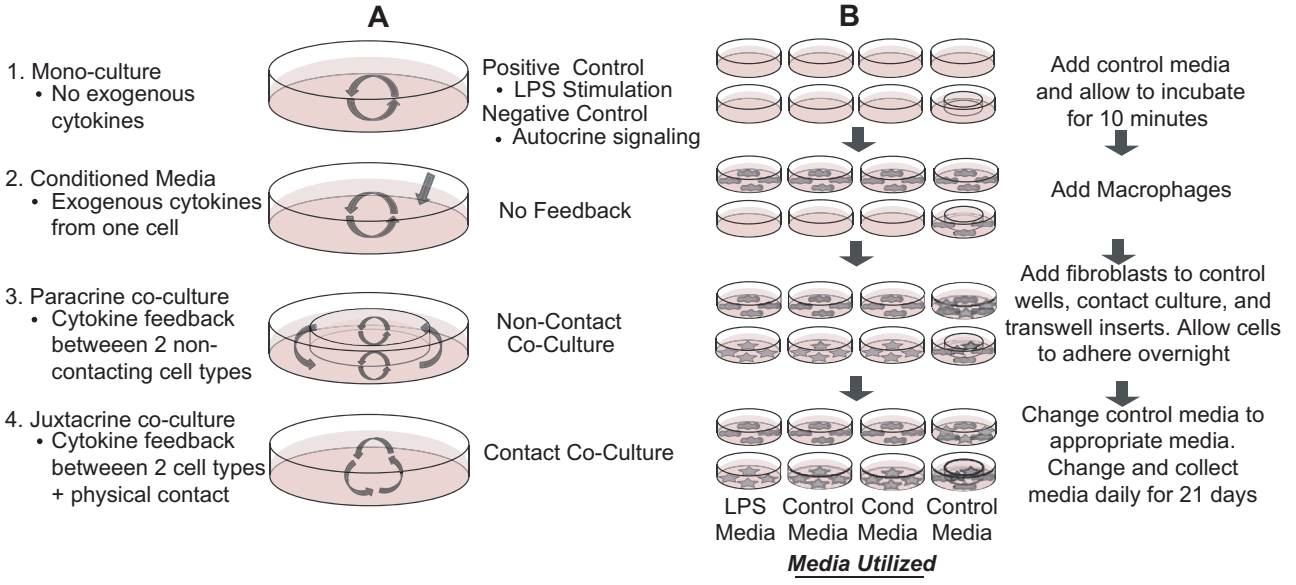

Fig. 1. A) Depiction of the four cell signaling feedback culture scenarios utilized in this *in vitro* study. B) Description of the culture process implemented to investigate each signaling condition.

served to normalize cytokine production as RAW cells are more highly metabolically active than 3T3 cells, as seen by their use of media (i.e., turning the phenol red indicator in the media from red to yellow more rapidly than 3T3s). Each conditioned medium was sterile filtered and 10% v/v was added to the control media for subsequent cell treatment. For positive cell activation controls, 1 μg/ml LPS (endotoxin, List Biological Laboratories Inc., Campbell, USA) was added to control media. Media (2 ml) in each well was changed daily, and analyzed on Days 1, 3, 7, 13 and/or 14, and 19 and/or 21, and stored at −70 °C for subsequent analysis. Media was analyzed on Days 13 and 19 due to fibroblast delamination from surfaces observed beyond those times.

2.2. Murine primary macrophage sourcing

Specific-pathogen-free female C57BL/6 mice, 6–8 weeks old, were purchased from Jackson Laboratory (Bar Harbor, USA). Animals were kept in the University of Utah ILAAC-approved animal facility and given water, mouse chow, bedding, and modes of enrichment *ad libitum* throughout this study.

2.3. Primary cell cultures

Bone marrow cells (BMCs) were collected from femurs and tibias of male C57BL/6 mice and differentiated into bone marrow macrophages (BMMΦs) using a previously described method [23,24]. On Day 7, cells were removed from plastic culture surfaces by incubation in Ca^{+2}/Mg^{+2}-free PBS and scraping with a rubber policeman. Cells were spun at 500 rcf for 5 min to form a pellet and then resuspended in BMMΦ control media (DMEM with 10% heat inactivated FBS, 1% antibiotic/antimycotic, 1% MEM non-essential amino acids, 1% HEPES, and 1% sodium pyruvate, Invitrogen, Carlsbad, USA). Transwell® inserts were utilized for non-contacting paracrine co-culture. BMMΦ cells were plated into mono-culture control wells (1.5×10^5 per well), conditioned media-treated mono-culture wells, wells beneath Transwell® inserts containing seeded fibroblasts (paracrine co-culture), and into contact culture wells (juxtacrine co-culture). NIH 3T3 cells (1.5×10^5 per well) were plated into Transwell® inserts, and in juxtacrine co-cultures. BMMΦs treated with conditioned media were grown in control BMMΦ media supplemented with 10% 3T3-conditioned media. Positive control media for BMMΦs was produced by adding 1 μg/ml LPS to BMMΦ control media (see Fig. 1 for pictorial summary representation of culture media and conditions).

2.4. Cytokine secretion assays

BD™ Cytometric Bead Array (CBA) assay was used to determine RANTES, TNF, MCP-1, MIP1-β, MIP1-α, IL-6, IL-2, IL-4, IL-5, IL-9, IL-10, IL-12P70, IL-13, and IFN-γ cytokine expression profiles over time. Media was collected from cells on Days 1, 2, 3, 7, 13 and/or 14, and 19 and/or 21 to be analyzed. The CBA has been shown to detect comparable levels of cytokines to an Enzyme Linked Immunosorbant Assay (ELISA) [25], and was implemented for this study due to its low technical error (attained by averaging the relative fluorescence of at least 300 beads per analyte) and ability to multiplex multiple cytokines simultaneously.

2.5. Flow cytometry analysis

Data acquisition for the CBA assay was performed using an upgraded 5-color FACScan Analyzer (BD Biosciences, Mountain View, USA), employing a benchtop analyzer with two lasers for fluorochrome excitation. The primary laser is a 15 mW argon (488 nm) laser and the secondary laser is a 25 mW red diode (637 nm) laser. The instrument uses seven detectors, two for light scattering (forward and 90°) and five for fluorescence. CellQuest 3.3 software (BD Biosciences, San Jose, USA) and Rainbow software 1.1 (Cytek, Fremond, USA), was used for data collection. WinMDI 2.9 (J. Trotter, The Scripps Research Institute, La Jolla, CA), Weasel (Walter & Eliza Hall Institute, Melbourne, Australia) and Summit software (Dako North America, Inc., Carpenteria, USA) were used for data analysis.

2.6. Cell quantification

Adherent cell counts in culture were taken from 40× objective phase contrast microscope images. For secondary cells, at least 3 frames per replicate, per condition, and per day were counted and the mean of the replicates was used for analysis. For primary cells, 10 frames per replicate, per condition, and per day were counted and the replicates averaged for analysis.

2.7. Imaging

Cells were imaged on Day 1, 3, 7, 13 and/or 14, and 19 and/or 21 using a Nikon Eclipse TE2000-U microscope (Nikon Inc., Melville, USA) equipped with fluorescent optics, CCD camera, and Metamorph (Molecular Devices, Sunnyvale, USA) and Q Capture Pro software (QImaging, Surrey, Canada). Each image presented was selected as a representative image of at least 3 independent replicates.

2.8. Cell staining

A hematoxylin and eosin stain (Fisher Scientific, Kalamazoo, USA) was employed according to manufacturer's instructions to stain for nuclei and cytoplasm respectively. For fluorescence staining, cells were fixed in 4% paraformaldehyde (Sigma–Aldrich, St. Louis, USA) for 10 min at room temperature and stained with rhodamine-phalloidin and counterstained with 4,6-diamidino-2-phenylindole (DAPI) (Molecular Probes, Eugene, OR) according to standard protocols. All wells were preserved with Fluoromount-G (Southern Biotech, Birmingham, USA). For live green fluorescent staining, fibroblasts were stained with Vybrant CFDA SE Cell Tracer Kit (Invitrogen) according to manufacturer's instructions prior to seeding with macrophages.

2.9. Multinucleated cell characterization

Primary and secondary macrophages were stained using a tartrate-resistant acid phosphatase (TRAP) assay (Sigma–Aldrich) according to manufacturer's instructions after being cultured on tissue culture polystyrene (TCPS) for 21 days in each culture condition.

2.10. Endotoxin (LPS) analysis

Levels of LPS contamination in cell culture materials, reagents, and laminar flow hood were tested using Limulus Amebocyte Lysate (LAL) Assay (Lonza, Basel, Switzerland). All solid samples were soaked for three days in pyrogen-free water, and the water was used in the LPS colorimetric assay.

2.11. Statistics

Endogenous levels of cytokines in conditioned media were subtracted from cell-produced cytokine profiles. All experimental results are presented as the mean ± SEM. Technical replicates using the CBA were taken as the geometric mean fluorescence of at least 300 beads. Replicates for secondary macrophages and fibroblasts are represented as 3 separate wells carried in parallel through the entire experimental protocol; this experiment was repeated on 3 independent occasions and revealed similar results (data not shown). Replicates for primary macrophages were harvested from 4 mice. A Single-Factor ANOVA was utilized to determine significance between groups of samples for the conditioned media and LPS test groups. A Two-Factor ANOVA without replication was utilized to determine significant differences between the co-cultures (paracrine and juxtacrine) and either the mono-cultured macrophages or fibroblasts, or sum of both mono-cultured macrophages and fibroblasts. A post-hoc student's *t*-test was used to determine statistically significant differences between samples ($p < 0.05$). Samples treated with conditioned media or LPS were compared against control mono-cultured wells, while paracrine and juxtacrine co-cultures were compared against the sum total of both control mono-cultured macrophages and fibroblasts at each discrete time point. This accommodates the problem of cytokines produced from both macrophages and fibroblasts in the co-cultures that should be considered. Particular comparisons to be tested were selected in advance and were reported individually rather than as a group and therefore were not appropriate for correction by a multiple comparison procedure [26]. In graphical representations, values below the assay detection limit were set to 0. The detectable limit was determined using the assay signal value of the 0 cytokine standard plus 1.5 times the standard deviation for that cytokine assay result.

3. Results

3.1. Cytokine production

From an initial screen of cytokines, IL-2, IL-3, IL-4, IL-5, IL-9, IL-10, IL-12P70, IL-13, IFN-γ, and GM-CSF were found to be below 40 pg/ml (with the exception of GM-CSF, which increased above this value only in the presence of LPS) and were not included in this study (data not shown). IL-6, TNF, MCP-1, RANTES, MIP-1α, and MIP-1β were detected above this value and were considered the most relevant to the foreign body response and were thus included in this study.

3.1.1. Conditioned media treated sample

Secondary and primary macrophages primarily decreased their production of inflammatory cytokines in the presence of fibroblast-conditioned media, compared to control macrophages, with the exception that they both increased their production of MCP-1 within the first 3 days (Figs. 2 and 3). In contrast, primary

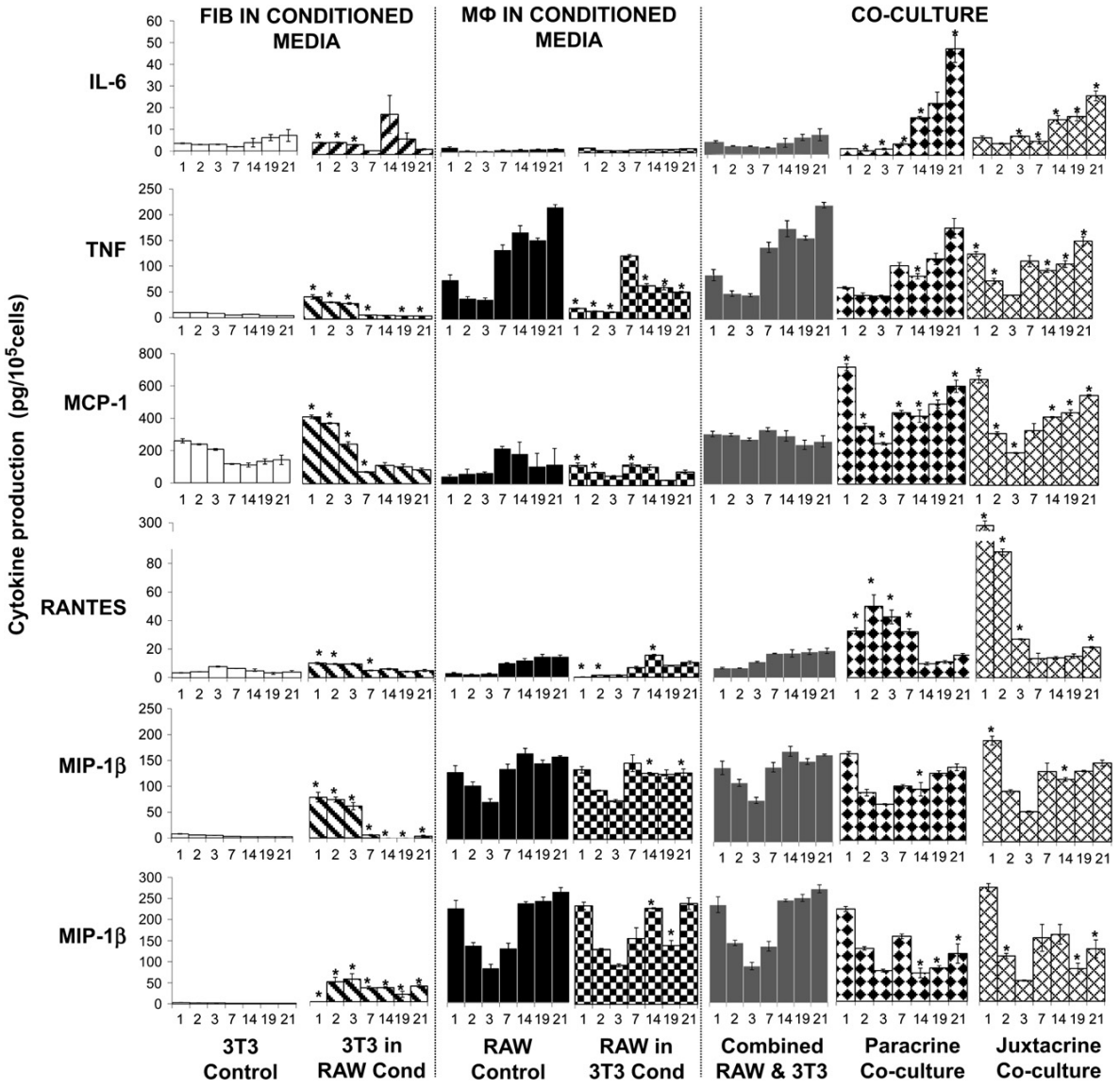

Fig. 2. Cytokine production profiles for secondary RAW macrophages and fibroblasts. Profiles were normalized to the sum total of all cells in the well including macrophages and fibroblasts during co-cultures. Cytokine production represents the average from 3 separate wells; each experiment was repeated four times with similar results and trends (data not shown). IL-6, TNF, MCP-1, RANTES, MIP-1β, and MIP-1α were detected using a BD™ Cytometric Bead Array. Significant difference from each internal control condition ($p < 0.05$) is indicated by an *. Controls are represented by solid bars, combined RAW & 3T3 control represents the mathematical sum of mono-cultured 3T3 and RAW control cells for comparison with co-cultures. Values below the assay detection limit were set to zero. All cells grown in wells were cultured on tissue culture polystyrene. Fibroblasts delaminated on Day 19. Background endogenous levels of cytokines in conditioned media were subtracted from each data set.

macrophages increased their production of MIP-1β, while secondary macrophages did not. Interestingly, fibroblasts increased their production of all inflammatory cytokines tested in the presence of macrophage-conditioned media compared to control fibroblasts, even after subtracting the background values for cytokines in the macrophage-conditioned media (Fig. 2).

3.1.2. Co-cultures

Macrophage responses (both primary and secondary) during paracrine and juxtacrine co-culture were more similar to each other than to their cultures in conditioned media (Figs. 2 and 3). In contrast to cultures with conditioned media, secondary macrophages during co-culture with fibroblasts dramatically increased their production of IL-6, MCP-1, and RANTES compared to controls (i.e., mono-cultures). More similar to samples treated with fibroblast-conditioned media, primary macrophages during co-culture increased only their production of MCP-1 significantly compared to controls.

3.1.3. LPS stimulation

LPS stimulation produced the greatest amount inflammatory cytokines in both primary and secondary macrophages compared to all other culture conditions. Primary macrophages produced higher maximum concentrations of inflammatory cytokines than secondary cells upon LPS stimulation. Additionally, primary macrophages decreased inflammatory cytokine production with repeated LPS treatments, while secondary macrophages primarily increased cytokines in the presence of repeated LPS stimulation (Fig. 4). Interestingly, 3T3 fibroblasts also appeared highly

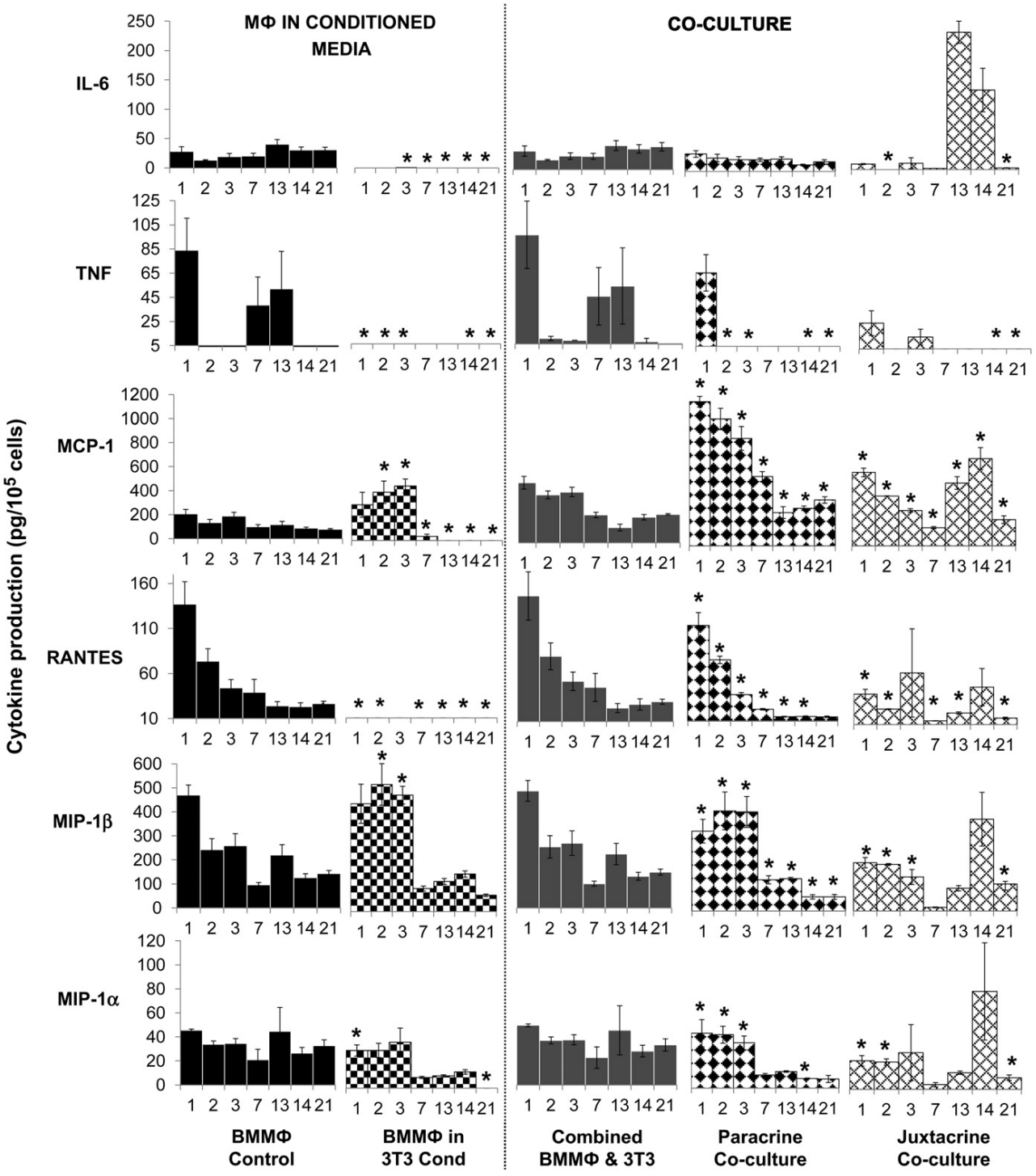

Fig. 3. Cytokine production profiles for cultures containing primary macrophages and secondary fibroblasts. Profiles were normalized to the sum total of all cells in the well including macrophages and fibroblasts during co-cultures. Cytokine production represents the average from 4 mice. IL-6, TNF, MCP-1, RANTES, MIP-1β, and MIP-1α were detected using a BD™ Cytometric Bead Array. Significant difference from each internal control (represented by solid bars) ($p < 0.05$) is indicated by an *. Mono-cultured BMMΦ macrophages were used as the control for BMMΦs in conditioned media. The mathematical sum of mono-cultured BMMΦ and 3T3s were used as the control for paracrine and juxtacrine co-culture (3T3 mono-cultured cell control data were taken from Fig. 2). All cells grown in wells were cultured on tissue culture polystyrene. Values below the assay detection limit were set to zero (see Methods and materials). Fibroblast delamination during juxtacrine co-culture occurred on Day 13. Background endogenous levels of cytokines in conditioned media were subtracted from the above data.

responsive to LPS addition, significantly increasing nearly every cytokine tested. A qualitative summary of these relative changes compared to controls is shown in Table 1.

3.2. Adherent cell morphology

Secondary macrophages during paracrine and juxtacrine co-culture and those stimulated with conditioned media all retained similar morphologies to mono-cultured control cells, displaying a more-rounded phenotype and growing near, or on top of, neighboring cells at both early (Supplementary Fig. 1) and late time points (Fig. 5) (also previously observed [4,27,28]). Primary macrophages in conditioned media and in paracrine and juxtacrine co-culture all exhibited similar morphologies at early (Supplementary Fig. 1) and late culture time points (Fig. 5), exhibiting more cell attachments than secondary macrophages and remaining relatively contact-inhibited. However, control BMMΦs (mono-cultured in the absence of fibroblast stimulation), by contrast, lost their contact inhibition over time, forming large dense clusters of cells in multi-layers. Over time, both primary and secondary macrophages developed a few scattered larger single-nucleated cells, with RAW macrophages occasionally producing multinucleate giant-like cells (Fig. 5). These

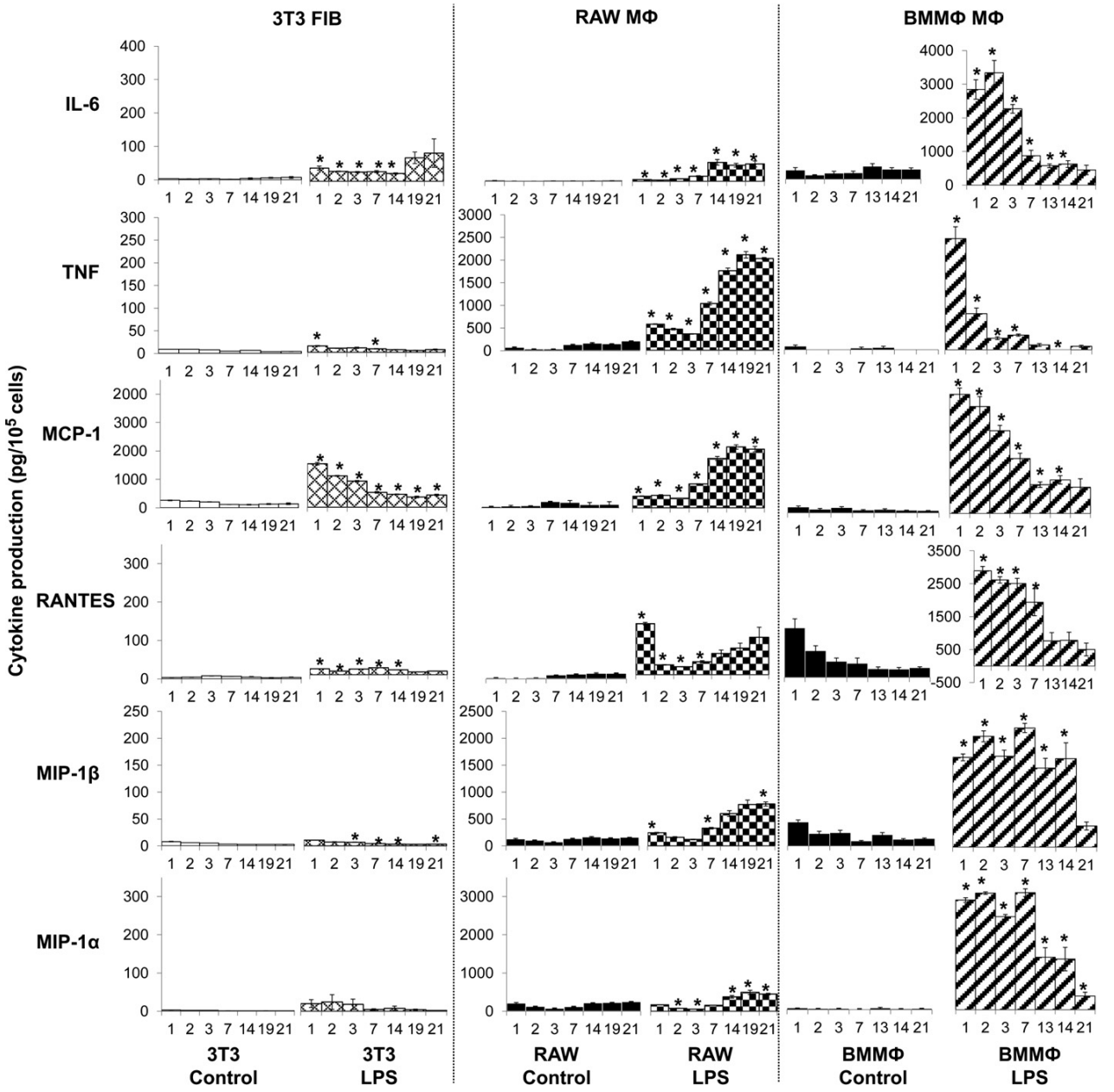

Fig. 4. Cytokine production normalized to cell number comparing mono-cultures both with and without LPS stimulation. Mono-cultured 3T3 fibroblasts, RAW macrophages, and BMMΦ macrophages were used as the control for their respective cell type repeatedly stimulated with LPS daily. Significant difference from each internal control (represented by solid bars) ($p < 0.05$) is indicated by an *. All cells grown in wells were cultured on tissue culture polystyrene. Values below the assay limit of detection for each cytokine were set to zero.

Table 1
A) Summary of relative changes in inflammatory cytokine production for secondary macrophages and fibroblasts, and B) primary macrophages in the presence of conditioned media, during co-culture, and after repeated stimulation with LPS. Arrows represent relative trends over 21 days in culture, and multiple arrows indicate changes in trends over the time course of the experiment. Background endogenous levels of cytokines in conditioned media were subtracted from the data.

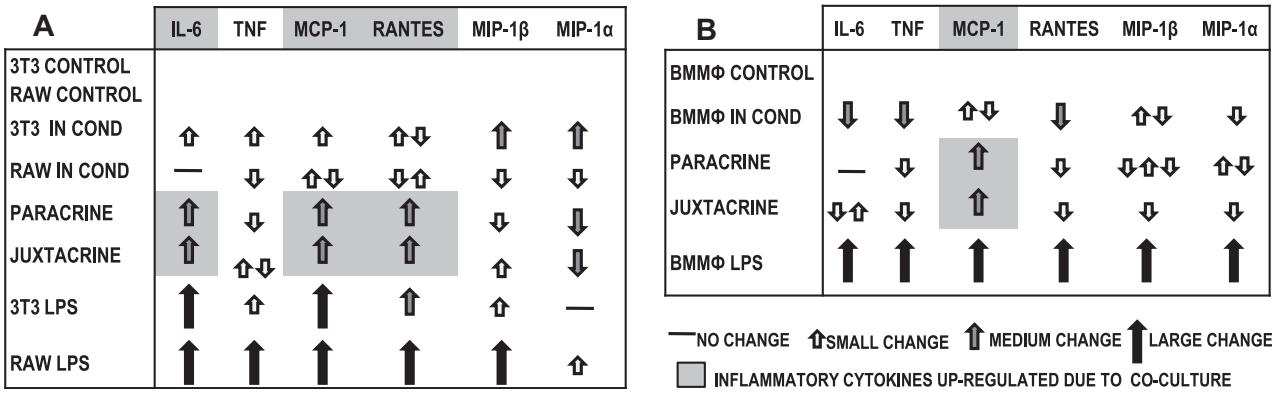

multinucleated cells were far larger than co-existing mononuclear cells, with centrally clustered nuclei, and consistently stained negative for TRAP (Supplementary Fig. 2). The frequency of multinucleate cells in RAW cultures remained similar for every treatment condition with the exception of LPS-stimulated cells that resulted in far more fused cells. In the presence of LPS stimulation, both primary and secondary macrophages developed highly activated morphologies compared to controls, displaying a high frequency of larger cell bodies with cytoplasmic vesicles (e.g., foamy appearance) and occasionally multiple nuclei. In all primary macrophage cultures, LPS-stimulation was the only condition that produced multinucleate cells (Fig. 5).

Fibroblasts maintained similar adherent morphologies in every condition tested. During secondary cell co-culture experiments, fibroblasts cultured alone, in RAW-conditioned media, and LPS media all began to delaminate from the culture surface on Day 19 (Figs. 2 and 4), a phenomenon also observed in previous extended fibroblast cultures [27,29]. During primary juxtacrine co-culture experiments, fibroblasts delaminated on Day 13 (Fig. 3). Due to this delamination, few fibroblasts remained, but began to repopulate past those time points.

3.3. Cell proliferation kinetics

Secondary RAW cells in 3T3-conditioned media and in paracrine and juxtacrine co-cultures possessed similar proliferation profiles as secondary RAW cells. Primary macrophages appeared to increase in cell number slightly in the presence of 3T3-conditioned media and during co-culture. Secondary and primary macrophages displayed distinct proliferation kinetics in culture (Fig. 6). Secondary macrophages proliferated rapidly within the first week, peaking at Day 3, and then decreased until Day 21, while primary macrophages proliferated at much slower rates during the first week, peaking at Day 7, and then decreased very slowly during the remaining time periods. Primary and secondary cells showed no apparent correlations between cell proliferation and cytokine production (Figs. 2–4,6). Juxtacrine co-culture cell density dropped on Day 13 due to fibroblast delamination. Macrophage cultures below the fibroblast Transwell inserts in paracrine co-culture wells often became contaminated by rapidly growing fibroblasts around Day 13, resulting in observed dramatic cell density increases to Day 21 (see Fig. 6).

3.4. LPS assay

An LAL assay, employed to detect endotoxin contamination, showed that all samples and materials had LPS levels below the assay detection limit (0.06 EU/ml) with the exception of the LPS-treated cultures (data not shown). This validates that differences observed in cell culture were not due to unwanted adventitious LPS contamination.

4. Discussion

Cell co-culture systems incorporating macrophages and fibroblasts, two primary effector cell types in the FBR, might better reflect actual FBR inflammatory profiles than their respective mono-cultures. Therefore, primary and secondary cells were both co-cultured in several different communication conditions in this assessment. Macrophages were treated with fibroblast-conditioned media and vice versa in order to determine if cytokine presence alone, without direct feedback from the other cell type in real-time, produced distinctly different responses from direct contact co-culture or mono-cultures. Transwell® inserts were used to physically separate the two cell types in co-culture, allowing cytokine transport between cell types to mimic paracrine signaling. Both cell types were co-cultured together in physical contact to mimic juxtacrine signaling. As a positive control of cell activation, primary- and secondary-derived macrophages and fibroblasts were stimulated with LPS, shown to activate macrophages [30,31]. Each cell mono-culture served as a negative control.

Cytokines TNF, IL-6, MIP-1α and MIP-1β, and chemokines MCP-1 and RANTES are some of the most potent inflammatory signals responsible for orchestrating the cellular responses to foreign material, frequently up-regulated in the presence of a foreign material *in vivo* [5,11,32,33]. They were monitored as a quantitative metric for cell behavioral changes arising from culture conditions and cell origin. Cell proliferation was assessed to normalize cytokine production to cell number to account for cell density changes in each condition. Cell morphology was used as a qualitative metric of phenotype. Murine cells were chosen due to the cost-effectiveness, abundant reagent base, and relevant comparisons to the many implant reaction studies performed in mice.

4.1. Cytokine response

4.1.1. LPS-stimulated cell cultures

LPS dramatically affected 3T3 fibroblasts, statistically increasing production of all cytokines with the exception of MIP-1α. Fibroblasts are not considered primary contributors of inflammatory cytokines upon endotoxin exposure. However, others have also reported increased IL-6 and other inflammatory cytokines by fibroblasts in

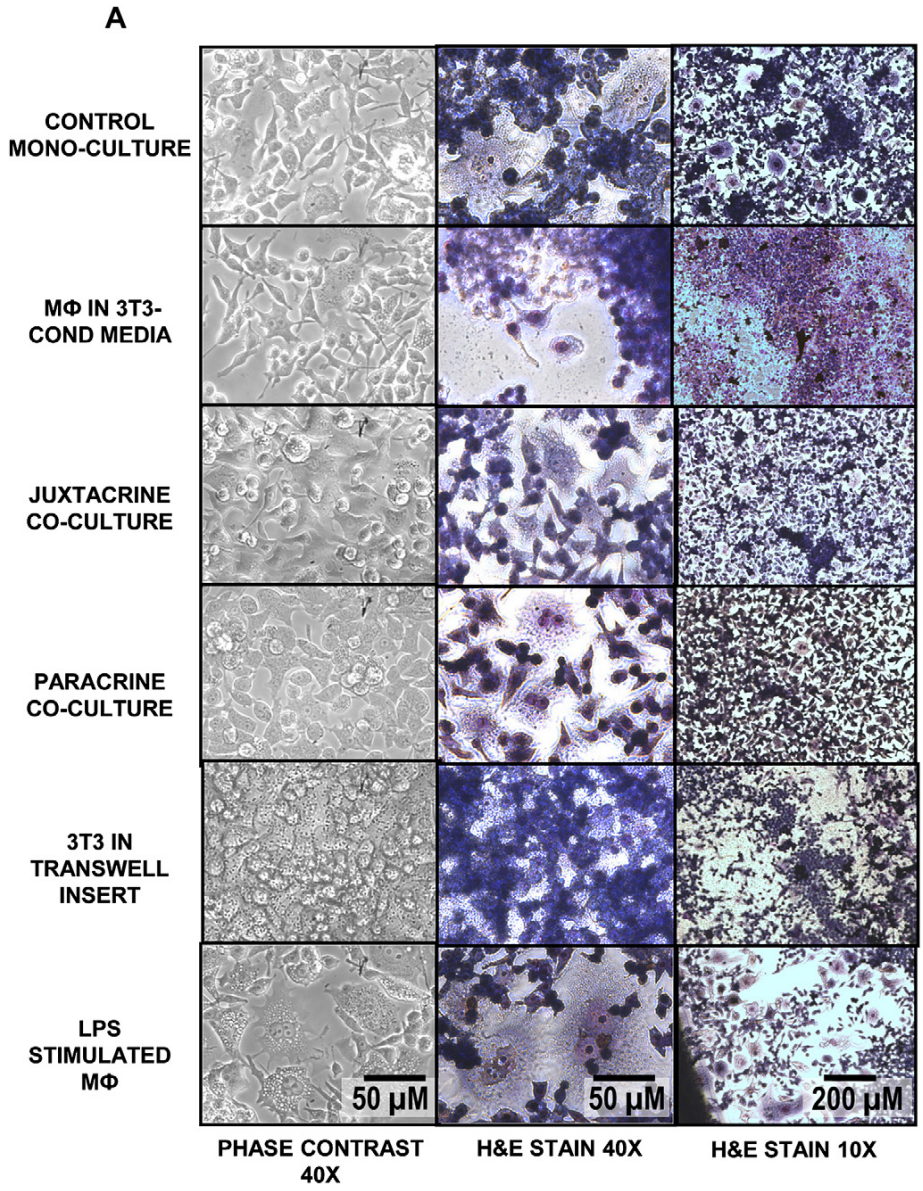

Fig. 5. Fluorescence and phase contrast microscope images of A) secondary RAW macrophages, and B) primary BMMΦ macrophages, in various 3T3 fibroblast signaling conditions after 21 days of culture. For fluorescence staining, phalloidin (red) was used to stain cytoskeleton and DAPI (blue) was used to stain cell nuclei.

response to LPS [34–36]. Strong LPS response by all cell types shows that both primary and secondary macrophages and fibroblasts are not maximally activated simply by *in vitro* culture on a synthetic surface, another contrast to cell activation by polystyrene and nearly every other synthetic material *in vivo* [37,38]. This discrepancy is most pronounced with IL-6, shown in this and other studies to be secreted at low *in vitro* and very high *in vivo* concentrations even in the absence of LPS stimulation [6,11]. Lack of cell activation against biomaterials *in vitro* has been a common challenge to such biomaterials assays, requiring use of exogenous stimulants such as LPS and phorbol esters to mimic *in vivo* activation (*vide supra*). This finding suggests that even in co-culture, cells may not be capable of biomaterials-based activation levels shown *in vivo*.

Published *in vivo* studies show a general decrease in inflammatory cytokine production from macrophages after repeated LPS dosing, a phenomenon known as LPS or endotoxin tolerance [39,40]. This effect is considered a natural cellular response to prevent uncontrolled inflammation [41–43], and is readily apparent in cultured primary-derived macrophages in this and other studies [44]. However, the opposite effect was observed in secondary-derived RAW macrophages, where this and other studies show increasing inflammatory cytokine production after repeated LPS stimulation [45]. Though RAW 264.7 macrophages have exhibited endotoxin tolerance [43,46], it has only been over the span of a few hours and with one repeated dose, compared to the continual LPS stimulation seen in this study over the course of 21 days. This general increasing

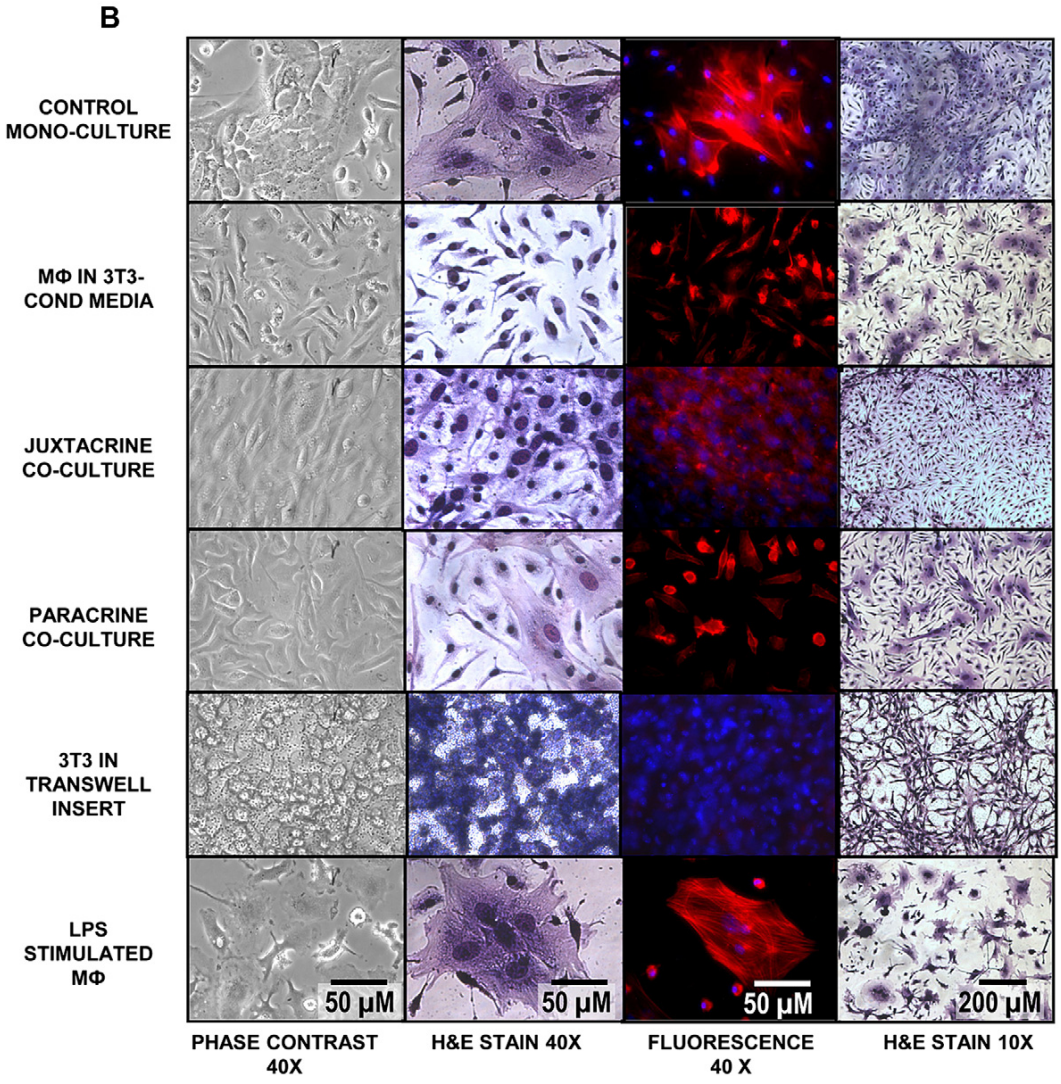

Fig. 5. (*continued*).

inflammatory cytokine production from secondary macrophages over a three-week period may result from their transformed oncogenic phenotype, impeding the normal down-regulation of inflammatory cytokines observed *in vivo* and in primary cultures.

Additionally, primary macrophages exposed to LPS in this study produced comparable relative increases of inflammatory cytokines as *in vivo* serum levels produced in response to LPS stimulation [11,47] (compared to non-stimulated controls). In contrast, secondary macrophages stimulated with LPS exhibited less dramatic increases in cytokine production, most pronounced with IL-6 and MIP-1α (Fig. 4). These data suggest that endotoxin sensitivity in primary cells may better reflect *in vivo* LPS response that in than secondary cells.

4.1.2. Conditioned media-treated cell cultures

Primary macrophage mono-cultures showed more dramatic decreases in IL-6, TNF, and RANTES in the presence of 3T3-conditioned media compared to controls than their paracrine and juxtacrine co-cultures (Table 1). Secondary macrophages in fibroblast-conditioned media displayed less drastic changes in cytokine production compared to primary macrophages, more similar to control cells. As RAW cells are oncogenically transformed, passaged many times, displaying a more monocytic phenotype [4,14,15], they may exhibit less sensitivity to cellular cues in fibroblast-conditioned media than primary cells. This decreased primary and secondary cytokine production falls below that in their co-cultures (Table 1). Distinct differences in primary and secondary cell response to conditioned media versus co-culture could result from lack of dynamic cell feedback and reaction: co-culture allows for real-time cell processing and feedback between macrophages and fibroblasts, prompting unique signaling profiles.

Another contrast is that 3T3 fibroblasts increased production of pro-inflammatory cytokines in RAW-conditioned media, while RAW and BMMΦ cells generally decreased their pro-inflammatory cytokine production in the presence of 3T3-conditioned media. Cytokines present in fibroblast-conditioned media may inhibit macrophage production of cytokines tested while macrophage-conditioned media may induce cytokine production in fibroblasts. This complex balance of cell–cell signaling determines the host's response to an implanted biomaterial, and importantly, that factor is missing in frequently used mono-cultures of isolated cell types.

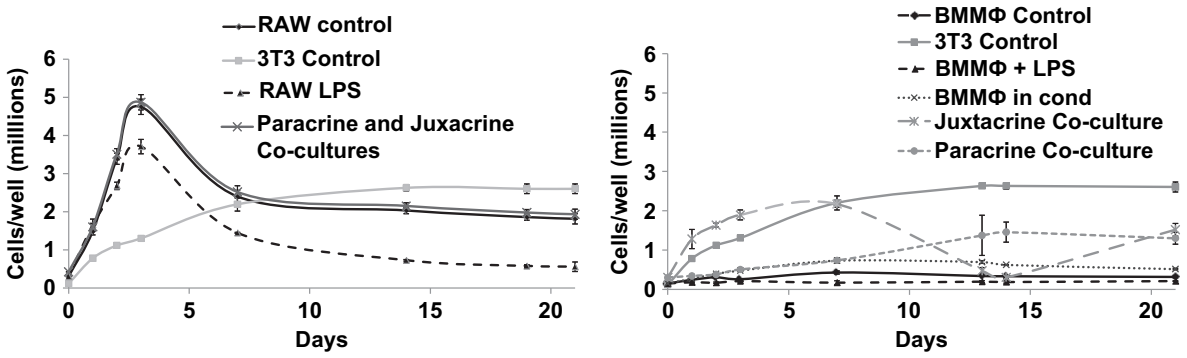

Fig. 6. A) Proliferation profiles for secondary macrophage and fibroblast mono-cultures. Profiles for 3T3s stimulated with LPS and treated with conditioned media were comparable to mono-cultured 3T3s, and RAWs in conditioned media were comparable to mono-cultured RAWs (not shown). B) Proliferation profiles for primary BMMΦs in various culture conditions. Juxtacrine co-culture cell density dropped on Day 13 due to fibroblast delamination. Macrophage cultures below the fibroblast Transwell® insert in the paracrine co-culture wells became contaminated by rapidly growing fibroblasts around Day 13, resulting in dramatic cell density increases until Day 21. Cells in all conditions reached confluence by Day 1. Error bars not seen are smaller than symbols.

4.1.3. Contact and non-contact co-cultures

Co-cultured primary and secondary macrophages both generally decrease production of MIP-1β, MIP-1α, and TNF compared to mono-cultured controls. Previous studies also document reductions of these cytokines in the presence of fibroblast-released cytokines [48,49]. Primary macrophages in co-culture also generally decreased RANTES and IL-6 production compared to mono-cultured controls, related possibly to mutual cytokine down-regulation (Table 1). RANTES and IL-6 down-regulation were not observed in secondary cell cultures: by contrast, IL-6 and RANTES were highly up-regulated in both paracrine and juxtacrine co-cultures compared to controls. This *in vitro* discrepancy between primary and secondary macrophages cytokine expression may again be due to intrinsic differences in cell sensitivity and responses to cytokine signaling.

Notably, both primary and secondary paracrine and juxtacrine macrophage-fibroblast co-cultures displayed significant increases in MCP-1 at nearly all time points (Figs. 2 and 3). MCP-1 could participate in a positive feedback loop between cultured macrophages and fibroblasts (seen in a schematic of known cytokine communication between macrophages and fibroblasts, Fig. 7), resulting in its increased production in the presence of the other cell type (Table 1). Importantly, this dramatic increase in MCP-1 was not seen in primary or secondary macrophage mono-cultures treated with fibroblast-conditioned media – a system that inherently lacks cell–cell reciprocal feedback signals found *in vivo*. This MCP-1 increase is consistent with a positive feedback mechanism for MCP-1 previously proposed to perpetuate the FBR [50]. Increasing levels of TNF are shown to increase MCP-1 production [51,52] and act as a mitogen for fibroblasts [53] (Fig. 7) which may also then contribute to high MCP-1 levels seen during co-culture (Table 1). Increased MCP-1 production during 3T3 co-culture with both primary and secondary macrophages relative to mono-cultured macrophages could reflect an important fibroblast transition to a fibrotic phenotype, as fibrotic fibroblasts are known to increase TNF-induced MCP-1 [54], proliferation [55], and protein secretion [56]. Though co-cultures do not replicate all comprehensive aspects of *in vivo* reactions, they are capable of cell signaling patterns more representative of the *in vivo* environment than their mono-cultures with or without conditioned media.

Interestingly, all cytokines significantly increased in co-cultures (compared cytokines produced from *the arithmetic sum total* from both mono-cultured macrophages and fibroblasts) were only those appearing to be produced in greater amounts by fibroblasts over macrophages during mono-culture. Mono-cultured fibroblasts exhibited greater IL-6, MCP-1, and RANTES cytokines than mono-cultured secondary macrophages, and produced greater MCP-1 cytokine amounts than primary cells. Relatively strong fibroblast cytokine response compared to macrophages may initiate positive feedback during co-culture. As cytokines are pleiotropic [57], their dynamic production kinetics and fluctuations are expected, prompting dynamic production and fluctuations of other cytokines.

4.2. Adherent cell morphology

At early time points, adherent secondary RAW 264.7 macrophages behaved very differently from primary-derived BMMΦs, showing no contact inhibition and readily growing in multi-layers. BMMΦs maintained larger cell bodies, more cell attachments, frequent lamellipodia, and elongated morphologies, while RAWs had smaller cell bodies and maintained a more-rounded phenotype compared to primary cells during mono-culture, a characteristic of their less differentiated and more monocytic phenotype (images of all cells on Day 1 are found in Supplementary Fig. 1) [4]. However, over time both cell populations transitioned to larger cell bodies, showing differentiation over time (Fig. 5). RAW control cells in frequently developed into FBGCs with large cell bodies and centrally clustered nuclei, while primary control macrophages did not. These cells consistently stained negative for TRAP (Supplementary Fig. 2). This supports an FBGC-like phenotype [58,59] over an alternative osteoclastic phenotype also known to be derived from RAW 264.7 cells [60]. Osteoclasts tend to have multiple nuclei lining the cell periphery as opposed to clustered centrally (arrows, Supplementary Fig. 2), have larger cell bodies than FBGCs, and stain positive for TRAP [61].

Both in the presence of conditioned media and co-culture, RAW cells maintained a similar phenotype to control cells, unlike BMMΦs in these conditions that remained contact-inhibited in the presence of fibroblast signaling. Both primary and secondary control macrophage cultures, absent of fibroblast signaling, lost their contact inhibition, began to grow much larger cell bodies, and formed dense multilayered clusters (notably not multinucleated as for LPS-stimulated cells). Perhaps without appropriate signals, these cells may not be able to retain their original macrophage phenotype in culture.

LPS activates all macrophage cultures, influencing morphology of both primary and secondary macrophages more than any other condition, leading to the production of intracellular vesicles, enlarged cell bodies, and occasionally multiple nuclei, seen previously [30]. Kyriakides *et al.* identified a loss of peripheral actin rings

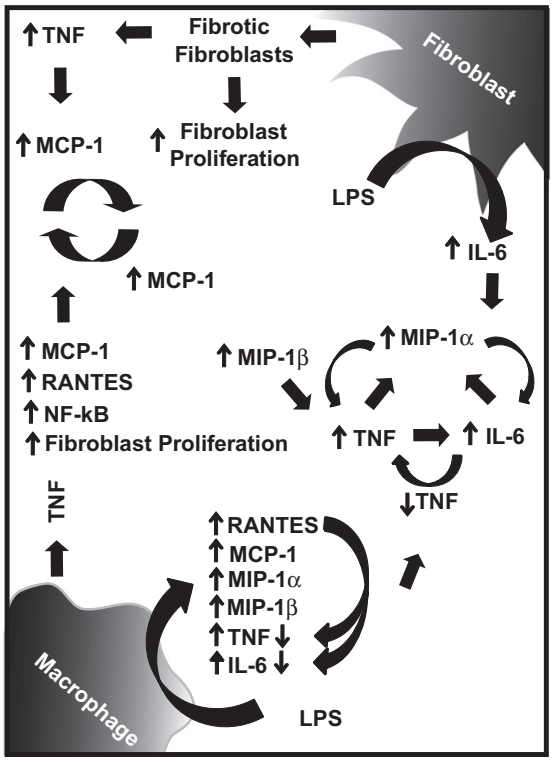

Fig. 7. Overview of the select cytokine signaling pathways known between fibroblasts and macrophages [12,33,50–56,64–73].

and extended lamellipodia in cells destined to become FBGCs [62]. This is witnessed in LPS-stimulated BMMΦs (see Fig. 5 – the only treatment of BMMΦs leading to FBG-like cells). Neither primary nor secondary macrophages appeared activated by culture surfaces compared to LPS-stimulated cells, consisting with cytokine data. This absence of cell activation during *in vitro* co-culture of macrophages and fibroblasts may be due to the absence of acute wound-derived inflammatory cues always produced *in vivo* during device implantation, or insufficient cell types, numbers and signals necessary to accurately recapitulate host inflammatory reactions or produce a clear foreign body response.

During contact co-culture, one cell type grew more aggressively than the other, eventually creating a layer over the other cell type. RAW cells over-layered 3T3 fibroblasts, while 3T3 fibroblasts over-layered BMMΦs, both within the first 3 days. However, even with this covering layer, the cells underneath did not die, but also did not appear to proliferate. Supplementary Fig. 3 shows viable fluorescent 3T3s beneath unlabeled RAWs, still maintaining a normal morphology. But these cells did not reach confluence like mono-cultured fibroblasts. Similarly, in the primary contact co-culture on Day 13, the 3T3s delaminated, revealing a layer of viable BMMΦs underneath, which appeared to have retained their original plating density and phenotype (Supplementary Fig. 4). Cell culture conditions that enabled fibroblasts to grow to confluence all resulted in eventual longer-term cell-substrate delamination seen previously [29,63].

4.3. Cell culture proliferation kinetics

Secondary RAW macrophages proliferated rapidly in the first week of culture, and then decreased cell numbers at later time points (seen previously [28]). Primary macrophages grew at far slower rates, maintaining a relatively constant cell density. These primary macrophages did not reach confluency until Day 7, after which their density decreased very slowly. By Day 3, secondary cells were at their highest proliferative rate (Fig. 6), however, they exhibited low cytokine secretion profiles during that time. Proliferation of primary cells peaked at Day 7, but their highest cytokine secretion levels were during the first 3 days. These results suggest that cell inflammatory signaling activity is independent of proliferation. Also supporting this idea, LPS-stimulated secondary and primary cells secreted the largest amounts of inflammatory cytokines, but while undergoing the least proliferation.

RAW cell treatment with fibroblast-conditioned media or direct co-culture did not appear to affect their proliferation. These cultures maintained comparable proliferation rates to control RAW cells (as RAWs proliferated at much higher rates than 3T3 fibroblasts and therefore dominated co-culture kinetics). However, primary BMMΦs in conditioned media and their paracrine co-culture with fibroblasts show slightly increased proliferation rates compared to control BMMΦs. This increased cell number compared to mono-cultured BMMΦ controls is due to cell size in each culture: control BMMΦs without fibroblast stimulation grew very large cell bodies, while those with fibroblast signaling maintained much smaller cell bodies (Fig. 5), altering the cell densities. LPS-stimulated primary- and secondary-macrophage cultures displayed an overall decreased cell number compared to controls. This reduced cell density may be due to this same cell size transition to larger cells, toxic effects of LPS, or a phenotypic shift to a less proliferative cell during LPS stimulation. Cell proliferation kinetics in primary juxtacrine co-culture were comparable to mono-cultured fibroblasts, because secondary fibroblasts proliferate faster than primary macrophages. With both secondary and primary macrophage juxtacrine co-cultures, growth kinetics are determined by this more highly proliferative cell type.

5. Conclusions

Several differences in cell signaling, adherent cell morphology, and proliferation between primary- and secondary-derived macrophages are shown in cultures, with greater apparent fidelity in primary over secondary cells to *in vivo* responses. Primary and secondary macrophage cell sources also exhibit unique responses in culture that provide different cell–cell feedback mechanisms, with reciprocal feedback (i.e., in paracrine and juxtacrine co-cultures) eliciting more representative characteristics found *in vivo* than mono-cultured cells in conditioned media. In general, co-culture feedback signaling in primary macrophage co-cultures with fibroblasts improves on *in vitro* models currently employing secondary cell mono-cultures. Despite co-culture feedback, without cell-derived wounding cues or implant-associated healing cascades in cell culture, FBR *in vitro* assays may exclude other acute cellular reactions associated with implant placement *in vivo*. Additionally, 2-D monolayer cell culture on rigid substrates and absence of other inflammatory cells such as T-cells may also limit *in vitro* approaches to duplicate the cell signaling observed *in vivo*. *In vitro* cell assays may only be adequate to represent specific cell types, functions, and simple biomaterials-associated signaling, but may be insufficient to approach or accurately represent more dynamic cell-interactive acute inflammatory or resulting FBR mechanisms found *in vivo*. The many *in vitro* assays (especially those using secondary-derived cell cultures and/or mono-cultured cells) used for FBR models, cell toxicity screening, drug and materials testing, and basic cell signaling research should all be validated by comparisons to primary cell cultures, cell co-cultures, and *in vivo*

contexts in order to assert fidelity and relevance to the specific *in vivo* phenomena they claim to represent.

Acknowledgments

This research was supported by National Institutes of Health grant R01EB00894. Dr. G. Stoddard (Biostatistics Core Facility, University of Utah) is thanked for discussions and guidance on statistical analysis.

Appendix. Supplementary data

Supplementary data associated with article can be found in the online version, at doi:10.1016/j.biomaterials.2010.07.101.

Appendix

Figures with essential color discrimination. Figs. 1 and 5 in this article are difficult to interpret in black and white. The full color images can be found in the online version, at doi:10.1016/j.biomaterials.2010.07.101.

References

[1] Anderson JM. Mechanisms of inflammation and infection with implanted devices. Cardiovasc Pathol 1993;2:33S–41S [Chapter 4].
[2] Zhao Q, Topham N, Anderson JM, Hiltner A, Lodoen G, Payet CR. Foreign-body giant cells and polyurethane biostability: in vivo correlation of cell adhesion and surface cracking. J Biomed Mater Res 1991;25:177–83.
[3] Murray DW, Rushton N. Macrophages stimulate bone resorption when they phagocytose particles. J Bone Jt Surg Br 1990;72:988–92.
[4] Chamberlain LM, Godek ML, Gonzalez-Juarrero M, Grainger DW. Phenotypic non-equivalence of murine (monocyte-) macrophage cells in biomaterial and inflammatory models. J Biomed Mater Res A 2009;88:858–71.
[5] Luttikhuizen DT, Harmsen MC, Van Luyn MJ. Cellular and molecular dynamics in the foreign body reaction. Tissue Eng 2006;12:1955–70.
[6] Schutte RJ, Parisi-Amon A, Reichert WM. Cytokine profiling using monocytes/macrophages cultured on common biomaterials with a range of surface chemistries. J Biomed Mater Res A 2009;88:128–39.
[7] Ung DY, Woodhouse KA, Sefton MV. Tumor necrosis factor (TNFalpha) production by rat peritoneal macrophages is not polyacrylate surface-chemistry dependent. J Biomed Mater Res 1999;46:324–30.
[8] Scheibenbogen C, Andreesen R. Developmental regulation of the cytokine repertoire in human macrophages: IL-1, IL-6, TNF-alpha, and M-CSF. J Leukoc Biol 1991;50:35–42.
[9] Whelan RD, Kiley SC, Parker PJ. Tetradecanoyl phorbol acetate-induced microtubule reorganization is required for sustained mitogen-activated protein kinase activation and morphological differentiation of U937 cells. Cell Growth Differ 1999;10:271–7.
[10] Gretzer C, Emanuelsson L, Liljensten E, Thomsen P. The inflammatory cell influx and cytokines changes during transition from acute inflammation to fibrous repair around implanted materials. J Biomater Sci Polym Ed 2006;17:669–87.
[11] Schutte RJ, Xie L, Klitzman B, Reichert WM. In vivo cytokine-associated responses to biomaterials. Biomaterials 2009;30:160–8.
[12] Roumestan C, Michel A, Bichon F, Portet K, Detoc M, Henriquet C, et al. Anti-inflammatory properties of desipramine and fluoxetine. Respir Res 2007;8:35.
[13] Hayflick L, Moorhead PS. The serial cultivation of human diploid cell strains. Exp Cell Res 1961;25:585–621.
[14] Hughes P, Marshall D, Reid Y, Parkes H, Gelber C. The costs of using unauthenticated, over-passaged cell lines: how much more data do we need? Biotechniques 2007;43(575):7–8. 81-2 passim.
[15] Sandeep Varma R, Ashok G, Vidyashankar S, Patki P, Nandakumar KS. Anti-inflammatory properties of septilin in lipopolysaccharide activated monocytes and macrophage. Immunopharmacol Immunotoxicol 2010, doi:10.3109/08923971003739236.
[16] Lin NJ, Hu H, Sung L, Lin-Gibson S. Quantification of cell response to polymeric composites using a two-dimensional gradient platform. Comb Chem High Throughput Screen 2009;12:619–25.
[17] Yoon WJ, Ham YM, Yoo BS, Moon JY, Koh J, Hyun CG. Oenothera laciniata inhibits lipopolysaccharide induced production of nitric oxide, prostaglandin E2, and proinflammatory cytokines in RAW264.7 macrophages. J Biosci Bioeng 2009;107:429–38.
[18] Kelly M, Kolb M, Bonniaud P, Gauldie J. Re-evaluation of fibrogenic cytokines in lung fibrosis. Curr Pharm Des 2003;9:39–49.
[19] Liu X, Li J, Zhang J. STAT3-decoy ODN inhibits cytokine autocrine of murine tumor cells. Cell Mol Immunol 2007;4:309–13.
[20] Anderson JM, Rodriguez A, Chang DT. Foreign body reaction to biomaterials. Semin Immunol 2008;20:86–100.
[21] Ask K, Bonniaud P, Maass K, Eickelberg O, Margetts PJ, Warburton D, et al. Progressive pulmonary fibrosis is mediated by TGF-beta isoform 1 but not TGF-beta3. Int J Biochem Cell Biol 2008;40:484–95.
[22] Higgins DM, Basaraba RJ, Hohnbaum AC, Lee EJ, Grainger DW, Gonzalez-Juarrero M. Localized immunosuppressive environment in the foreign body response to implanted biomaterials. Am J Pathol 2009;175:161–70.
[23] Godek ML, Sampson JA, Duchsherer NL, McElwee Q, Grainger DW. Rho GTPase protein expression and activation in murine monocytes/macrophages is not modulated by model biomaterial surfaces in serum-containing in vitro cultures. J Biomater Sci Polym Ed 2006;17:1141–58.
[24] Rhoades ER, Orme IM. Similar responses by macrophages from young and old mice infected with *Mycobacterium tuberculosis*. Mech Ageing Dev 1998;106:145–53.
[25] Morgan E, Varro R, Sepulveda H, Ember JA, Apgar J, Wilson J, et al. Cytometric bead array: a multiplexed assay platform with applications in various areas of biology. Clin Immunol 2004;110:252–66.
[26] Dunnett C, Goldsmith C. When and how to do multiple comparisons. In: Buncher CR, Tsay J-Y, editors. Statistics in the pharmaceutical industry. 3rd ed. New York: Chapman and Hall/CRC; 2006. p. 421–52.
[27] Godek ML, Michel R, Chamberlain LM, Castner DG, Grainger DW. Adsorbed serum albumin is permissive to macrophage attachment to perfluorocarbon polymer surfaces in culture. J Biomed Mater Res A 2009;88:503–19.
[28] Godek ML, Duchsherer NL, McElwee Q, Grainger DW. Morphology and growth of murine cell lines on model biomaterials. Biomed Sci Instrum 2004;40:7–12.
[29] Takahashi H, Emoto K, Dubey MG, Castner DG, Grainger DW. Imaging surface immobilization chemistry: correlation with cell patterning on non-adhesive hydrogel thin films. Adv Funct Mater 2008;18:1–10.
[30] Kim DH, Smith JT, Chilkoti A, Reichert WM. The effect of covalently immobilized rhIL-1ra-ELP fusion protein on the inflammatory profile of LPS-stimulated human monocytes. Biomaterials 2007;28:3369–77.
[31] Gordon S, Taylor PR. Monocyte and macrophage heterogeneity. Nat Rev Immunol 2005;5:953–64.
[32] Volin MV, Shah MR, Tokuhira M, Haines GK, Woods JM, Koch AE. RANTES expression and contribution to monocyte chemotaxis in arthritis. Clin Immunol Immunopathol 1998;89:44–53.
[33] Nath A, Chattopadhya S, Chattopadhyay U, Sharma NK. Macrophage inflammatory protein (MIP)1alpha and MIP1beta differentially regulate release of inflammatory cytokines and generation of tumoricidal monocytes in malignancy. Cancer Immunol Immunother 2006;55:1534–41.
[34] Isumi Y, Minamino N, Kubo A, Nishimoto N, Yoshizaki K, Yoshioka M, et al. Adrenomedullin stimulates interleukin-6 production in Swiss 3T3 cells. Biochem Biophys Res Commun 1998;244:325–31.
[35] Helfgott DC, May LT, Sthoeger Z, Tamm I, Sehgal PB. Bacterial lipopolysaccharide (endotoxin) enhances expression and secretion of beta 2 interferon by human fibroblasts. J Exp Med 1987;166:1300–9.
[36] Kitamura H, Kanehira K, Okita K, Morimatsu M, Saito M. MAIL, a novel nuclear I kappa B protein that potentiates LPS-induced IL-6 production. FEBS Lett 2000;485:53–6.
[37] Brown DM, Wilson MR, MacNee W, Stone V, Donaldson K. Size-dependent proinflammatory effects of ultrafine polystyrene particles: a role for surface area and oxidative stress in the enhanced activity of ultrafines. Toxicol Appl Pharmacol 2001;175:191–9.
[38] Ratner BD. Reducing capsular thickness and enhancing angiogenesis around implant drug release systems. J Control Release 2002;78:211–8.
[39] Draisma A, de Goeij M, Wouters CW, Riksen NP, Oyen WJ, Rongen GA, et al. Endotoxin tolerance does not limit mild ischemia-reperfusion injury in humans in vivo. Innate Immun 2009;15:360–7.
[40] Porta C, Rimoldi M, Raes G, Brys L, Ghezzi P, Di Liberto D, et al. Tolerance and M2 (alternative) macrophage polarization are related processes orchestrated by p50 nuclear factor kappaB. Proc Natl Acad Sci U S A 2009;106:14978–83.
[41] Ziegler-Heitbrock HW. Molecular mechanism in tolerance to lipopolysaccharide. J Inflamm 1995;45:13–26.
[42] Sly LM, Rauh MJ, Kalesnikoff J, Song CH, Krystal G. LPS-induced upregulation of SHIP is essential for endotoxin tolerance. Immunity 2004;21:227–39.
[43] Zhu MF, Zhang J, Qu JM, Zhang HJ, Zhou SC, Dong SF, et al. Up-regulation of growth factor independence 1 in endotoxin tolerant macrophages with low secretion of TNF-alpha and IL-6. Inflamm Res, 2010, doi:10.1007/s00011-010-0197-1.
[44] West MA, Hackam DJ, Baker J, Rodriguez JL, Bellingham J, Rotstein OD. Mechanism of decreased in vitro murine macrophage cytokine release after exposure to carbon dioxide: relevance to laparoscopic surgery. Ann Surg 1997;226:179–90.
[45] Jakobsen SS, Larsen A, Stoltenberg M, Bruun JM, Soballe K. Effects of as-cast and wrought cobalt–chrome–molybdenum and titanium–aluminium–vanadium alloys on cytokine gene expression and protein secretion in J774A.1 macrophages. Eur Cell Mater 2007;14:45–54. discussion -5.
[46] Vittimberga Jr FJ, Foley DP, Perugini RA, McDade TP, Callery MP. Endotoxin fails to stimulate inositol triphosphate production in macrophages. Int J Surg Investig 1999;1:229–35.
[47] Wang X, Lennartz MR, Loegering DJ, Stenken JA. Interleukin-6 collection through long-term implanted microdialysis sampling probes in rat subcutaneous space. Anal Chem 2007;79:1816–24.
[48] Oshikawa K, Yamasawa H, Sugiyama Y. Human lung fibroblasts inhibit macrophage inflammatory protein-1alpha production by lipopolysaccharide-stimulated macrophages. Biochem Biophys Res Commun 2003;312:650–5.

[49] Vancheri C, Crimi N, Conte E, Pistorio MP, Mastruzzo C, Lamicela M, et al. Human lung fibroblasts inhibit tumor necrosis factor-alpha production by LPS-activated monocytes. Am J Respir Cell Mol Biol 1996;15:460–6.
[50] Gosling J, Slaymaker S, Gu L, Tseng S, Zlot CH, Young SG, et al. MCP-1 deficiency reduces susceptibility to atherosclerosis in mice that overexpress human apolipoprotein B. J Clin Invest 1999;103:773–8.
[51] Satriano JA, Hora K, Shan Z, Stanley ER, Mori T, Schlondorff D. Regulation of monocyte chemoattractant protein-1 and macrophage colony-stimulating factor-1 by IFN-gamma, tumor necrosis factor-alpha, IgG aggregates, and cAMP in mouse mesangial cells. J Immunol 1993;150:1971–8.
[52] Kumar SN, Boss JM. Site A of the MCP-1 distal regulatory region functions as a transcriptional modulator through the transcription factor NF1. Mol Immunol 2000;37:623–32.
[53] Palombella VJ, Mendelsohn J, Vilcek J. Mitogenic action of tumor necrosis factor in human fibroblasts: interaction with epidermal growth factor and platelet-derived growth factor. J Cell Physiol 1988;135:23–31.
[54] Vancheri C, Sortino MA, Tomaselli V, Mastruzzo C, Condorelli F, Bellistri G, et al. Different expression of TNF-alpha receptors and prostaglandin E2 production in normal and fibrotic lung fibroblasts: potential implications for the evolution of the inflammatory process. Am J Respir Cell Mol Biol 2000;22:628–34.
[55] Sun LK, Reding T, Bain M, Heikenwalder M, Bimmler D, Graf R. Prostaglandin E2 modulates TNF-alpha-induced MCP-1 synthesis in pancreatic acinar cells in a PKA-dependent manner. Am J Physiol Gastrointest Liver Physiol 2007;293:G1196–204.
[56] Goldstein RH, Polgar P. The effect and interaction of bradykinin and prostaglandins on protein and collagen production by lung fibroblasts. J Biol Chem 1982;257:8630–3.
[57] Rosenquist JB, Ohlin A, Lerner UH. Cytokine-induced inhibition of bone matrix proteins is not mediated by prostaglandins. Inflamm Res 1996;45:457–63.
[58] Helming L, Gordon S. Macrophage fusion induced by IL-4 alternative activation is a multistage process involving multiple target molecules. Eur J Immunol 2007;37:33–42.
[59] MacLauchlan S, Skokos EA, Meznarich N, Zhu DH, Raoof S, Shipley JM, et al. Macrophage fusion, giant cell formation, and the foreign body response require matrix metalloproteinase 9. J Leukoc Biol 2009;85:617–26.
[60] Wang Y, Grainger DW. siRNA knock-down of RANK signaling to control osteoclast-mediated bone resorption. Pharm Res 27:1273–1284.
[61] Xiao XH, Liao EY, Zhou HD, Dai RC, Yuan LQ, Wu XP. Ascorbic acid inhibits osteoclastogenesis of RAW264.7 cells induced by receptor activated nuclear factor kappaB ligand (RANKL) in vitro. J Endocrinol Invest 2005;28:253–60.
[62] Jay SM, Skokos E, Laiwalla F, Krady MM, Kyriakides TR. Foreign body giant cell formation is preceded by lamellipodia formation and can be attenuated by inhibition of Rac1 activation. Am J Pathol 2007;171:632–40.
[63] Godek ML, Malkov GS, Fisher ER, Grainger DW. Macrophage serum-based adhesion to plasma-processed surface chemistry is distinct from that exhibited by fibroblasts. Plasma Process Polym 2006;3:485–97.
[64] Ghezzi P, Sacco S, Agnello D, Marullo A, Caselli G, Bertini R. LPS induces IL-6 in the brain and in serum largely through TNF production. Cytokines 2000;12:1205–10.
[65] Smith RE, Strieter RM, Phan SH, Lukacs N, Kunkel SL. TNF and IL-6 mediate MIP-1alpha expression in bleomycin-induced lung injury. J Leukoc Biol 1998;64:528–36.
[66] Fahey 3rd TJ, Tracey KJ, Tekamp-Olson P, Cousens LS, Jones WG, Shires GT, et al. Macrophage inflammatory protein 1 modulates macrophage function. J Immunol 1992;148:2764–9.
[67] Santavirta S, Konttinen YT, Bergroth V, Eskola A, Tallroth K, Lindholm TS. Aggressive granulomatous lesions associated with hip arthroplasty. Immunopathological studies. J Bone Jt Surg Am 1990;72:252–8.
[68] Jiranek WA, Machado M, Jasty M, Jevsevar D, Wolfe HJ, Goldring SR, et al. Production of cytokines around loosened cemented acetabular components. Analysis with immunohistochemical techniques and in situ hybridization. J Bone Jt Surg Am 1993;75:863–79.
[69] Neale SD, Sabokbar A, Howie DW, Murray DW, Athanasou NA. Macrophage colony-stimulating factor and interleukin-6 release by periprosthetic cells stimulates osteoclast formation and bone resorption. J Orthop Res 1999;17:686–94.
[70] Al-Saffar N, Revell PA. Differential expression of transforming growth factor-alpha and macrophage colony-stimulating factor/colony-stimulating factor-1R (c-fins) by multinucleated giant cells involved in pathological bone resorption at the site of orthopaedic implants. J Orthop Res 2000;18:800–7.
[71] Shahrara S, Park CC, Temkin V, Jarvis JW, Volin MV, Pope RM. RANTES modulates TLR4-induced cytokine secretion in human peripheral blood monocytes. J Immunol 2006;177:5077–87.
[72] Starkie R, Ostrowski SR, Jauffred S, Febbraio M, Pedersen BK. Exercise and IL-6 infusion inhibit endotoxin-induced TNF-alpha production in humans. FASEB J 2003;17:884–6.
[73] Elias JA, Rossman MD, Zurier RB, Daniele RP. Human alveolar macrophage inhibition of lung fibroblast growth. A prostaglandin-dependent process. Am Rev Respir Dis 1985;131:94–9.

CHAPTER 3

MULTINUCLEATED GIANT CELLS FROM FIBROBLAST CULTURES

Reprinted with permission from Holt DJ, Grainger DW. Multinucleated giant cells from fibroblast cultures. *Biomaterials* 2011;32:3977-87.

Biomaterials 32 (2011) 3977–3987

Contents lists available at ScienceDirect

Biomaterials

journal homepage: www.elsevier.com/locate/biomaterials

Multinucleated giant cells from fibroblast cultures

Dolly J. Holt [a], David W. Grainger [a,b,*]

[a] Department of Bioengineering, University of Utah, Salt Lake City, UT 84112-5820, USA
[b] Department of Pharmaceutics and Pharmaceutical Chemistry, University of Utah, Salt Lake City, UT 84112-5820, USA

ARTICLE INFO

Article history:
Received 11 January 2011
Accepted 12 February 2011
Available online 12 March 2011

Keywords:
Fibroblast
Macrophage
Co-culture
Foreign body response
Animal model
Cell culture

ABSTRACT

Many multinucleated giant cells are well-known to form from macrophage origin. Those formed from other cell types are less described, but may be as prevalent in pathological tissue. Giant multinucleated cells derived from secondary and primary fibroblast sources in various cultures with similar characteristics to foreign body giant cells are reported. Secondary-transformed NIH 3T3 fibroblasts rapidly fuse within 24 h in contact co-cultures with RAW 264.7 immortalized macrophages, while 3T3 monocultures, non-contact (transwell) co-cultures, and macrophage-conditioned media-treated 3T3 monocultures all do not fuse. Primary-derived murine fibroblasts also form multinucleated cells, both in the presence or absence of co-cultured macrophages that increase during long-term culture (5–30 days). In contrast to 3T3 fusion, this primary cell phenomenon is not due to fibroblast fusion, but rather to nuclear division without cytokinesis. That these multinucleated fibroblasts can originate via different mechanisms may influence and distinguish their behaviors in conditions under which they may arise, including various in vitro culture assays, and in certain fibroblastic pathologies such as the foreign body response, fibrosis, cancer and aged tissue.

Published by Elsevier Ltd.

1. Introduction

Fibroblasts are the most common cell type in the body and can become altered in various pathologies such as fibrosis, cancer, aging, and the foreign body response (FBR) [1–9]. One phenotypic alteration that is not widely acknowledged, but possible is fibroblast multinucleation [6–8]. Additionally, several other multinucleated giant cells including foreign body giant cells (FBGCs), Langhans' cells, and osteoclasts, all commonly derived from a macrophage cell origin are known [10].

Significantly, FBGCs can form from the fusion of multiple monocytes/macrophages [11] during the FBR, mounted by the host against implanted biomedical materials [12]. The FBR can cause device failure due to degradation by enzymes secreted by macrophages and abnormal collagen production by fibroblasts, resulting in an impeding collagen capsule [9,12,13]. Macrophages and fibroblasts are both primary FBR effector cells [9,12], though unlike macrophages, fibroblasts are not commonly considered to form multinucleated giant cells. However, the mileu surrounding implants is abnormal, can be toxic to cells [14], has been speculated to stimulate tumorigenesis [15,16], and can elicit altered cell phenotypes such as FBGCs [17]. This unusual environment may also prompt fibroblasts to alter their phenotype and form multinucleated giant cells.

Previous studies have identified multinucleated cells in vivo ostensibly of fibroblast origin [6,7], one describing cells appearing as "bizarre, atypical fibroblasts with hyperchromatic and large, pleomorphic nuclei and multinucleated floret-like giant cells" [8]. Several studies describe the presence of multinucleated fibroblasts in vitro [18–21] and in vivo in pathologies such as fibrosis and cancer and in aged tissue [1–8]. However, whether these cells multinucleate in vitro and in vivo via fusion similar to FBGCs [11] or through nuclear division without cytokinesis [18] is unclear.

This study definitively identifies fibroblasts that become multinucleated through both mechanisms—fusion and mitosis without cytokinesis—depending on fibroblast phenotype and culture conditions. Immortalized secondary fibroblasts formed multinucleate cells via fusion with other fibroblasts during contact co-culture with secondary-derived macrophages after 24 h. Primary fibroblasts formed multinucleate cells in mono-culture after becoming senescent and undergoing nuclear division without cytokinesis.

2. Methods and materials

2.1. Cell culture

2.1.1. Secondary cell culture

Macrophage-like cell line RAW 264.7 and fibroblast-like cell line NIH 3T3 were purchased from the American Type Culture Collection (TIB-71 for RAW and CRL-

* Corresponding author. Department of Pharmaceutics and Pharmaceutical Chemistry, University of Utah, Salt Lake City, UT 84112-5820, USA. Tel.: +1 801 581 3715; fax: +1 801 581 3674.
E-mail address: david.grainger@utah.edu (D.W. Grainger).

0142-9612/$ – see front matter Published by Elsevier Ltd.
doi:10.1016/j.biomaterials.2011.02.021

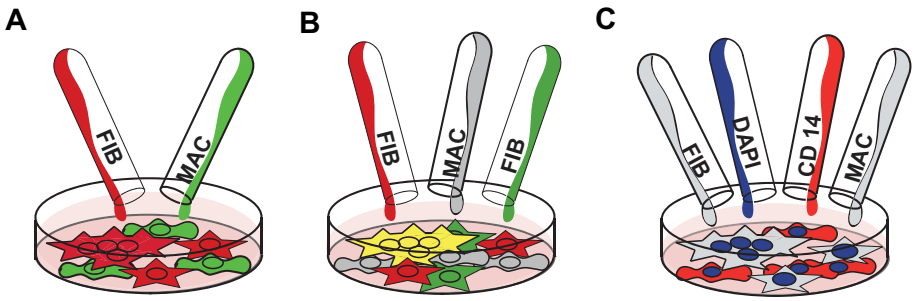

Scheme 1. Multinucleate cell origin was followed by fluorescent cell labeling. A) Macrophages were labeled green and fibroblasts were labeled red prior to co-culture. B) Cell fusion was visualized as a co-localization of two different labeled fibroblast populations (red and green) with macrophages receiving no dye (grey). Cell co-localization of red and green dyes appears yellow. C) After 24 h, macrophage and fibroblast cultures were labeled with DAPI (blue) and macrophage-specific anti-CD14(red)to identify possible macrophage contamination within the plated fibroblast population. (For interpretation of the references to colour in this figure legend, the reader is referred to the web version of this article).

1658 for 3T3 ATCC, Manassas, VA) and cultured in 96-well tissue culture treated polystyrene plates (BD Falcon, San Jose, CA) unless otherwise specified, during contact co-culture experiments at 37 °C with 5% supplemental CO_2 for 24–72 h. Fibroblasts were used at passages 6–30 and macrophages were used below passage 10. RAW cells were passaged by scraping with a rubber policeman. 3T3 cells were passaged using TripLE (Invitrogen, Carlsbad, CA). For optimal cell fusion, 2×10^4 fibroblasts and 1×10^4 macrophages were plated into co-culture wells. This same number of fibroblasts and macrophages were also plated into control wells for comparison. Cells were always cultured in complete media (Dulbecco's modified eagle medium (DMEM) with 10% fetal bovine serum, and 1% antibiotic/antimycotic (Invitrogen, Carlsbad, CA). Secondary NIH 3T3 fibroblasts were cultured for 24–72 h under four different conditions: 1) in direct co-culture contact with secondary RAW 264.7 macrophages, 2) co-culture but separated from RAW cells by a Transwell® microporous insert (RAWs in insert and 3T3s in well beneath), 3) in RAW-conditioned complete media, and 4) alone, devoid of macrophage signaling [22]. Mono-cultured RAW cells in complete media served as a control. Non-contact co-cultures utilized 3 μm porosity plasma-treated polycarbonate Transwell® Permeable Supports (Corning, Corning, NY) in 12-well tissue culture treated polystyrene plates (BD Falcon, San Jose, CA). Cell numbers were scaled linearly with respect to surface area from the 96-well culture dishes to accommodate larger sized wells. In the same 12-well plates all 4 culture conditions i.e., mono-culture, conditioned media, contact co-culture, and Transwell® co-culture—were also employed. Macrophage-conditioned media was collected after 24 h of exposure to RAW cells (density = 1×10^5 cells/well) and placed over mono-cultured fibroblasts in 12-well plates. New conditioned media was collected from the original RAW culture well every day for 3 days to be placed over the conditioned media-treated fibroblasts.

2.1.2. Murine primary cell sourcing

Specific-pathogen-free, 2–3 month-old male C57BL/6 mice were purchased from Jackson Laboratory (Bar Harbor, ME). Animals were kept in the University of Utah animal facility, and provided water, mouse chow, bedding, and modes of enrichment ad libitum throughout this study. Animals were euthanized via CO_2.

2.1.3. Primary macrophage cell culture

Bone marrow cells were collected from the femurs and tibias of 2–3 month-old male C57BL/6 mice and differentiated into bone marrow macrophages (BMMΦs) using a previously described method [23,24]. On day 7, the cells were removed from surfaces by incubation in Ca/Mg-free phosphate-buffered saline solution and scraping with a rubber policeman. Harvested cells were spun at 500 rcf for 5 min to form a pellet and then resuspended in DMEM with 10% heat-inactivated fetal bovine serum, 10% L929-conditioned media, 1% antibiotic/antimycotic, 1% MEM nonessential amino acids, 1% HEPES, and 1% sodium pyruvate. Also in 96-well plates, 1×10^4 primary macrophages per well were seeded alone or in contact co-culture with primary fibroblasts. Alternatively, primary monocyte-like cells were obtained by using the bone marrow cells on day 1, 2, or 4, before complete macrophage differentiation was expected [25–27]. Pure monocytes were obtained using the EasySep® Magnetic Mouse Monocyte Enrichment Kit (Stemcell Technologies Inc., Vancouver, BC) from bone marrow cells according to the manufacturer's instructions, typically producing monocyte purity of 80%–93%.

2.1.4. Primary fibroblast cell culture

Primary fibroblasts were obtained post-mortem from ear dermal tissue of 2–3 month-old freshly sacrificed male C57BL/6 mice. Ear tissue was clipped at the base of the ear and soaked in 70% ethanol for 5 min and then rinsed in sterile phosphate-buffered saline (BD Falcon, San Jose, CA). Tissues were placed in a Petri dish and diced using a sterile razor, placed into 2 ml of 5 mg/ml collagenase solution in DMEM and incubated for 2 h in a 37 °C water bath with agitation [25–27] then filtered though a 70 μm cell filter (BD, San Jose, CA). An equal portion of complete media was added to the filtrate and spun at 500 rcf for 5 min to create a cell pellet. Supernatant was aspirated off and the cell pellet was resuspended in primary cell media (DMEM with 10% fetal bovine serum, 1% antibiotic/antimycotic, and 1% MEM nonessential amino acids (Invitrogen, Carlsbad, CA), placed in T75 cell culture flasks (BD Falcon, San Jose, CA), and incubated at 37 °C with 5% supplemental CO_2. Cells required 3–7 days to become confluent and were subsequently passaged and used in further experiments. Cells were passaged by incubation with TripleE (Invitrogen, Carlsbad, CA). Primary fibroblasts (1×10^4 cells per well in 96-well plates, characterized by anti-CD14 and anti-vimentin labeling, as well as Oil Red O post-differentiation, vide infra) were cultured alone or in physical contact with primary macrophages for up to 30 days. On different occasions, primary ear-derived fibroblasts were also co-cultured with either secondary RAW 264.7 cells, primary monocyte-like cells or pure monocytes, to determine if more monocytic cells could prompt cell fusion.

2.2. Cell labeling

2.2.1. H&E

A hematoxylin and eosin (H&E) stain (Fisher Scientific, Kalamazoo, MI) was employed according to manufacturer's instructions to stain for nuclei and cytoplasm respectively.

2.2.2. Fluorescent cell labeling

For fixed fluorescence labeling, cells were fixed in 4% paraformaldehyde (Sigma–Aldrich, St. Louis, MO) for 10 min at room temperature and labeled with rhodamine-phalloidin and counterstained with 4,6-diamidino-2-phenylindole (DAPI) (Molecular Probes, Eugene, OR) according to manufacturer's instructions. Live cell in situ fluorescent detection used either a green Vybrant® CFDA SE Cell Tracer Kit or a red Cell Trace Far Red DDAO-SE long-lived intracellular dye (Invitrogen, Carlsbad, CA) according to manufacturer's instructions. These dyes label 100% of cells (data not shown) and have been shown not to transfer to neighboring cells [28]. Macrophages were labeled with the green live dye, while fibroblasts were labeled with the red live dye prior to seeding in both mono- and co-cultures in order to distinguish fibroblast and macrophage populations during co-culture and determine cellular origin of the resulting multinucleated cells (Scheme 1A). These same dyes and experimental procedure were used to determine FBGC fusion [11]. Analogously two fibroblast populations were labeled with either red or green live cell dye prior to seeding in mono- and co-cultures to determine fibroblast fusion by dye co-localization (Scheme 1B). These same procedures were employed for both secondary- and primary-derived fibroblast cultures.

2.2.3. Antibody labeling

A phycoerythrin-conjugated macrophage marker, anti-CD14 (clone Sa2-8, IgG2a, diluted 1:100, eBioscience, San Diego, CA) [29] was added to control RAW cells, 3T3 cells, and co-cultures of RAW and 3T3 cells to determine possible inadvertent macrophage contamination in fibroblast cultures and to confirm multinucleate cell origins (Scheme 1C). This marker was also added to primary-derived macrophages and fibroblasts to determine multinucleate cell origin. Cyanine3-tagged fibroblast marker anti-vimentin [30] (clone V9, IgG1, diluted 1:100, Sigma, St. Louis, MO) was added to primary fibroblasts to assert phenotype and multinucleate cell origin.

2.2.4. Senescence

Both primary and secondary macrophages and fibroblasts and primary adipose-derived stem cells (ASCs, isolation and characterization described in Supplementary Information) were stained with a senescence-labeling kit staining for beta-galactosidase [31] (Cell Signaling Technology, Danvers, MA) according to manufacturer's instructions.

2.2.5. Cell apoptosis

Primary fibroblasts were cultured for 3 days prior to apoptosis testing. Positive control fibroblasts were incubated with 1 mg/ml bupivicaine (Hospira, Lake Forest, IL) for 2 h at 37 °C. Primary fibroblasts were labeled with Poly Caspases FLICA™ in vitro Apoptosis Detection Kit (Immunochemistry Technologies, Bloomington, MN) according to manufacturer's instructions.

2.2.6. Mycoplasma assay

Mycoplasma testing was performed using DAPI labeling, according to standard protocols [32–34].

2.2.7. TRAP assay

Secondary fibroblast-derived multinucleated cells were stained using a tartrate resistant acid phosphatase (TRAP) assay (Sigma–Aldrich, St. Louis, MO), specific for osteoclasts [35], according to manufacturer's instructions.

2.3. Imaging

Fluorescent, brightfield, and colored microscopy images of cells in culture were acquired using a Nikon Eclipse TE2000-U microscope equipped with fluorescent optics, CCD camera, and Metamorph and Q Capture Pro software. Confocal images were captured using an FV1000 IX81 Olympus confocal microscope. Fluorescence and confocal images were used to identify dye co-localization within cells. At least 9 replicates from 3 separate cell experiments were imaged to determine representative image samples of all experiments in this study. Experiments producing multinucleated fibroblasts were repeated at least 6 times.

2.4. Video

Confocal time-lapse video was acquired using a Nikon A1 Confocal microscope over 24–48 h. In videos taken from 0 to 24 h, cultured cells did not readily adhere to the surface of the plate, most likely due to microscope micromotion (results not shown). Four 20× fields were digitally stitched together into a mosaic for the video included in this study.

2.5. Statistics

Numbers of giant cells per frame, percent nuclei fused, and percent multinucleated cells between short-term co-cultures and long-term monocultures compared to short-term mono-cultured fibroblasts were evaluated using a student's t-test with significance defined as $p < 0.05$. A Single-Factor ANOVA was utilized to determine significance between groups of samples. A post-hoc student's t-test was used to determine statistically significant differences between samples ($p < 0.05$). Cell counts were taken from 15× objective images. Three frames per replicate were counted and the mean was used for analysis. At least 3 independent replicates were counted with independent replicates defined as different experiments using different mice for primary cells, and different passage numbers for secondary cells.

3. Results

3.1. Mycoplasma detection

All cell cultures, both those derived from primary and secondary sources, stained negative for mycoplasma contamination using DAPI fluorescence (data not shown).

3.2. Secondary-derived multinucleate cells

Fig. 1 shows multinucleated cells appearing during contact co-culture with secondary RAW macrophages (Row 5). RAW and 3T3 cells cultured alone (Rows 1&2, respectively) and 3T3s in the presence of RAW-conditioned media (Row 3) do not form multinucleated cells. In order to test for signaling effects of short-lived excreted cytokines, 3T3s were co-cultured with RAWs separated by Transwell® inserts (Row 4), where the permeable polyester membrane prevents physical contact of each cell type, but permits mass transport of soluble culture components. No formation of multinucleated fibroblasts occurred in this co-culture system.

Multinucleated cells have been reported in vivo to have "increased nuclear-cytoplasmic ratio, pale pink scant cytoplasm, and indistinct cell boundaries (with rosette arrangement of hyperchromatic nuclei)" [8] similar to those seen in this study (Fig. 1, Row 5). This can be seen both with live cells (Fig. 1, column 1) and fixed cells stained with H&E (Fig. 1, Columns 2&3). 3T3 cells begin multinucleation immediately upon adherence to tissue culture surfaces in the presence of RAWs (data not shown) and is readily apparent at 24 h (Fig. 2).

3.3. Multinucleate cell origin

Fig. 3 shows RAW cells (Fig. 3A) labeled with a cytoplasmic fluorescent green dye prior to co-culture with fibroblasts, and 3T3s (Fig. 3B) labeled with a cytoplasmic fluorescent red dye prior to co-culture with macrophages. Resulting multinucleated cells (Fig. 3C) exhibited red fluorescence, with no detectable green fluorescence. Additionally, as proof of negligible macrophage contamination in the fibroblast population, anti-CD14 added to the mixed population readily bound all mono-cultured RAW cells (Fig. 3D) but not mono-cultured fibroblasts (Fig. 3E). In the co-culture system, no multinucleated cells were fluorescently labeled by anti-CD14 (Fig. 3F). Other external macrophage markers analyzed, including MHC-II, CD40, CD18, CD11b, and F4/80, were analyzed (data not shown). However, anti-CD14 provided the most reliable and prominent labeling and was thus presented in this study.

3.4. Secondary fibroblast fusion

Separate 3T3 fibroblasts cultures containing either green or red cytoplasmic dyes were added simultaneously to non-labeled RAW macrophage cultures (Fig. 3 G–L). Fig. 3 I&L shows that resulting multinucleated cells exhibit both red and green nuclei with yellow (i.e. both red and green co-localization) cell bodies. A video of these cells fusing between 24 and 48 h in culture is available online in Supplementary Data. This video also shows these cells to be highly motile, traveling hundreds of microns over the course of 24 h Fig. 4 shows still frames from that video and the corresponding approximate cell trajectories of one tracked multinucleated cell.

Multinucleated cells derived from 3T3 fibroblasts exhibit similar qualities to FBGCs, with enlarged cytoplasms, multiple cellular adhesions, and multiple centric nuclei [36]. However, they do not possess punctate podosomal actin [17,37] but do possess prominent stress fibers, features consistent with fibroblasts [38] but contrary to FBGCs and osteoclasts (Fig. 5A). Furthermore, secondary-derived multinucleated cells in this study did not stain positive for macrophage marker CD14 (Fig. 3 D–F) or osteoclast-marker TRAP (Supplementary Fig. 1).

Interestingly after passages greater than 20, 3T3s cultured on the same surface for extended periods of time (>5 days) began forming multinucleated cells even in the absence of macrophages (Fig. 5 C–D). The spontaneously formed multinucleated cells frequently had nuclei that appeared polymorphonuclear.

3.5. Primary-derived multinucleate cells

Primary murine ear dermal fibroblast isolations were confirmed to be dominantly fibroblastic using several cell phenotype assays (see Supplementary Information and Supplementary Fig. 4).

Fig. 6 shows that primary fibroblasts cultured in the presence of primary bone marrow-derived macrophages (Fig. 6 A–C) or secondary-derived RAW cells (Fig. 6 D–F) also become multinucleated, while the macrophages alone do not over the same culture time period. No noticeable differences between fibroblast fusion rates in the presence of either primary macrophages or monocytes were seen (data not shown). Primary-derived multinucleated cells are not macrophage-like. Primary macrophages containing cytoplasmic green dye cultured with primary fibroblasts containing cytoplasmic red dye for 24 h yield multinucleated cells with only red fluorescence (Fig. 6 G–I). Additionally, while both primary

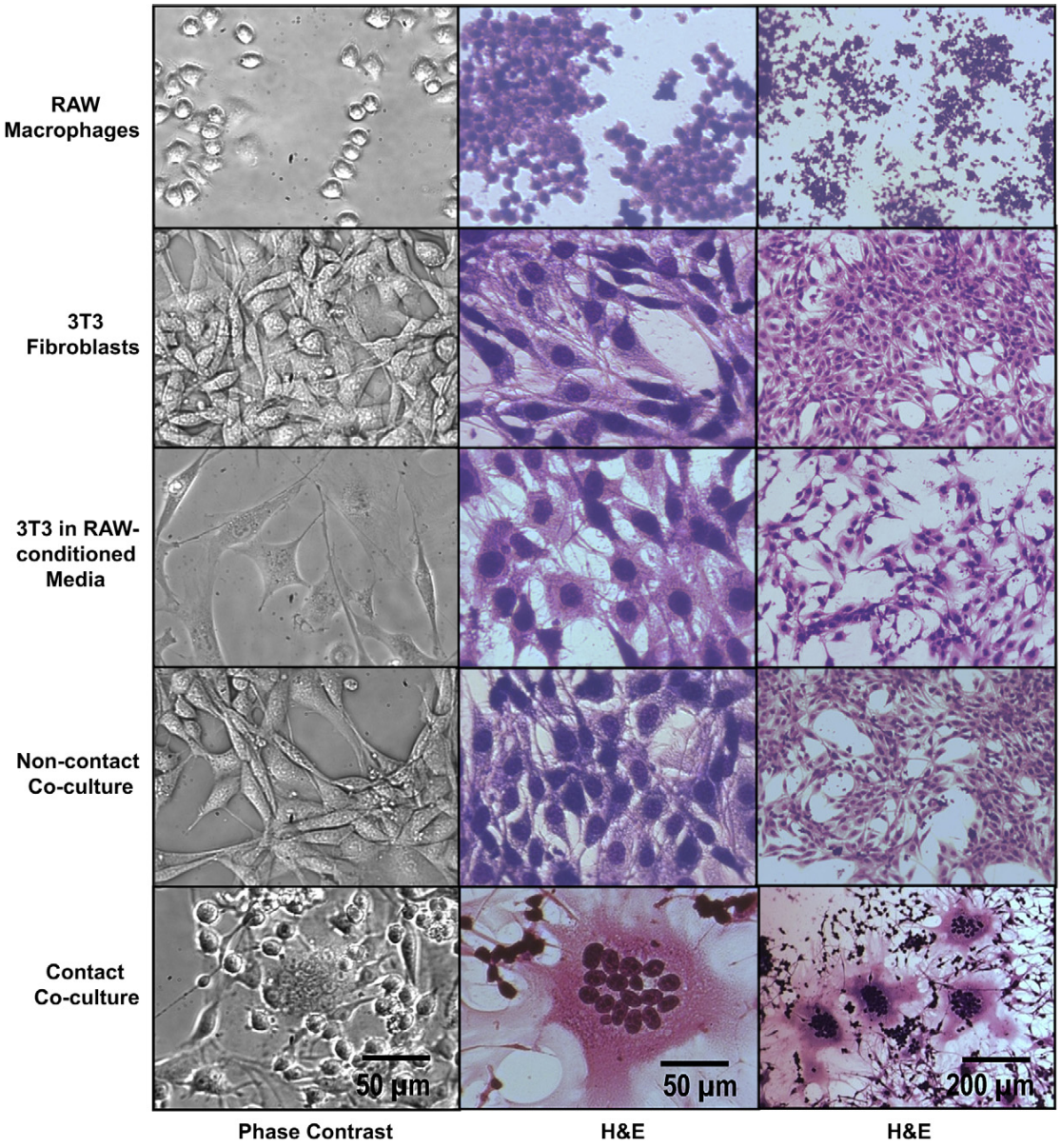

Fig. 1. Phase contrast and hematoxilin and eosin (H&E)-stained cell images. Cultured 3T3 fibroblasts form multinucleated cells in contact co-culture with RAW macrophages (bottom row), but not during mono-culture (top 2 rows), treatment with conditioned media (3rd row) or non-contact co-culture (4th row). Images shown after 3 days of culture in complete media.

macrophages and fibroblasts stained positive for CD14, upregulated in macrophages [29,39], primary BMMΦs stained strongly positive (Fig. 6J), while fibroblasts exhibited only very dim fluorescence (Fig. 6K). Differentiation between the two cell types is clear. Additionally, fibroblasts stained positive for the fibroblast-specific marker, vimentin, including cells with multiple nuclei (Fig. 6 L&O).

Fig. 6 also shows primary multinucleated cells in monocultures of fibroblasts containing no added macrophages. No significant differences are noted between fibroblasts cultured alone or during co-culture both at short time points (<3 days) (Fig. 2). Primary multinucleated cells do not appear to form via cell–cell fusion. Fig. 6 M&N shows two populations of primary fibroblasts labeled green or red prior to co-culture together. Resulting multinucleated cells were either green or red, but not both, i.e., yellow, demonstrating that primary multinucleated cells do not appear to form via cell–cell fusion.

3.6. Primary multinucleate cell morphology

Multinucleated cells from fibroblasts can be seen as early as 1 day post-culture, though the frequency of multinucleated cells and number of nuclei per cells increases at days 5–30 as seen in Figs. 2 and 7. Nonetheless, even after extended culture periods (5–30 days), the frequency of multinucleated cells from primary fibroblasts was far less than those from secondary-derived fibroblasts during co-culture at short time periods (24 h, Fig. 2).

Over time, multinucleated cells from primary-derived fibroblasts change their morphology, developing larger, more-extended

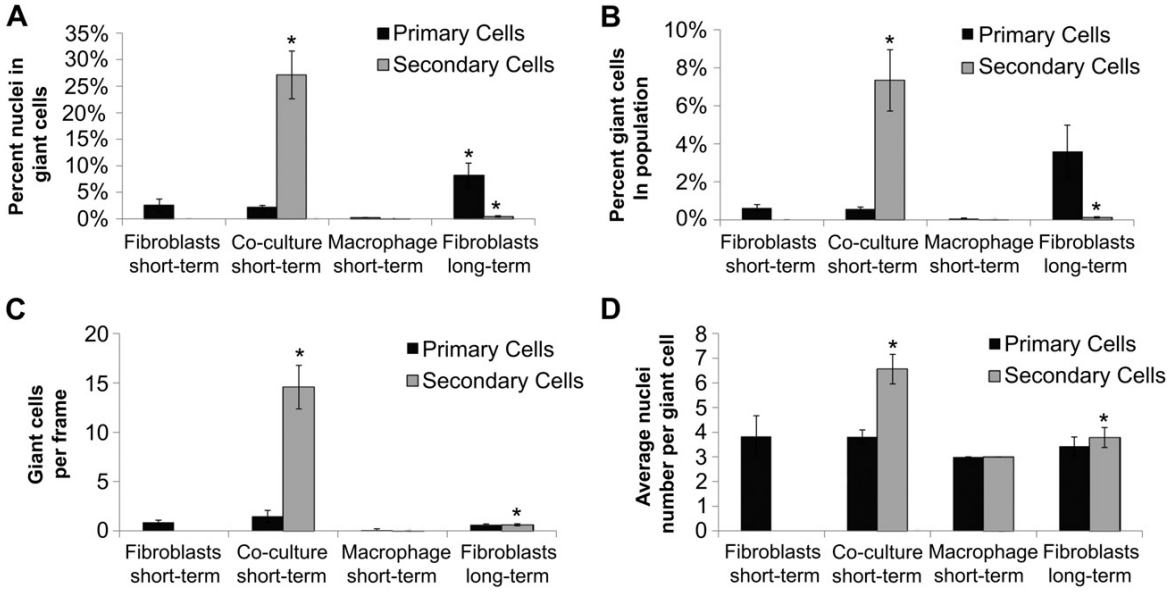

Fig. 2. Multinucleate cell characterization. A) Percent nuclei found in multinucleate giant cells, B) percent multinucleate giant cells found in cell population, C) number of multinucleate giant cells per frame, and D) average number of nuclei per giant cell for primary and secondary-derived fibroblasts and macrophages alone (short-term, 1–3 days, and long-term, 30 days) and in co-culture (short-term, 1–3 days) without the addition of exogenous cytokines. So few giant cells per frame in the long-term fibroblast culture condition is due to the increase in size of those fibroblasts compared to those cultured for short-term, consequently decreasing the overall number of cells per frame (see Fig. 7). Data represent the mean ± SEM from 3 independent replicates. Significance ($p < 0.05$) was analyzed between primary and secondary fibroblast short-term monocultures and short-term co-cultures and between primary and secondary fibroblast short-term monocultures and long-term monocultures. Images were taken with a 15× objective and yielded a frame size of 260, 891 μm^2.

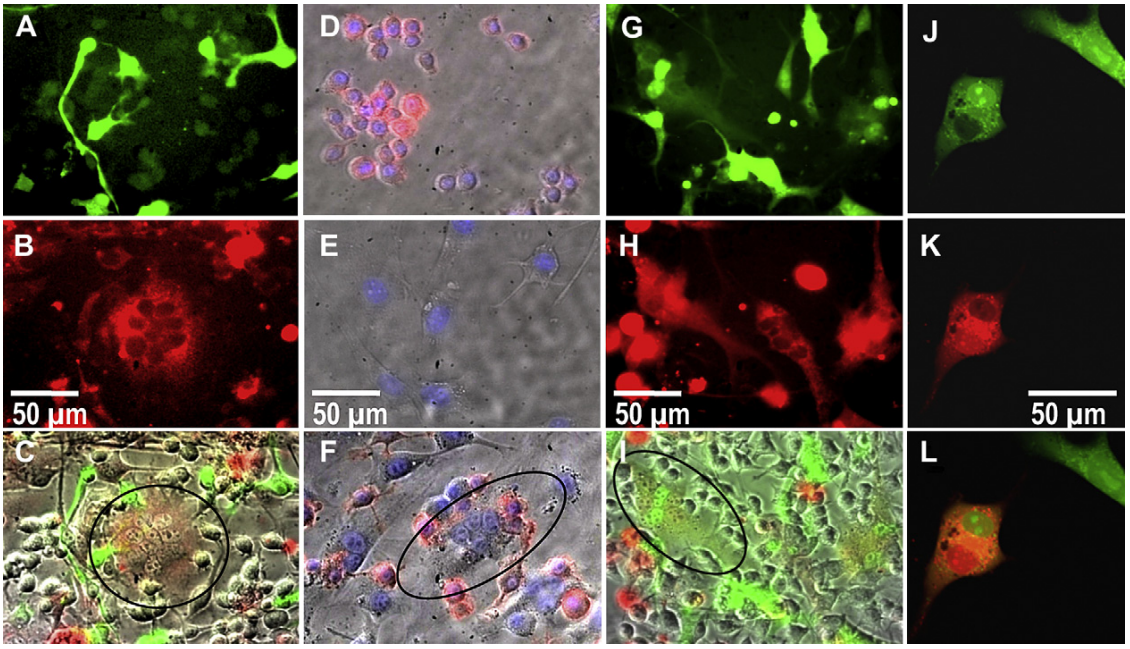

Fig. 3. Fluorescence images showing A) RAW macrophages labeled green, B) 3T3 fibroblasts labeled red, and C) an overlay of brightfield and red and green channels showing a red (circled), and therefore fibroblastic, multinucleated cell. Fluorescence images showing D) macrophages and E) fibroblasts incubated with DAPI (blue) and also fluorescently labeled anti-CD14 (red), revealing F) fibroblasts that stain negative for CD14, are multinucleated (circled), and are therefore not macrophages. Fluorescent G–I) and confocal J-K) images revealing co-localization of a red-labeled population of fibroblasts fused with a green-labeled population of fibroblasts in the presence of non-labeled macrophages, where G and J are the green channel, H and K are the red channel, and I and L are overlays of I) brightfield and red and green fluorescent channels and L) red and green channels (co-localization experiments with 3 replicates each were repeated 3 times). Images shown after 24 h of culture. (For interpretation of the references to colour in this figure legend, the reader is referred to the web version of this article).

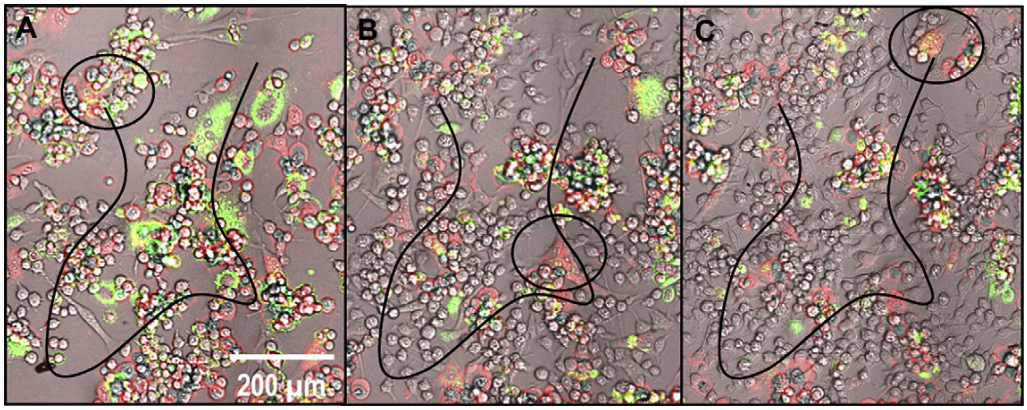

Fig. 4. Frames A–C show the approximate motility trajectory (black line) of a secondary-derived multinucleated fibroblast (circled) traveling hundreds of microns over the course of 24 h (from 24 to 28 h). This time-lapse image series also appears to show the fibroblast beginning as only a few red-labeled cells and ending with several more nuclei including those from green-labeled fibroblasts (full video available online in supplementary data).

cell bodies and even developing what appears to be polymorphonuclei (Fig. 5 E&F). Cultured adipose-derived stem cells (ASCs) (Supplementary Fig. 2, description of ASC isolation and identification are found in Supplementary Information) and cardiomyoblasts (data not shown) were also observed to form multinucleate cells under identical culture conditions, occasionally possessing polymorphonuclei as well. Interestingly, primary-derived multinucleated cells possessed prominent stress fibers but lacked punctate podosomal actin (Fig. 5B), consistent with fibroblasts [38], but not FBGCs or osteoclasts [17,37].

3.7. Primary multinucleate cell senescence

A senescence assay [31] was employed for primary fibroblasts on Days 1, 2, 3, 10, and 20. Fibroblasts stained positive for senescence first on Days 10 and 20 (Fig. 8, Panel A). ASCs, also seen to create multinucleate cells, were also tested for senescence during the same time frame and began staining positive for senescence as early as Day 1, though not prevalently until Day 3 onward (Supplementary Fig. 3). Secondary-derived multinucleate cells were also tested with this assay and found to exhibit no detectable

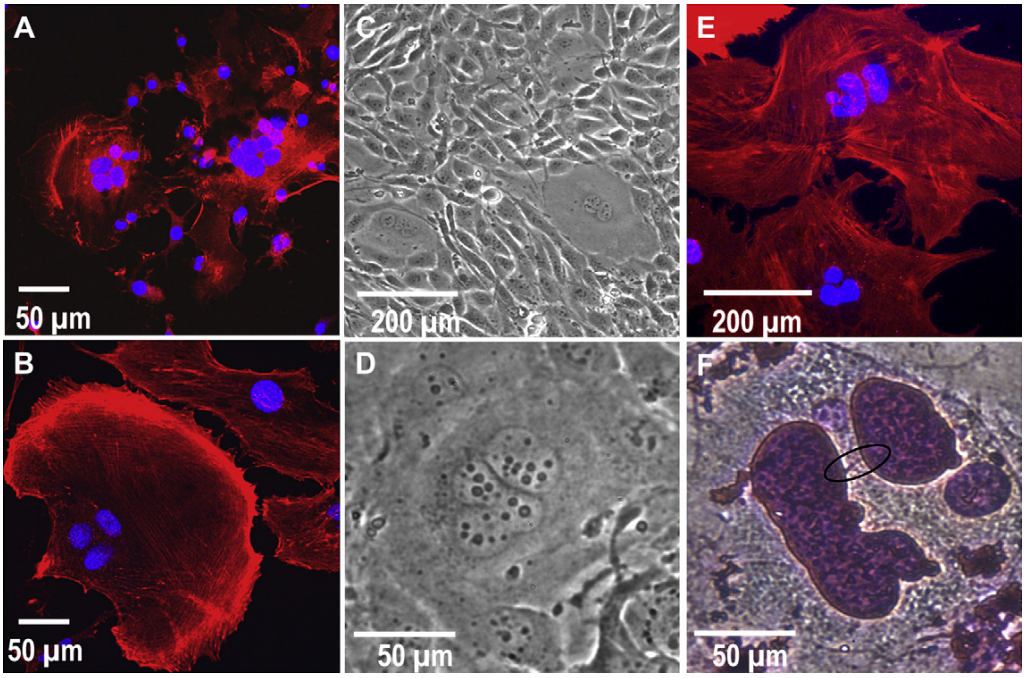

Fig. 5. Actin (red) and nuclei (blue) labeling for A) secondary-derived multinucleate fibroblasts and B) primary-derived multinucleate fibroblasts. These images show prominent stress fibers (more prevalent in primary versus secondary multinucleate cells) and the absence of podosomes surrounding single and multinucleate cells, features contrary to those seen in macrophage-derived FBGCs. Secondary multinucleate cells are shown after 1 day and primary cells are shown after 30 days of culture. C&D) Phase contrast images (C 10× and D 40×) of secondary fibroblasts which spontaneously formed polymorphonuclear multinucleated cells after >20 passages and culture for >5 days. E&F) Primary fibroblasts contain several pleomorphic and budding nuclei seen in E) a confocal image of DAPI (blue) and phalloidin (red) labeled cells and F) an H&E-stained cell (purple line, potentially chromatin, circled in black),shown after 30 days in culture. (For interpretation of the references to colour in this figure legend, the reader is referred to the web version of this article).

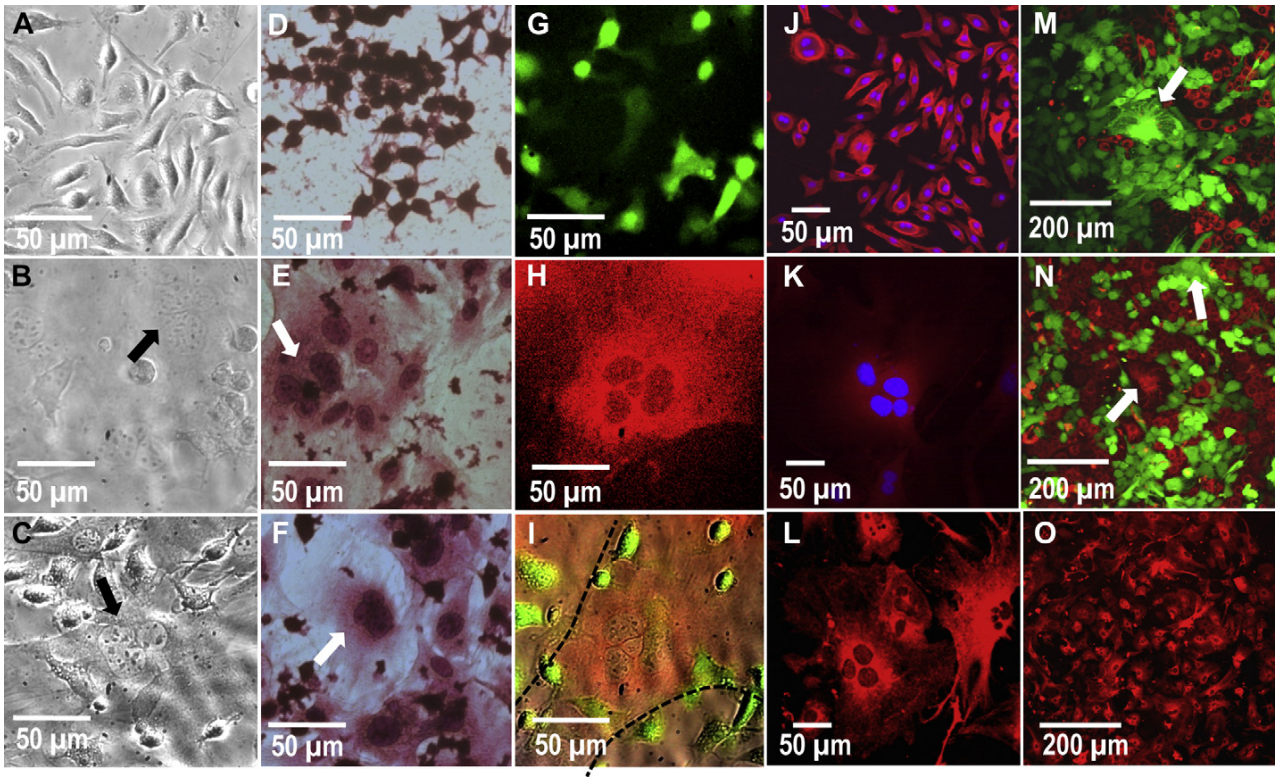

Fig. 6. Phase contrast images of A) primary-derived BMMΦs alone, B) primary fibroblasts alone and C) contact co-culture of BMMΦs and fibroblasts. Note multinucleate cells in both the mono-culture fibroblasts and contact co-cultures (arrows). H&E-stained images showing D) secondary-derived RAWs cultured alone, E) ear fibroblast cultured alone and F) contact co-culture of RAW cells and primary fibroblasts. Multinucleate cells can be seen in fibroblast mono-culture as well as contact co-culture with RAW cells (arrows). G–I) Fluorescent images of contact co-cultured primary macrophages (green channel, G), fibroblasts (Red channel, H) and an overlay of red, green and brightfield channels (I). These images show that the multinucleated cell is red and therefore of fibroblastic origin (H and delineated by dotted lines in I). Confocal images of primary-derived J) BMMΦs and K) fibroblasts labeled with DAPI (blue) and macrophage marker CD14 (red), revealing a strong CD14 stain in macrophages but not fibroblasts. L and O) show 40× and 20× confocal images, respectively, of primary-derived fibroblasts labeled with fibroblast marker vimentin (red), showing that the majority of cells in this culture stain positive for fibroblasts, including multinucleate cells. M and N) Confocal images of mono-cultured primary fibroblasts pre-labeled with red or green long-lived intracellular fluorescence prior to culture, where the multinucleated cells (arrows) found were either green or red, but not both (representative images from 3 separate experiments and a total of 9 replicates). This lack of co-localization indicates an absence of fusion to produce cell multinucleation. Images are shown after 3 days of culture. (For interpretation of the references to colour in this figure legend, the reader is referred to the web version of this article).

positive senescence in either 3T3s or RAWs during either co-culture or mono-culture (data not shown). Significantly, all multinucleate cells regardless of the culture time period stained positive for senescence and negative for apoptosis (Fig. 8, Panel B).

4. Discussion

The majority of multinucleated cells are believed to originate from macrophages [10]. However fibroblasts, the most prevalent cell type in the body, are also capable of forming multinucleate cells both in vitro [18] and in vivo [1–8]. Though some studies claim they form via fusion [4,7] and others mitosis without cytokinesis [18], this study found that both of these mechanisms can create multinucleated fibroblasts, depending on cell sourcing and culture conditions.

Secondary fibroblast-derived multinucleated cells formed when 3T3 fibroblasts were in direct physical contact with secondary-derived RAW macrophages after 24 h (Fig. 1, Row 5). This was not only seen during co-culture between RAW macrophages and 3T3 fibroblasts but also in identical co-cultures between RAW and L929 fibroblast cells (data not shown). Importantly, cell multinucleation in secondary cultures did *not* occur 1) during 3T3 fibroblast mono-culture in either complete or RAW macrophage-conditioned complete media, or in non-contact Transwell® macrophage co-cultures with soluble media-phase diffusive exchange between macrophages and fibroblasts. Consistent with a previous study, contact co-cultures of RAW 264.7 macrophages and NIH 3T3 fibroblasts formed multinucleate cells while those with 3T3 fibroblasts and primary bone-derived macrophages did not [22]. Additionally, cell multinucleation in secondary cultures did not occur when either cell type was allowed to adhere prior to adding the other cell type (data not shown). Lack of observed cell fusion in secondary cell cultures of both macrophage-conditioned media and Transwell® co-cultures indicates that cell fusion requires 3T3 fibroblasts in physical contact with RAW macrophages rather than just soluble signal exchange [22]. Necessity for physical cell–cell contact may suggest involvement of external cell membrane receptors such as inter-cellular adhesion molecule (ICAM) 1 on observed secondary cell multinucleation. ICAM is deemed responsible for many interactions between macrophages and fibroblasts [40], and significantly, fusion between macrophages to form FBGCs [41]. In this study, cultured RAW macrophages were very motile, making contact with many cells over a 24-h period. Surprisingly, multinucleated cells derived from 3T3 fibroblasts were also found to be highly motile, traveling hundreds of microns during the same 24-h period (Fig. 4 and video in Supplementary Data). Cell mobility in these secondary-derived cultures, enabling facile macrophage-fibroblast and fibroblast–fibroblast interactions,

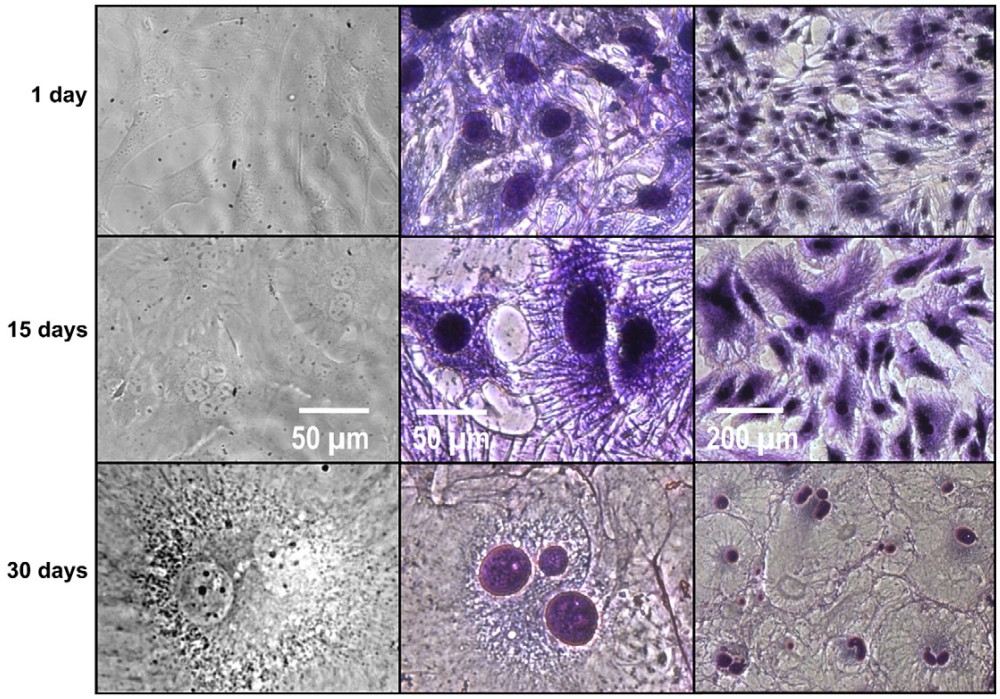

Fig. 7. Phase contrast (column 1) and H&E-stained (columns 2 &3) cell images show changes in primary fibroblast morphology over time. Columns 1 and 2 are at a 40× magnification and column 3 is at a 10× magnification. Day 1 cells possessed spindle and stellate morphologies. By Day 15, cells began to develop larger cell bodies and nuclei. By day 30, the cells possessed very large cell bodies, with some containing multiple and pleomorphic nuclei.

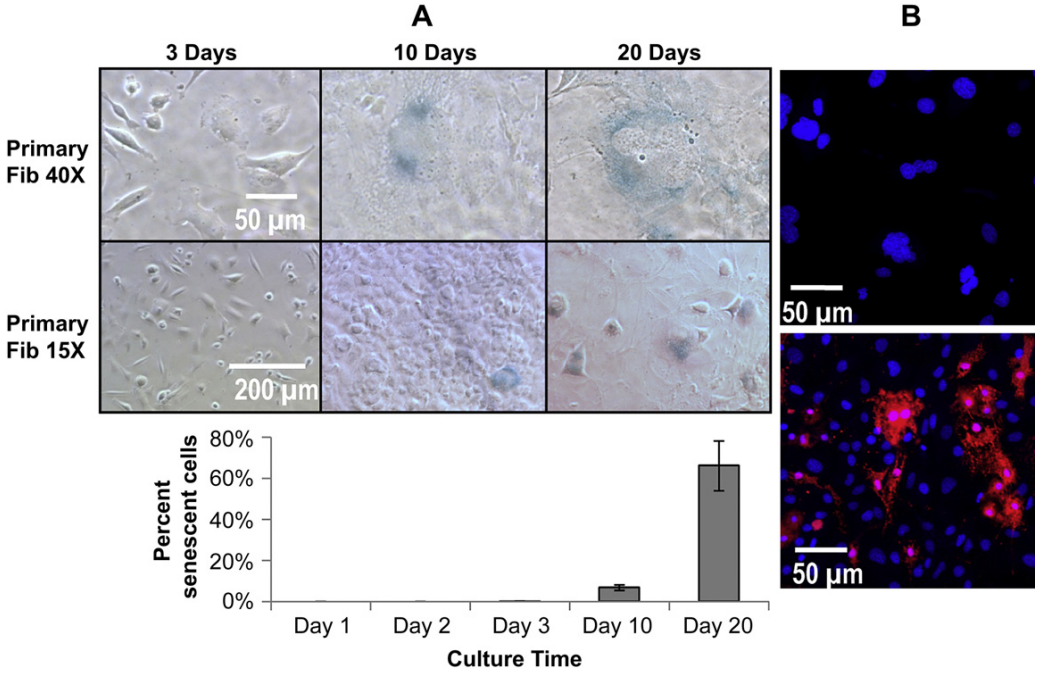

Fig. 8. Panel A) Senescence staining (blue) in primary fibroblasts after 3, 10, and 20 days expressed qualitatively as representative images and quantitatively in graph below. These data show that at longer time points near day 10, senescence becomes prevalent in primary fibroblasts. Data are represented as the mean ± SEM from 3 independent replicates. Importantly, all multinucleated fibroblasts regardless of time point, stained positive for senescence. Panel B) Confocal images showing DAPI (blue) and apoptosis staining (red) in primary fibroblasts (top image) left untreated and (bottom image) treated with bupivicaine as a positive control. Multinucleate fibroblastic cells even with highly polymorphic nuclei did not stain positive for apoptosis. Images shown after 3 days in culture. (For interpretation of the references to colour in this figure legend, the reader is referred to the web version of this article).

increases the likelihood of physical stimulation of 3T3 fibroblasts by RAW macrophages and subsequent fusion with other 3T3 fibroblasts (Fig. 3 I&L).

Multinucleated cells from RAW macrophage contact co-cultures with 3T3 fibroblasts arise from the fibroblast, not macrophage, population. 3T3 fibroblast cultures do not contain contaminating macrophages: CD14 antibodies specifically bound RAW macrophages but not 3T3 fibroblasts and multinucleated cells. Assayed for TRAP, a prominent marker for multinucleate osteoclasts [35], cultured RAW macrophages, 3T3 fibroblasts, and multinucleate cells all stained negative (supplementary data), indicating that these cells were not osteoclastic.

In secondary 3T3 cell contact co-cultures with RAW macrophages, multinucleation is shown to result from fusion of two or more fibroblasts. Two separate populations of secondary-derived fibroblasts labeled with either a red or green cytoplasmic dye prior to plating with non-labeled secondary-derived macrophages, an experiment analogous to that used to determine macrophage fusion to FBGCs [11], produced multinucleated cells with both red and green nuclei and yellow (red plus green) cell bodies. Co-localization of both red and green dyes was seen with both fluorescent and laser scanning confocal microscopy (Fig. 3 I&L, respectively). Red and green coloration occupied the same volume, shape, and focal plane (optical cross-section was 0.45 μm, less than a cell thickness), confirming cytoplasm fusion (Fig. 3L). All secondary multinucleated cells displayed this colour co-localization, with multinucleate cell density being approximately 15 giant cells per 15× frame (Fig. 2). A 24 h time-lapse video (supplementary data) shows a red 3T3 fibroblast traveling approximately 1 mm and apparently fusing with several green and red 3T3 fibroblasts to accumulate approximately 5 nuclei that, conjoined together, move within the same membrane containing both red and green fluorescence.

Primary ear-derived dermal fibroblasts formed multinucleated cells in physical contact with primary bone marrow-derived macrophages (Fig. 6 A–C), secondary RAW macrophages (Fig. 6 D–F) and primary bone marrow monocyte-like cells and monocytes (data not shown) in 24–72 h. Primary and secondary macrophages formed extremely rare or no multinucleated cells during the same culture time under these conditions (Fig. 2). Primary fibroblasts loaded with a red cytoplasmic dye and primary macrophages containing a green cytoplasmic dye produce red multinucleated cells (Fig. 6 G–I) (i.e., from the fibroblast population, not from macrophages). Interestingly, primary fibroblasts also form multinucleated cells in mono-culture (complete absence of macrophages, shown by very dim CD14 labeling (Fig. 6K) over the same time frame, increasing in their density over 30 culture days (Fig. 2). Though primary fibroblasts are commonly cultured, multinucleated fibroblasts are not commonly reported, likely due to the fact that any rarely occurring multinucleated cells may be dismissed as contaminating cells or phenotypic anomalies. Fig. 6 M&N shows mono-cultured primary fibroblasts loaded with either red or green cytoplasmic dye prior to seeding. In these representative images, multinucleated cells display only one colour (either red or green) supporting a non-fusion mechanism to create multinucleated cells in primary fibroblast cultures. Similar multinucleated cells are also observed in primary ASCs (Supplementary Fig. 2) and cardiomyoblasts (data not shown).

This observed multinucleation event that retains colour fidelity in primary fibroblasts is consistent with nuclear division without cytokinesis. This phenomenon has been described previously [18–21], and the dye co-localization studies performed here further substantiate this phenomenon. This asserted nuclear division in the absence of cytokinesis is also supported by Supplementary Fig. 5 E&F, showing the presence of globular or pleomorphic nuclei sharing a membrane with one or more nuclei. *In vivo* presence of multinucleated giant fibroblasts with pleomorphic nuclei has also been reported in a fibroma [8]. Polymorphonuclei exhibiting only 1 nucleus but with multiple lobes are also possible. Fig. 5F shows a thread-like feature (circled) that may represent a strand of chromatin often seen connecting lobes of a polymorphonucleus [42]. This has also been seen previously in fibroblasts cultured in vitro, displaying tumor-like phenotypes [43]. After high passage numbers (>20), and extended culture beyond 5 days, secondary 3T3 fibroblasts in mono-culture also occasionally express multiple nuclei and develop amorphic nuclei similar to those seen in the mono-cultured primary cells (Fig. 5C&D). That this type of multinucleation is more apparent in primary fibroblasts after 1 week in mono-culture and in secondary fibroblasts at high passage numbers in mono-culture, both in cells that appear to be non-dividing, is likely due to aging. Previous work found multinucleated fibroblasts with pleomorphic nuclei in 17% of fibroblasts in periodontal ligaments of aged mice (20 months), while no such cells were seen in young mice (5 weeks) [7].

Aging has been shown to manifest as replicative senescence [44], and is suggested to result from damage to the mitotic machinery of dividing cells [45]. To prove if multinucleation events in primary fibroblasts are correlated with cellular age, as seen previously in fibroblasts [18], primary fibroblasts were cultured for 20 days in complete media, and stained for β-galactosidase, a common marker for replicative senescence [31]. At Day 10, (i.e., approximate time when multinucleation in primary cells was observed to increase) senescent cells also became more frequent and all multinucleated cells, regardless of the culture time point, stained positive for senescence (Figs. 2 and 8). Both multinucleation and polyploidy (nuclear replication without nuclear division) have been seen in senescent fibroblasts [18,19]. Multinucleation and polyploidy are also well-known in trophoblasts [46,47] and cancerous tissue [20,43]. Though senescence has been proposed as a mechanism to prevent cells from oncogenesis [48], the nuclear material in senescent multinucleate fibroblasts is considered highly unstable, and on occasion cells can escape senescence by a nuclear budding process known as neosis [20,21,49]. During neosis multinucleate senescent cells can shed karyoplasts to become highly mitotically active and tumorigenic Raju cells [20,21,49]. Interestingly, this nuclear budding process has also been reported in osteoclasts in order to create mononuclear cells from a multinucleate osteoclast [50].

The two types of multinucleated fibroblasts identified in this study in vitro in both secondary and primary fibroblasts correlate with those proposed in vivo due to fusion [4,7] and nuclear division without cellular fission [43,45]. Depending on conditions, some multinucleated fibroblasts found in vivo seen in aged tissue, fibrosis, and fibromas [1–8] may be senescent cells either undergoing nuclear division without cytokinesis or fusion-derived fibroblasts, although direct evidence for either mechanism is scant. A clinical cancer study described multinucleated fibroblast histology with large numbers of nuclei (7–20), less prominent actin staining, and a prevalence of 10–30% multinucleated cells per microscopic field [3], characteristics similar to fused secondary fibroblasts in this study. Multinucleate fibroblasts with polymorphic nuclei seen in vivo [7,8,43] are better compared to the primary multinucleate fibroblasts formed from nuclear division without cytokinesis as reported in this study. Cells resulting from each mechanism are multinucleate, yet as they derive from different pathways, they may possess distinct traits characteristic of the pathologies in which they arise. Understanding these distinctions should provide better insight into the etiology of pathologies such as fibrosis, cancer, aging, and the FBR, where multinucleate fibroblasts may play a significant role.

Secondary fibroblasts in macrophage co-culture did not form the same type of multinucleated cells as primary cells in co- or monocultures. Secondary cells formed multinucleated cells readily after 1 day, while primary cell multinucleation required several days and was never as frequent (Fig. 2). Additionally, far more nuclei per cell were observed in multinucleate cells produced from secondary cells than from primary cells (Fig. 2), but primary cells possessed more prominent stress fibers (Fig. 5). Most interestingly, secondary cells fused to form multinucleated cells that stained negative for senescence (data not shown), while primary cells did not appear to fuse but became multinucleated instead by nuclear division without cytokinesis, correlated with replicative senescence. These differences most likely reside in secondary cells that are transformed, passaged many times, and display oncogenic phenotypes, such as rapid proliferation, lack of contact inhibition and immortalization. Distinct behaviors between primary and secondary fibroblasts in such cell–cell fusions should be considered both in model culture studies employing or clinical histopathological observations invoking this cell type.

5. Conclusions

Multinucleated cells are shown to form in both secondary- and primary-derived fibroblasts cultures in vitro under distinct conditions. Differences are noted in multinucleation mechanism between cultured fibroblasts from primary and secondary sources. Secondary cells produce multinucleation by fusion of multiple fibroblasts only in direct contact culture with macrophages. Primary cells do not multinucleate by fusion, but rather from senescent cells no longer undergoing cytokinesis, and in the absence of co-cultured macrophages. Clinical studies identify multinucleated fibroblasts with pleomorphic nuclei, similar to those derived from primary cells here, as well as the frequent appearance of claimed-fused fibroblasts similar to those from immortalized fibroblast cultures in this study, suggesting that both types of fibroblast-dependent multinucleation may be present in vivo in different pathologies. Understanding the impetus for the formation of each atypical multinucleated fibroblast type is essential in understanding multinucleate fibroblast involvement in pathologies such as the FBR, aging, and fibrotic diseases.

Acknowledgments

We acknowledge J.M. Anderson and T.R. Kyriakides for scientific critique and expert insight. This research was supported by National Institute of Health grant R01EB000894.

Appendix. Supplementary data

Supplementary data associated with this article can be found in online version at doi:10.1016/j.biomaterials.2011.02.021.

References

[1] Powell CM, Cranor ML, Rosen PP. Multinucleated stromal giant cells in mammary fibroepithelial neoplasms. A study of 11 patients. Arch Pathol Lab Med 1994;118:912–6.
[2] Ryska A, Reynolds C, Keeney GL. Benign tumors of the breast with multinucleated stromal giant cells. Immunohistochemical analysis of six cases and review of the literature. Virchows Arch 2001;439:768–75.
[3] Tse GM, Law BK, Chan KF, Mas TK. Multinucleated stromal giant cells in mammary phyllodes tumours. Pathology 2001;33:153–6.
[4] El-Labban NG, Lee KW. Myofibroblasts in central giant cell granuloma of the jaws: an ultrastructural study. Histopathology 1983;7:907–18.
[5] Min KW, Gillies E. Multinucleated giant stromal tumor of the omentum: report of a case with immunohistochemical and ultrastructural investigation. Ultrastruct Pathol 1996;20:89–99.
[6] Regezi JA, Courtney RM, Kerr DA. Fibrous lesions of the skin and mucous membranes which contain stellate and multinucleated cells. Oral Surg Oral Med Oral Pathol 1975;39:605–14.
[7] Cho MI, Garant PR. Formation of multinucleated fibroblasts in the periodontal ligaments of old mice. Anat Rec 1984;208:185–96.
[8] Hassanein A, Telang G, Benedetto E, Spielvogel R. Subungual myxoid pleomorphic fibroma. Am J Dermatopathol 1998;20:502–5.
[9] Anderson JM. Chapter 4 Mechanisms of inflammation and infection with implanted devices. Cardiovasc Pathol 1993;2:33S–41S.
[10] Anderson JM. Multinucleated giant cells. Curr Opin Hematol 2000;7:40–7.
[11] Helming L, Gordon S. Macrophage fusion induced by IL-4 alternative activation is a multistage process involving multiple target molecules. Eur J Immunol 2007;37:33–42.
[12] Anderson JM, Rodriguez A, Chang DT. Foreign body reaction to biomaterials. Semin Immunol 2008;20:86–100.
[13] Wisniewski N, Reichert M. Methods for reducing biosensor membrane biofouling. Colloids Surf B Biointerfaces 2000;18:197–219.
[14] Moilanen E, Moilanen T, Knowles R, Charles I, Kadoya Y, al-Saffar N, et al. Nitric oxide synthase is expressed in human macrophages during foreign body inflammation. Am J Pathol 1997;150:881–7.
[15] Brand KG, Buoen LC, Johnson KH, Brand I. Etiological factors, stages, and the role of the foreign body in foreign body tumorigenesis: a review. Cancer Res 1975;35:279–86.
[16] Tazawa H, Tatemichi M, Sawa T, Gilibert I, Ma N, Hiraku Y, et al. Oxidative and nitrative stress caused by subcutaneous implantation of a foreign body accelerates sarcoma development in Trp53 mice. Carcinogenesis 2007;28:191–8.
[17] DeFife KM, Jenney CR, Colton E, Anderson JM. Cytoskeletal and adhesive structural polarizations accompany IL-13-induced human macrophage fusion. J Histochem Cytochem 1999;47:65–74.
[18] Walen KH. Human diploid fibroblast cells in senescence; cycling through polyploidy to mitotic cells. Vitro Cell Dev Biol Anim 2006;42:216–24.
[19] Ohshima S. Abnormal mitosis in hypertetraploid cells causes aberrant nuclear morphology in association with H2O2-induced premature senescence. Cytometry A 2008;73:808–15.
[20] Sundaram M, Guernsey DL, Rajaraman MM, Rajaraman R. Neosis: a novel type of cell division in cancer. Cancer Biol Ther 2004;3:207–18.
[21] Walen KH. Budded karyoplasts from multinucleated fibroblast cells contain centrosomes and change their morphology to mitotic cells. Cell Biol Int 2005;29:1057–65.
[22] Holt DJ, Chamberlain LM, Grainger DW. Cell-cell signaling in co-cultures of macrophages and fibroblasts. Biomaterials 2010;31:9382–94.
[23] Godek ML, Sampson JA, Duchsherer NL, McElwee Q, Grainger DW. Rho GTPase protein expression and activation in murine monocytes/macrophages is not modulated by model biomaterial surfaces in serum-containing in vitro cultures. J Biomater Sci Polym Ed 2006;17:1141–58.
[24] Rhoades ER, Orme IM. Similar responses by macrophages from young and old mice infected with Mycobacterium tuberculosis. Mech Ageing Dev 1998;106:145–53.
[25] Shao C, Deng L, Henegariu O, Liang L, Raikwar N, Sahota A, et al. Mitotic recombination produces the majority of recessive fibroblast variants in heterozygous mice. Proc Natl Acad Sci U S A 1999;96:9230–5.
[26] Szulc J, Wiznerowicz M, Sauvain MO, Trono D, Aebischer P. A versatile tool for conditional gene expression and knockdown. Nat Methods 2006;3:109–16.
[27] Marino G, Salvador-Montoliu N, Fueyo A, Knecht E, Mizushima N, Lopez-Otin C. Tissue-specific autophagy alterations and increased tumorigenesis in mice deficient in Atg4C/autophagin-3. J Biol Chem 2007;282:18573–83.
[28] Hodgkin PD, Lee JH, Lyons AB. B cell differentiation and isotype switching is related to division cycle number. J Exp Med 1996;184:277–81.
[29] Gordon S, Taylor PR. Monocyte and macrophage heterogeneity. Nat Rev Immunol 2005;5:953–64.
[30] Chang HY, Chi JT, Dudoit S, Bondre C, van de Rijn M, Botstein D, et al. Diversity, topographic differentiation, and positional memory in human fibroblasts. Proc Natl Acad Sci U S A 2002;99:12877–82.
[31] Severino J, Allen RG, Balin S, Balin A, Cristofalo VJ. Is beta-galactosidase staining a marker of senescence in vitro and in vivo? Exp Cell Res 2000;257:162–71.
[32] Russell WC, Newman C, Williamson DH. A simple cytochemical technique for demonstration of DNA in cells infected with mycoplasmas and viruses. Nature 1975;253:461–2.
[33] Jung H, Wang SY, Yang IW, Hsueh DW, Yang WJ, Wang TH, et al. Detection and treatment of mycoplasma contamination in cultured cells. Chang Gung Med J 2003;26:250–8.
[34] Uphoff CC, Brauer S, Grunicke D, Gignac SM, MacLeod RA, Quentmeier H, et al. Sensitivity and specificity of five different mycoplasma detection assays. Leukemia 1992;6:335–41.
[35] Wang Y, Grainger DW. siRNA knock-down of RANK signaling to control osteoclast-mediated bone resorption. Pharm Res 2010;27:1273–84.
[36] McNally AK, Anderson JM. Beta1 and beta2 integrins mediate adhesion during macrophage fusion and multinucleated foreign body giant cell formation. Am J Pathol 2002;160:621–30.
[37] Akisaka T, Yoshida H, Inoue S, Shimizu K. Organization of cytoskeletal F-actin, G-actin, and gelsolin in the adhesion structures in cultured osteoclast. J Bone Miner Res 2001;16:1248–55.
[38] Ridley AJ, Hall A. The small GTP-binding protein rho regulates the assembly of focal adhesions and actin stress fibers in response to growth factors. Cell 1992;70:389–99.

[39] Chamberlain LM, Godek ML, Gonzalez-Juarrero M, Grainger DW. Phenotypic non-equivalence of murine (monocyte-) macrophage cells in biomaterial and inflammatory models. J Biomed Mater Res A 2009; 88:858–71.
[40] Steinhauser ML, Kunkel SL, Hogaboam CM, Evanoff H, Strieter RM, Lukacs NW. Macrophage/fibroblast coculture induces macrophage inflammatory protein-1alpha production mediated by intercellular adhesion molecule-1 and oxygen radicals. J Leukoc Biol 1998;64:636–41.
[41] Fais S, Burgio VL, Silvestri M, Capobianchi MR, Pacchiarotti A, Pallone F. Multinucleated giant cells generation induced by interferon-gamma. Changes in the expression and distribution of the intercellular adhesion molecule-1 during macrophages fusion and multinucleated giant cell formation. Lab Invest 1994;71:737–44.
[42] Briggs DK. The individuality of nuclear chromatin with particular reference to polymorphonuclear neutrophil leukocytes. Blood 1958;13:986–1000.
[43] Gisselsson D, Bjork J, Hoglund M, Mertens F, Dal Cin P, Akerman M, et al. Abnormal nuclear shape in solid tumors reflects mitotic instability. Am J Pathol 2001;158:199–206.
[44] Johnson FB, Sinclair DA, Guarente L. Molecular biology of aging. Cell 1999;96:291–302.
[45] Ly DH, Lockhart DJ, Lerner RA, Schultz PG. Mitotic misregulation and human aging. Science 2000;287:2486–92.
[46] Soloveva V, Linzer DI. Differentiation of placental trophoblast giant cells requires downregulation of p53 and Rb. Placenta 2004;25:29–36.
[47] Zybina EV, Zybina TG, Bogdanova MS, Stein GI. Whole-genome chromosome distribution during nuclear fragmentation of giant trophoblast cells of Microtus rossiaemeridionalis studied with the use of gonosomal chromatin arrangement. Cell Biol Int 2005;29:1066–70.
[48] O'Brien W, Stenman G, Sager R. Suppression of tumor growth by senescence in virally transformed human fibroblasts. Proc Natl Acad Sci U S A 1986;83:8659–63.
[49] Mosieniak G, Sikora E. Poliploidy: the link between senescence and cancer. Curr Pharm Des 2010;16:734–40.
[50] Solari F, Domenget C, Gire V, Woods C, Lazarides E, Rousset B, et al. Multinucleated cells can continuously generate mononucleated cells in the absence of mitosis: a study of cells of the avian osteoclast lineage. J Cell Sci 1995;108 (Pt 10):3233–41.

CHAPTER 4

SENESCENCE AND QUIESCENCE INDUCED COMPROMISED FUNCTION IN CULTURED MACROPHAGES

Accepted for publication in Holt DJ, Grainger DW. Senescence and quiescence induced compromised function in cultured macrophages. *Biomaterials* (July 2012)

SENESCENCE AND QUIESCENCE INDUCED COMPROMISED FUNCTION IN CULTURED MACROPHAGES

Dolly J. Holt[1] and David W. Grainger[1,2]

[1]Department of Bioengineering

[2]Department of Pharmaceutics and Pharmaceutical Chemistry

University of Utah

Salt Lake City, UT 84112-5820 USA

Short Title: *Senescent cultured macrophages*

*Correspondence: Department of Pharmaceutics and Pharmaceutical Chemistry

University of Utah, Salt Lake City, UT 84112 USA

Phone +1 801-581-3715, Fax +1 801-581-3674; E-mail: david.grainger@utah.edu

Abstract

Implants are predisposed to infection even years after implantation, despite ostensibly being surrounded by innumerable macrophages as part of the host foreign body response. The local implant environment could adversely influence the implant-associated macrophage phenotype, proliferative capacity, activation states, and ability to neutralize pathogens. This study monitored cultured macrophage proliferative states and phagocytotic competence on tissue culture plastic to address the hypothesis that extended contact with foreign materials alters macrophage phenotype. That such macrophage alterations might also occur around implants has significance to the foreign body response, infection, cancer, autoimmune and other diseases. Specifically, multiple indicators of macrophage proliferation in various culture conditions, including cell confluence, long-term culture (21 days), lipopolysaccharide (LPS) stimulation, passaging, and mitogenic stimulation are reported. Importantly, primary murine macrophages became quiescent at high confluence and senescent during long-term culture. Senescent macrophages significantly reduced their ability to phagocytose particles, while quiescent macrophages did not. Cell senescence and quiescence were not observed with repeated passaging. Primary macrophage stimulation with LPS delayed senescence but did not eliminate it. These results prompt the conclusion that both cell quiescence and senescence are observed under common macrophage culture conditions and could alter macrophage behavior and phenotypes in extended in vitro culture, such as the ability to phagocytose. Such macrophage transitions around foreign bodies in vivo are not documented: quiescence and senescence reported here in macrophage culture could be relevant to macrophage behavior both in vitro in bioassays and in vivo in the foreign body response and implant-centered infection.

Introduction

Macrophages play a primary role in modulating the foreign body response, immediately localizing to surfaces of every implanted material [1]. At the implant site, they are responsible for removing cell debris, foreign bodies and pathogens. After acute phase inflammation subsides, macrophages may reside at implant surfaces throughout the duration of the implantation, possibly for decades [2, 3], in some case producing multi-cellular macrophage layers around monolithic

implants [1, 4], completely infiltrating porous implants [5], and fusing to form foreign body giant cells at these surfaces [1, 4, 6-8]. That any of these commonly observed chronic responses result from macrophage in situ proliferation versus continual new cell recruitment is not clear. However, a recent study found that during T helper 2 (Th2) inflammation, macrophages were capable of undergoing rapid proliferation in vivo [9]. Importantly, changes in their resident phenotypes, functional competence and capabilities to address infection risk over this implant duration, prompted by or correlated with their prolonged exposure and reaction to a foreign body (e.g., implant) are largely unknown.

Despite macrophage persistence at surfaces of implanted materials, implants retain substantial infection risk even years after implantation [10, 11]. This may be due to the fact that unlike host tissue that is continuously renewed, thereby limiting opportunities for bacterial colonization, tissue surrounding implanted materials remains relatively unchanged, encapsulated in fibrous scar tissue [1, 12-14]. This suggests that while abundant macrophages are present, they may be transformed by their chronic reactions to implants into states of relative inactivity, incapable of addressing microbial presence as effectively as during initial implant site recruitment.

Many cells in normal tissue are quiescent, a reversible, viable, nondividing state-of-rest. Importantly, quiescent cells can be stimulated to divide [15, 16]. Cells can also become senescent, a viable but irreversible nondividing state that cannot be overcome even with mitogenic stimuli [17]. Senescent and quiescent cells are distinguished by altered patterns of gene expression [18, 19]. Senescent and quiescent transitions in macrophages at implant surfaces could explain their inability to adequately address bacterial infection in vivo in this context.

Previous studies have demonstrated a decreased phagocytic ability in aged macrophages [20] and a susceptibility of cells under oxidative stress to senesce [20, 21]. That macrophages demonstrate increased intracellular reactive oxygen species with age [22] and reside in high oxidative stress environments surrounding foreign bodies [13] could indicate their propensity to senesce and their subsequent incompetence to phagocytose pathogens at implant surfaces over time. Interestingly, foreign body giant cells, the chronic multinucleated macrophage-derived phenotypic hallmark surrounding implanted materials, also display decreased phagocytic

ability [23], and increased lysosomal activity [23, 24], consistent with senescent cells [25] also known to multinucleate [26]. Macrophages have also been purported to undergo frustrated phagocytosis, an exhausting metabolic phenomenon that could compel macrophages to senesce around implants [1, 4, 7, 8]. However, macrophage senescence and phagocytosis around chronically implanted foreign bodies or in long-term cultures on materials remains unaddressed in current literature.

Cultured macrophages are commonly employed in assays seeking information on aspects of their involvement in pathologies such as cancer, autoimmune diseases, and the foreign body response [27-32]. As an immunomodulatory cell, macrophages are highly susceptible to telomere attrition [22], increasing their potential to senesce. However, they are not commonly assayed for this phenotype. As both quiescence and senescence alter cell genetic profiles [18, 19], macrophage transitions to these states during in vitro culture likely influence assay outcomes, potentially leading to false conclusions, irreproducible results, and inconsistencies, especially when compared to in vivo phenotypes they intend to mimic. Maintenance of consistent macrophage phenotypes and activation states between in vivo and in vitro conditions is likely critical to ensuring proper in vitro model fidelity. Therefore, understanding the possible consequences of macrophage senescent and quiescent transitions has important implications both in vitro and in vivo.

This study identified proliferation states for both primary and secondary macrophages in several experimental culture conditions, including cell confluence, culture time, passage number, and biochemical stimulation. Cultured macrophage capacity to phagocytose in quiescent and senescent states raises important questions about macrophage phenotypic competence in extended contact with materials. Should this behavior also be observed in vivo, it has important implications for implanted biomaterials in the context of the foreign body response.

Methods and materials

Cell culture

Immortalized RAW cell culture

Macrophage-like transformed murine cell line RAW 264.7 was purchased from the American Type Culture Collection (TIB-71, ATCC, Manassas, USA) and cultured in 96-well tissue culture-treated polystyrene plates (BD Falcon, San Jose, USA), unless otherwise specified, at 37°C with 5% supplemental CO_2 according to the experiments detailed below. All RAW cells were used below passage 10 after purchase, unless passage number was explicitly specified. RAW cells were passaged by scraping with a rubber scraper (Starstedt, Newton, USA). Cells were always cultured in complete media (Dulbecco's modified eagle medium (DMEM) with 10% fetal bovine serum (FBS), and 1% antibiotic/antimycotic, Invitrogen, Carlsbad, USA). Full media exchanges were performed every other day.

Murine primary cell sourcing

Specific pathogen-free, 2-3 month-old male C57BL/6 mice were purchased from Jackson Laboratories (Bar Harbor, USA). Animals were kept in the University of Utah animal facility, and provided water, mouse chow, bedding, and modes of enrichment ad libitum throughout this study. For primary macrophage harvests, animals were euthanized via CO_2.

Primary macrophage cell culture

Bone marrow cells were collected from the femurs and tibias of 4-5 month-old euthanized male C57BL/6 mice and differentiated into bone marrow macrophages (BMMΦs) using a previously described method [33, 34]. On day 7, cells were removed from surfaces by rinsing cells 3X and incubating them in Ca^{+2}/Mg^{+2}-free phosphate buffered saline (PBS, Invitrogen) for 30 minutes at 37°C, and then rinsed from the surface using a 1 ml pipette tip, and collected. Cells were counted using a hemocytometer and cultured in 96-well tissue culture-treated polystyrene plates (BD Falcon, San Jose, USA), unless otherwise specified, at 37°C with 5% supplemental CO_2 according to the experiments outlined below. At least an equal volume of complete BMMΦ media (DMEM with 10% heat-inactivated FBS, 10% L929-conditioned media, 1%

antibiotic/antimycotic, 1% MEM nonessential amino acids, 1% HEPES, and 1% sodium pyruvate, Invitrogen) was added to the suspended cells after plating, and fresh media was replaced every 2-3 days. Unless otherwise specified, all BMMΦs were passaged once after their differentiation for experimental use.

In vitro culture conditions for senescence examination

Cell confluence

Immortalized RAW macrophages were plated at densities of 5 $x10^3$, 1 $x10^4$, 2 $x10^4$, 4 $x10^4$, and 8 $x10^4$ cells/well, and primary macrophages were plated at densities of 5 $x10^3$, 1 $x10^4$, 2 $x10^4$, 4 $x10^4$, 8 $x10^4$, and 1.6 $x10^5$ cells/well and cultured for 24 hours prior to fixing. To determine cell senescence versus quiescence, an equivalent cell density of 1.60 $x10^5$ cells/well was cultured in a 30-mm Petri dish (BD Falcon) in parallel and passaged and plated at low confluence. These cells were then cultured for 7 days further (seen previously to be the time for maximum proliferation). Both control media and media with 50% serum (to encourage growth) were utilized to confirm macrophage proliferative capacity.

Comparisons of longterm macrophage cultures

Primary and immortalized macrophages were plated at 5 $x10^3$ cells/well and cultured for 1, 2, 3, 5 and 7 days for secondary RAW 264.7 macrophages and 1, 2, 3, 5, 7, 10, 12, 14, 17, 19, and 21 days for primary BMMΦs prior to fixing. To determine senescence or quiescence in primary macrophages, a 30mm Petri dish (BD Falcon) with the same cell seeding density as the longterm experiment was passaged on Day 21 and plated at 5 $x10^3$ cells/well and analyzed for proliferation 5, 7, and 10 days later (i.e., the time at which the greatest proliferation during the initial 21 days was seen). Both control media and media with 50% serum (to encourage proliferation) were utilized to confirm macrophage proliferative capacity.

Lipopolysaccharide (LPS) treatment of cell cultures

For LPS-treated conditions, primary and immortalized macrophage cultures were treated with their respective media supplemented with 1 μg/ml LPS replaced every 2-3 days until the end

of the experiment (i.e., 7 days for RAWs and 21 days for BMMΦs). This concentration was selected because it has been shown to effectively activate macrophages [35, 36]. RAW cells were also stimulated with LPS during studies of increasing confluence (details listed above).

Cell passaging

RAW 264.7 macrophages were cultured in 30-mm tissue culture-treated polystyrene Petri dishes (BD Falcon, San Jose, USA) and passaged 30 times and subsequently plated into 96-well plates and assayed for senescence and proliferation markers. Primary BMMΦs were cultured in 100-mm tissue culture-treated polystyrene Petri dishes (BD Falcon), passaged and plated into 96-well plates for subsequent characterization. This was repeated up to 10 passages, where passage 1 was the first passage after differentiation. Passages were fixed after 24 hours of culture for characterization. Both primary and secondary macrophage culture passages were performed every other day, to allow stock cultures sufficient time to properly adhere before serial passaging.

Cell culture biochemical stimulation

Primary BMMΦs were plated at 5 x10^3 cells/well and cultured for 21 days and then treated for 48 hours with cytokines IFN-gamma, IL-6, MCP-1, TNF, GM-CSF, MIP-1β, MIP-1α, IL-4, RANTES, and IL-10, and mitogens TGF-β, IL-1β, MCP-1, and also 50% and 100% serum prior to fixing. This 48-hour incubation period was selected as the time reported for quiescent cells to reactivate [37].

Predifferentiated BMMΦ cultures

Bone-marrow cells were plated into 96-well plates and characterized on Days 1, 3, 5, and 7 post-harvest for proliferation markers prior to full differentiation into macrophages.

Phagocytosis

Phagocytosis was measured in both senescent and quiescent cells. Blue-green fluorescent polystyrene beads (diameter 1 μm, Invitrogen) at a dilution of 0.5 μl stock to 100 μl

media were added to macrophage cultures and allowed to incubate at 37°C with 5% supplemental CO_2 for 12 hours. After this incubation time, cells were washed to remove any beads not internalized and fixed with 4% paraformaldehyde (PFA, Sigma-Aldrich, St. Louis, USA), diluted in Ca^{+2}/Mg^{+2}-free PBS (Invitrogen) for 20 min at room temperature for subsequent imaging. Fixed cells were incubated with propidium iodide diluted 1:100 in PBS (Invitrogen) for 20 minutes which successfully stained the entire cell body. Using ImageJ (NIH freeware) the area of the cell occupied by beads was divided by the total cell area to determine the percentage of beads occupying the cells in each frame.

Cell labeling

Cell phenotypic makers

Mature macrophage-specific marker anti-F4/80 [38, 39] (clone BM8, rat anti-mouse IgG2a, pre-conjugated to phycoerythrin (PE), eBioscience ,San Diego, USA) and M2 macrophage marker anti-CD206, macrophage mannose receptor [40] (clone MR5D3, rat anti-mouse IgG2a, preconjugated to fluorescein isothiocyanate (FITC), AbD Serotec, Raleigh, USA) were used to label macrophages on Days 1,7, and 21. Representative images from Day 21 are shown in Supplementary 4.1.

Cell proliferation markers

Primary anti-mouse Ki-67 (IgG_1, Novacastra, Buffalo Grove, USA) and phospho-histone H3 (Ser10) (Cell Signaling Technology, Danvers, USA) antibodies, both markers of actively proliferating cells [41, 42], were used at dilutions of 1:50 and 1:100, respectively. Secondary IgG_1 goat-anti-mouse antibody conjugated to Alexa 488 (Invitrogen), used against both Ki-67 and phospho-histone H3, was diluted 1:500. Samples were rinsed 2X in PBS+Ca^{+2}/Mg^{+2} (Invitrogen,) and fixed in 4% PFA (Sigma-Aldrich), diluted in Ca^{+2}/Mg^{+2}-free PBS for 20 min at room temperature. They were rinsed 2X in Ca^{+2}/Mg^{+2}-free PBS and then incubated in block solution (4% goat serum plus 0.1% triton-X 100, Invitrogen) for 1 hour at room temperature on a shaker plate. Each primary antibody, diluted in block solution, was added to the samples and the plate was sealed and placed at 4°C overnight. The primary antibody media was removed and the

samples were washed 3X in Ca^{+2}/Mg^{+2}-free PBS. The secondary antibody, diluted in block solution, was added to the samples and incubated at room temperature for 1 hour on a shaker plate. The samples were washed 3X in Ca^{+2}/Mg^{+2}-free PBS and counterstained with 4',6-diamidino-2-phenylindole (DAPI, Invitrogen) according to manufacturer's instructions prior to imaging.

Cell senescence assay

A colorimetric assay for senescence-associated beta-galactosidase (SA beta-gal) used as a labeling kit (Cell Signaling Technology, Danvers, USA) was used according to manufacturer's instructions [21]. This commonly employed assay [17] labels fixed cells positive for SA beta-gal with a blue precipitate and allows for subsequent visualization of percent positive cells (imaging described below). A second quantitative fluorescence-based SA beta-gal assay, employed according to a previously established protocol [17] requires cell lysis and subsequently measures the relative fluorescence of total SA beta-gal in the culture well, rather than distinct SA-positive cells. Relative SA beta-gal fluorescence yield was analyzed using a plate reader (BioTek Synergy 2, Winooski, USA). All conditions were analyzed on the same plate at the same time, making comparison of RFUs meaningful between conditions. The quantitative fluorescent SA beta-gal lysate assay was normalized to cell density by dividing the relative fluorescence of the SA beta-gal assay by the BCA protein content from each culture well (described below). Both colorimetric and fluorescent senescence assays were conducted at pH 6, which suppresses the activity of native lysosomal beta-galactosidase that is only active at pH 4 [17]. Therefore, only SA beta-gal active at pH 6 could cleave the chromogenic substrate 5-bromo-4-chloro-3-indolyl-beta-D-galactopyranoside (X-gal), reducing non-senescent cell staining and increasing signal:noise ratios [17].

BCA cell protein assay

Cell density was approximated using cell-derived protein content from each culture well detected by the microBCA assay (Pierce Thermo Scientific, USA) used according to manufacturer's instructions. Relative fluorescence from the assay was analyzed using a plate

reader (BioTek Synergy 2, Winooski, USA). All conditions were analyzed on the same plate at the same time, making comparison of RFUs meaningful between conditions.

Cell imaging

Fluorescent false-color, brightfield, and true color microscopy images of cells in culture were acquired using a Nikon Eclipse TE2000-U microscope equipped with fluorescent optics, CCD camera, and Metamorph and Q Capture Pro software. Confocal images were captured using a FV1000 IX81 Olympus confocal microscope. Representative images were selected from 3 independent replicates.

Statistics

Statistics were performed using a one-way ANOVA with post-hoc Dunnett Multiple Comparisons Test or Student's t-test, where specified. Cell counts were taken from 15X objective images in low confluency cultures and 40X images in high confluency cultures so that ~50-100 cells occupied each frame. For the colorimetric SA beta-gal assay, Three frames per replicate were counted from three replicates from three mice per condition. For the Ki-67 assay, two frames from two replicates were counted from three mice per condition. For the fluorescent SA beta-gal assay, lysates from three replicates were combined from each of three mice. For RAW cells, six wells were counted in each condition for the colorimetric SA beta-gal and Ki-67 assays, and lysates from three wells were combined for each condition for the fluorescent SA beta-gal assay. For the colorimetric senescent assay, only dark blue cells were counted as they (and not any lighter blue cells) corresponded to cells that did not label for Ki-67. Ki-67-positive cells with a definite labeled nucleus were counted as positive. No values for primary cells were below the limit of detection for any of the assays. For bead quantification in phagocytosis assays, two frames from two replicates were counted from three mice per condition.

Results

Macrophage phenotype

Macrophages maintained strong F4/80 staining throughout 21 days of culture, supporting their mature macrophage phenotype [38, 39] (Supplementary Figure 4.1). Macrophages also maintained the strong M2 phenotypic marker, CD206 [40] (macrophage-mannose receptor), labeling to 21 days (Supplementary Figure 4.1), a macrophage polarization state shown capable of proliferation in vivo during inflammation [9]. Macrophage proliferation, peaked in culture near day 7 (Figure 4.1). Isotype controls for F4/80 and CD206 revealed some background staining; however, previous work also reported strong staining for these two markers after 21-day cultures (unpublished data, submitted 2012).

Culture confluence

Increasing adherent macrophage confluence increased expression of senescence marker, SA beta-gal, and decreased expression of proliferation marker, Ki-67, in primary BMMΦ cells (Figure 4.2). Both the colorimetric qualitative and fluorescent quantitative senescence assays yielded the same trends. After confluence was reached, cells were passaged and re-plated at a low density and found capable of being restimulated to divide (Figure 4.3).

BMMΦ proliferation over 21 days

Primary BMMΦs initially increased and then later decreased their percent proliferation over the course of 21 days, peaking at day 7 and 10 (Figure 4.1). This same trend in proliferation was seen previously by our lab [36]. The colorimetric senescence assay inversely correlated with the Ki-67 assay, while the fluorescent quantitative senescent assay diverged, showing a general increasing trend over 21 days. Cells passaged and re-plated after 21 days were not capable of being restimulated to divide, even with mitogenic stimulation (Figure 4.3).

Phagocytosis

Primary BMMΦs showed reduced ability to phagocytose subsequent to passaging after 21 days (Figure 4.4), under the same conditions by which the majority of cells within the culture

were shown to be senescent (Figure 4.3). Cells at high confluence (i.e., those deemed quiescent) compared to those at low confluence showed a non-significant reduction in phagocytosis (Figure 4,4).

LPS stimulation

LPS stimulation in primary BMMΦs delayed SA beta-gal staining over the course of 21 days, but did not eliminate it. The colorimetric senescence assay showed least amounts of staining for SA beta-gal from day 5 to day 10, with proliferation rates decreasing after day 14 (Figure 4.5). Similar but delayed trends for both senescence assays were seen in the LPS-stimulated condition compared to the non-LPS stimulated condition described above.

Passaging

Increasing passages of BMMΦs did not correlate to a definite increasing or decreasing trend of SA beta-gal or Ki-67 expression up to 10 passages. The qualitative colorimetric percent positive cell and quantitative cell lysate senescent assays followed relatively similar trends. The Ki-67 assay was inversely related at some passage numbers, but not all (Figure 4.6).

Biochemical stimulation

After 21 days of culture, BMMΦs positive for SA beta-gal and negative for Ki-67 could not be stimulated to proliferate using cytokines, mitogens, or passaging at a lower confluency as determined by an insignificant change in either SA beta-gal or Ki-67 expression after stimulation (Figure 4.3, Supplementary Figure 4.2).

Figure 4.1. Proliferative capacity of primary BMMΦ cultures over 21 days. Fluorescence and color images of: A) DAPI and Ki-67, and B) SA beta-gal staining, respectively, in primary BMMΦs over 21 days. Graphical representation of: C) percent positive Ki-67 cells; D) percent positive SA beta-gal cells (from fixed colorimetric beta-gal assay); E) relative fluorescence units (from lysed fluorescent SA beta-gal assay); and F) cells per frame, all over 21 days. These data show a decrease in Ki-67 staining and an increase in SA beta-gal staining after 21 days, suggesting an increase in macrophage senescence over 21 days. One-way ANOVA with post-hoc Dunnett Multiple Comparisons Test was applied, comparing all days to the day 1 time point. Significance is noted as $p<.05$ * and $p<.001$ **. No significant increase in Ki-67 expression after passaging (C) indicates macrophage senescence.

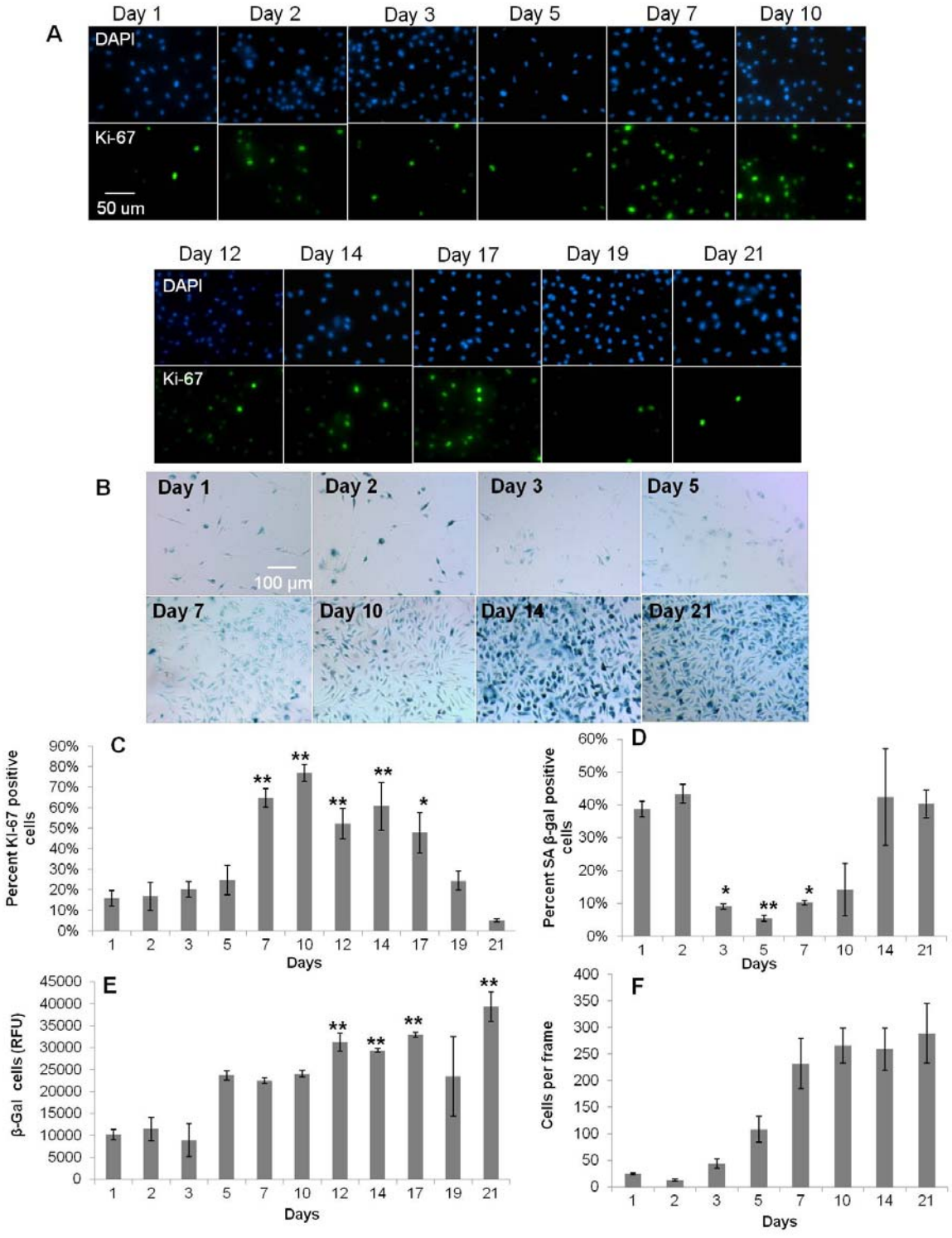
A
Day 1
Day 2
Day 3
Day 5
Day 7
Day 10
DAPI
Ki-67
50 um
Day 12
Day 14
Day 17
Day 19
Day 21
DAPI
Ki-67
B
Day 1
Day 2
Day 3
Day 5
100 µm
Day 7
Day 10
Day 14
Day 21
C
Percent KI-67 positive cells
Days
D
Percent SA β-gal positive cells
Days
E
β-Gal cells (RFU)
Days
F
Cells per frame
Days

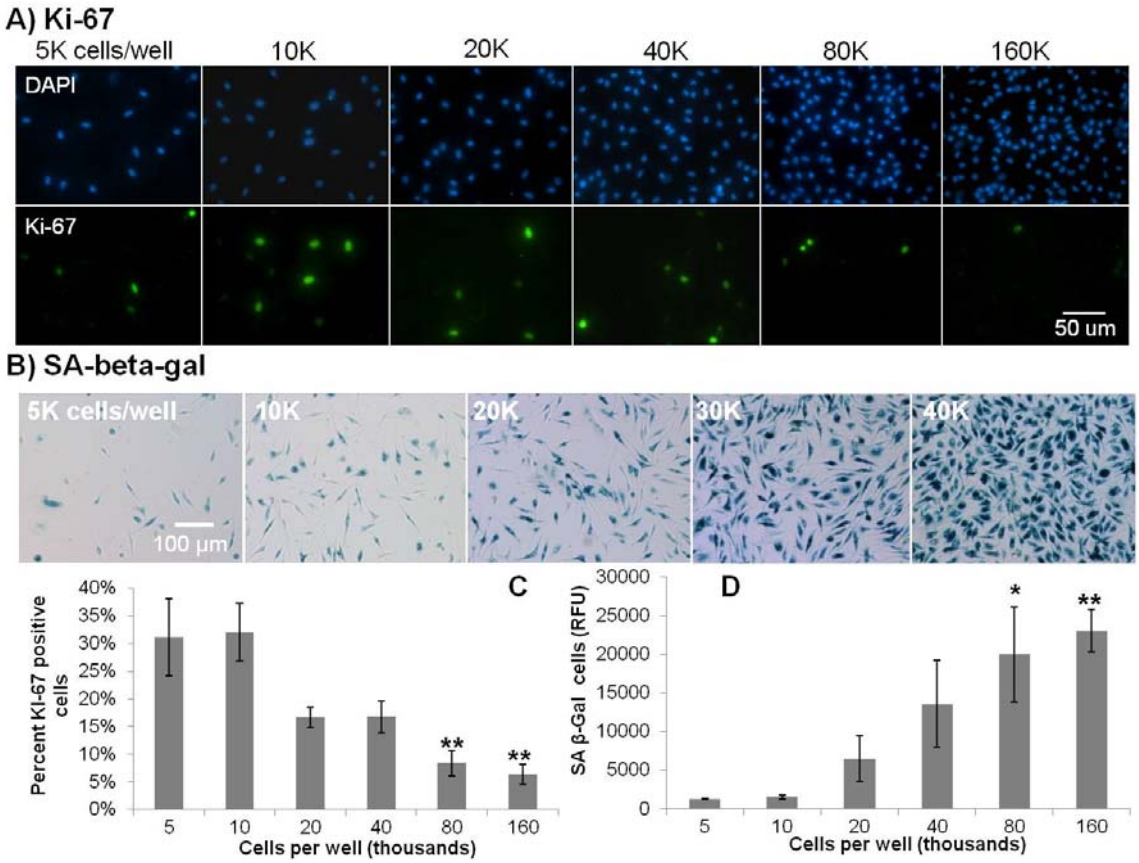

Figure 4.2. Effect of increasing cell confluence on macrophage proliferation in culture. Fluorescence and color micrograph images of: A) DAPI and Ki-67, and B) SA beta-gal staining, respectively, in primary BMMΦs with increasing confluence on tissue culture plastic. Graphical representation of C) percent positive cells for Ki-67, and D) relative fluorescent signal, from lysed fluorescent SA beta-gal assay, showing increased SA beta-gal with increasing confluence in BMMΦ cultures. These data show decreased percent proliferative cells as seen by Ki-67 and an increase in SA beta-gal with increasing cell density. These data also confirm the ability of SA beta-gal to represent non-proliferative cells and the decrease in proliferative capacity of macrophages with increasing concentration. One-way ANOVA with post-hoc Dunnett Multiple Comparisons Test was applied, comparing all concentrations the 5K condition. Significance is noted as $p<0.05$ * and $p<0.001$ **.

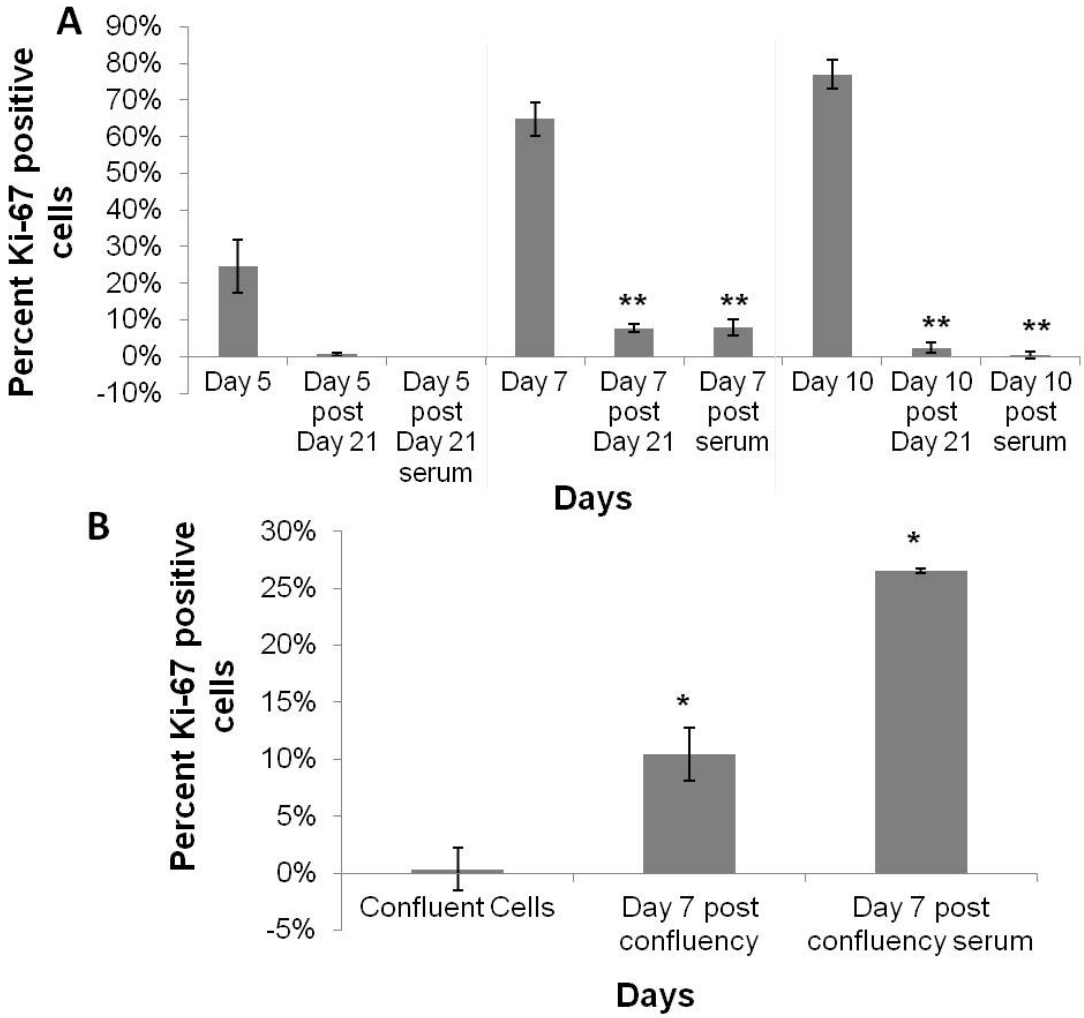

Figure 4.3. Discrimination of senescent versus quiescent BMMΦs using Ki-67 staining of cultures. A) cells passaged after 21 days and allowed to grow for 5, 7, and 10 days. Passaged cells with and without serum as a mitogenic stimulator were compared to their respective time point prior to day 21, indicating that after 21 days, cells decrease their ability to proliferate, reflecting senescence. B) proliferation of cells cultured for 1 day at high confluence and 7 days after those cells were passaged and plated at low confluence in the presence and absence of serum. These data indicate regained proliferative capacity of cells after being plated at sub-confluency, indicating confluent cells become quiescent and not senescent. One-way ANOVA with post-hoc Student's t-test was applied, comparing post-passages to the pre-passaged condition (i.e. Day 5, 7, and 10 in A and confluent cells in B). Significance is noted as $p<0.05$ * and $p<0.001$ **.

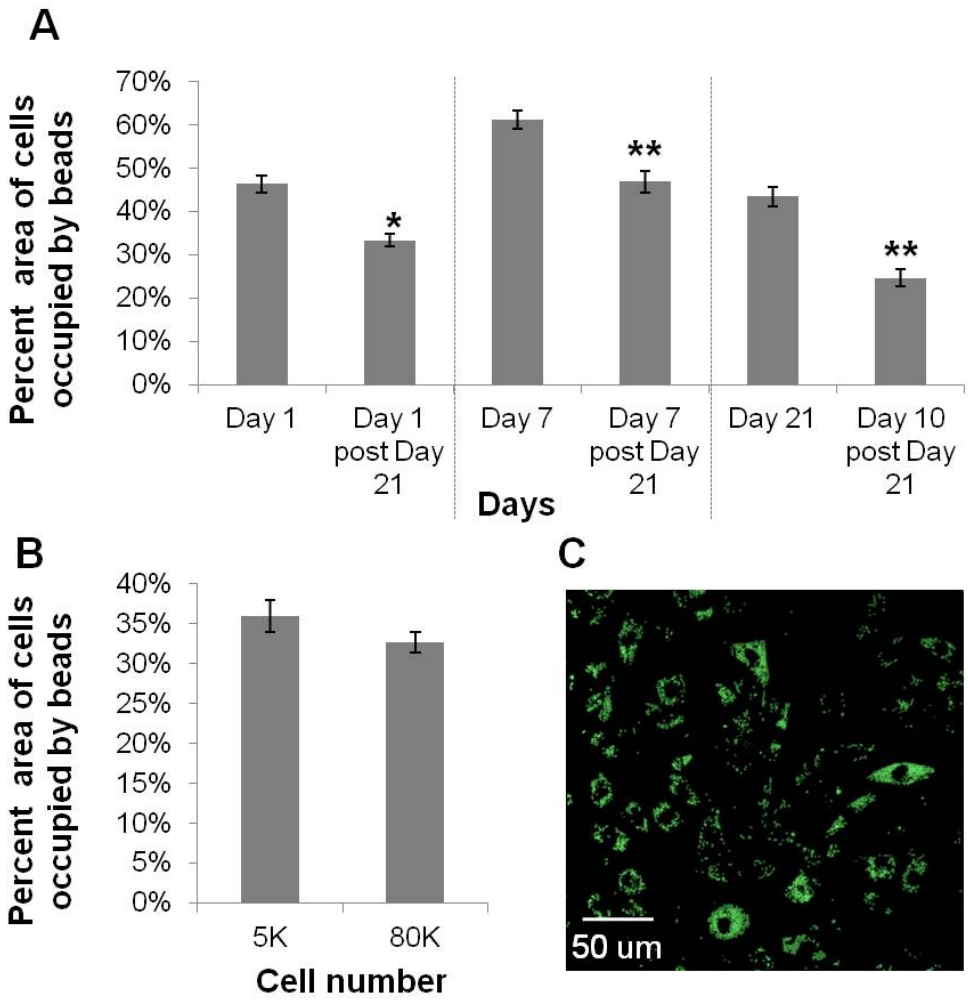

Figure 4.4. Macrophage phagocytosis in quiescent and senescent cells. A) Bead phagocytic uptake in macrophages passaged after 21 days (shown in Figure 4.3 to be senescent) and cultured for 10 days were compared with bead uptake of their corresponding time point prior to 21 days. Data show a reduction in phagocytosis in cells at time points past 21 days. B) Bead uptake in macrophages at low and high confluency, indicating no significant change in phagocytosis at high confluence (shown in Figure 4.3 to be quiescent). One-way ANOVA with posthoc Student's t-test was applied, comparing postpassages to the prepassaged condition (i.e. Day 1, 7, and 21). Significance is noted as $p<.05$ * and $p<.001$ **. C) Representative confocal image of BMMΦs with internalized beads. This image is an overlay of 10 z-sections through the cell, indicating beads are internalized by phagocytosis.

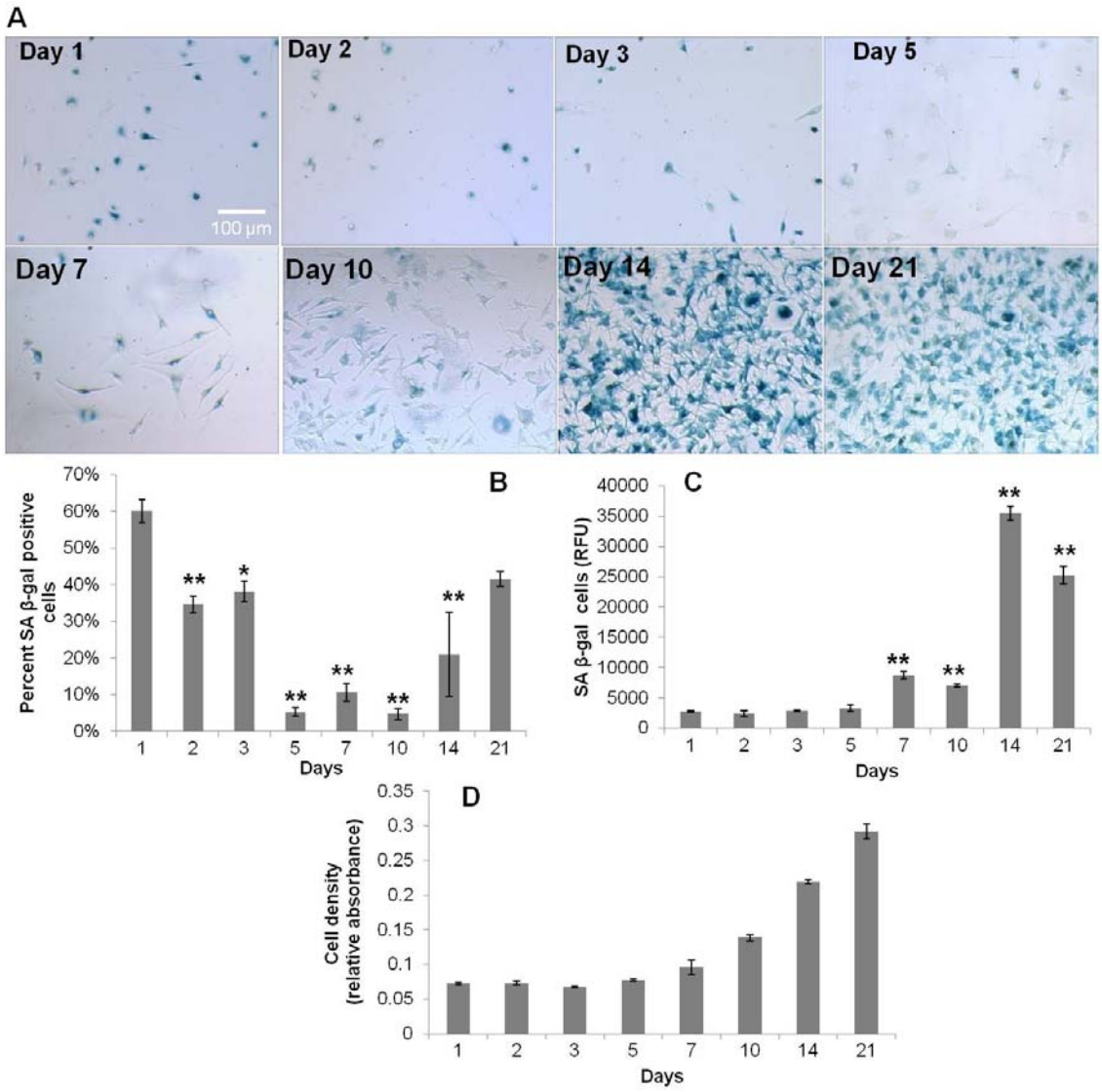

Figure 4.5. Proliferative capacity of primary BMMΦs over 21 days in culture in the presence of continual LPS stimulation. A) Color images of SA beta-gal staining in primary BMMΦs over 21 days in the presence of LPS. Graphical representation of: B) percent SA beta-gal positive cells from the colorimetric SA beta-gal assay, C) relative fluorescence from the fluorescent SA beta-gal assay, and D) cell density shown as relative absorbance from the microBCA assay. These data show a delay in the SA beta-gal response compared to non-LPS treated macrophages (Figure 4.1). One-way ANOVA with post-hoc Dunnett Multiple Comparisons Test was applied, comparing all days to the day 1 time point. Significance is noted as $p<0.05$ * and $p<0.001$ **.

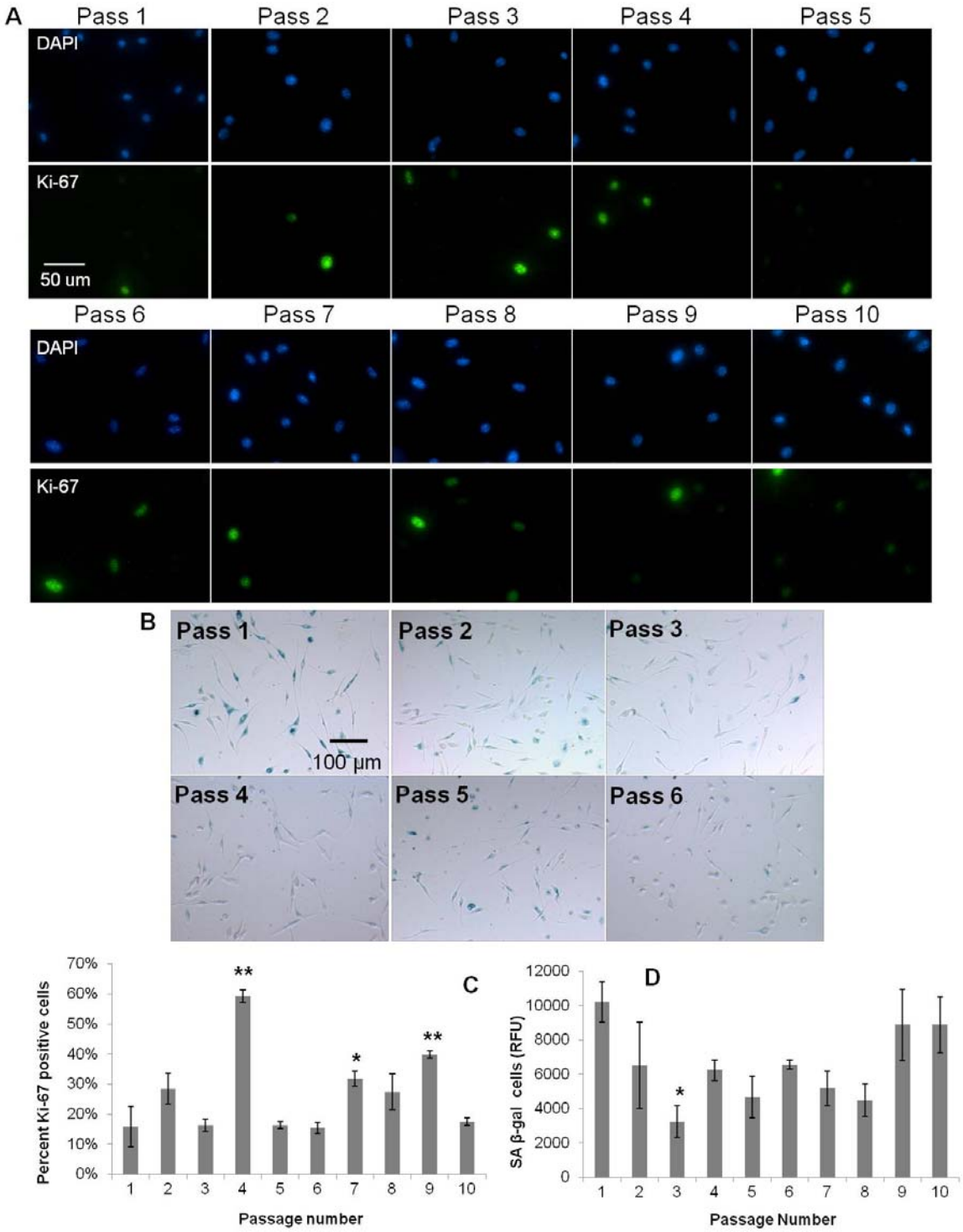

Figure 4.6. Effect of serial passaging on BMMΦ proliferation. Fluorescence and color images of: A) DAPI and Ki-67, and B) SA beta-gal staining, respectively, in primary BMMΦ cultures with increasing passage numbers. Graphical representation of: C) percent positive cells for Ki-67 markers, and D) SA beta-gal (from fluorescent senescence assay) with increasing passaging in BMMΦs. These data show no dramatic increasing or decreasing trends in senescence with increased passaging. One-way ANOVA with post-hoc Dunnett Multiple Comparisons Test was applied, comparing all passages to the passage 1 condition. Significance is noted as $p<0.05$ * and $p<0.001$ **.

Predifferentiated BMMΦs

SA beta-gal increased while Ki-67 decreased during the first 7 days of macrophage differentiation from bone marrow hematopoietic cell precursors (Supplementary Figure 4.3). Though by day 7 many now-differentiated macrophages expressed SA beta-gal, they were still able to be restimulated to divide when passaged at lower confluency. This is seen in Figure 4.1, representing recently differentiated macrophages after passage and plating at a lower confluency, exhibiting decreased SA beta-gal and increased Ki-67 expression after a couple days of culture.

Transformed RAW cell cultures

RAW 264.7 cells stained positive for SA beta-gal with increasing time and confluency. LPS exposure decreased SA beta-gal staining over long-term culture and with increasing confluency (Supplementary Figure 4.4). RAWs always responded to restimulation to proliferate regardless of culture time (data not shown) and passage number (passaged up to 30 times, Supplementary Figure 4.5).

Discussion

Macrophage culture duration to 21 days was selected as a terminal time point as it is the approximate time required for the foreign body response (FBR) to mature in vivo [43]. After 21 days in culture, macrophages were found to be senescent and decrease their ability to phagocytose (Figure 4.4). This is consistent with the observed propensity of implants to infect [10, 11], and implies that macrophages could lose their ability to phagocytose bacteria after extended exposure to biomaterials. Importantly, Jenkins et al. recently discovered that macrophages proliferate in vivo during Th2 inflammation [9]; thus, their senescence shown in culture over time could suggest a decreased ability to properly proliferate at implant sites in the presence of infection. A previous study also found that macrophages decrease their production of inflammatory cytokines over 21 days [36]. All these findings support a phenotypic shift over time that decreases macrophage competence, contributing to their inability to respond to bacterial invasion at the surface of an implant over time. Macrophages from aged animals have also shown a decreased ability to be stimulated to divide [22] and a decreased phagocytic capacity

[20]. Thus, the longer the implant resides in the body and the older the individual [44] may increase their susceptibility to implant-centered infection.

Various culture conditions are known to affect cell senescence in other cultured cell types including confluency, culture time, and passage number [17, 21, 45]. Passaging macrophages up to 10 times did not appear to have observable effects on their proliferation (Figure 4.6). Confluent culture disposes macrophages to quiescence but not senescence. This was substantiated by the ability of macrophages to be restimulated to divide upon passaging and mitogenic stimulation post-confluence (Figure 4.3). This result is consistent with contact inhibition-induced quiescence [21, 37] shown in other cell types to also stain positive for SA beta-gal. Decreasing SA beta-gal staining at early time points during the 21-culture is attributed to confluence-induced quiescence of predifferentiated BMMΦ-staged cells (which were passaged and plated at lower cell confluence for the 21-day experiment, Supplementary Figure 4.3). Dimri *et al.* have also shown reduced SA beta-gal staining 2 days after highly confluent cultures of normal human fetal lung fibroblasts were passaged [37]. Confluent cultures stained positive for SA beta-gal, indicating that although this assay is specific for senescence in other cell lines [21, 37], it stains both quiescent and senescent macrophages. Interestingly, we found a slight decrease in phagocytosis in confluent versus nonconfluent cultures. This decrease was not significant and was not as dramatic as in senescent cultures (Figure 4.4).

Two metrics were used to determine senescence: 1) senescence-associated beta-galactosidase (SA beta-gal) activity at pH 6 [37, 46], and 2) active cell proliferation (i.e., absence from the cell cycle G_0 phase).[41] Many cells produce beta-galactosidase at pH 4-5 in lysosomes, but it is unique among senescent cells to exhibit beta-gal activity at pH 6 [37]. Senescent cells have been postulated to provide an environment wherein modified lysosomal beta-gal structure remains active at neutral or alkaline pH [21] and that its increased lysosomal content characteristic in senescent cells makes it detectable [25]. While macrophages frequently up-regulate lysosomal activity [47], the SA beta-gal assay used here may not selectively reflect macrophage senescence. Therefore, despite common cell culture use of the SA beta-gal assay, its validation for macrophage senescence -- to our knowledge not yet reported -- was required. Therefore, senescence used was anti-Ki-67 antibody labeling of cells to target a protein

expressed only during active cell proliferation [41] in parallel with SA beta-gal staining. Significantly, anti-Ki-67 labels all cells in all active cell cycle phases (i.e., interphase and mitosis). Therefore cells were also labeled with phospho-histone H3, which labels cells only during S-phase of interphase [42]. Results showed similar trends between Ki-67 and phospho-histone H3 labeling (data not shown), validating the proliferative activity of cultured macrophages using Ki-67. Inverse correlation between cell Ki-67 expression and SA beta-gal staining suggests that SA beta-gal labels macrophages with decreasing proliferation tendency and not nonspecifically as a general function of increased macrophage lysosomal activity.

As senescent cells are incapable of being restimulated to divide [48], passaging, mitogens, and both passaging and subsequent mitogenic stimulation were all employed in culture to determine if macrophages could be restimulated to divide. Macrophages were allowed to first grow for at least 7 days in the presence and absence of mitogenic stimulation after passaging to determine if cells were quiescent (capable of being restimulated to divide) or senescent (incapable of being restimulated to divide) at the time when greatest cell proliferation is seen (Figure 4.1).

The cell lysate-based fluorescent SA beta-gal assay did not correlate with the fixed cell colorimetric assay during extended culture time, showing instead an increase in SA beta-gal over the 21 day time-course in both LPS-stimulated and non-LPS-stimulated BMMΦ culture conditions (Figures 4.1 and 4.5, respectively). This discrepancy is attributed to the observation that over 21 days of culture, cells becoming senescent produced increasing SA beta-gal amounts within positive cells (Figure 4.1) so that total SA beta-gal amounts in culture wells after cell lysis increased over 21 days. This explanation is also supported by observations from increased cell confluence-dependent culture experiments where initially different plated cell densities were cultured for identical times. These results showed that both SA beta-gal senescence assays consistently correlated with each other and also inversely with Ki-67 expression. Percent of cells positive for SA beta-gal detected in fixed cells using the colorimetric SA beta-gal assay correlated inversely with percent cells positive for Ki-67, suggesting that over increased culture time, determining senescence on a percent positive cell basis is more representative of changes in proliferation than cell lysis methods.

As a positive control for Ki-67 and a negative control for senescence, secondary RAW 264.7 macrophages that also have intrinsically high lysosomal activity [49] were labeled with these markers. These immortalized cells were always shown capable of being restimulated to divide and subsequently expressed high levels of Ki-67 regardless of culture time or passage number, displaying 100% Ki-67 staining even at passage 30 (Supplementary Figure 4.5). Interestingly, these cells began to express SA beta-gal and decrease Ki-67 with increasing confluence, seen previously in immortalized fibroblast cultures at high confluence [21, 50]. This is significant as the ability of immortalized and essentially transformed cancer-like cells to quiesce is not commonly known. Primary bone-derived murine macrophage cultures on plastic have already been shown to exhibit several characteristic features distinct from the transformed macrophage-like murine RAW 264.7 cell line commonly employed as a macrophage surrogate in cultures [51-53]. These differences include variances in morphology, cytokine secretion, receptor expression, proliferation, response to LPS, and metabolic output [31, 36]. These studies now confirm integral changes in macrophage proliferative capacity.

Endotoxin, a lipopolysaccharide (LPS) found on the membrane surface of gram negative bacteria [54], is commonly used to stimulate macrophages [36, 55]. To determine if macrophages might avoid senescence during perpetual stimulation that may occur at an infected implant site, both primary and immortalized transformed macrophages were treated with LPS in serum-based culture [31]. LPS delayed the onset of SA beta-gal expression in primary BMMΦs, but did not eliminate it (Figure 4.5), and also ameliorated SA beta-gal expression in RAW cells (Supplementary Figure 4.4). We previously reported reduced inflammatory cytokine secretion from primary macrophage cultures in continued presence of LPS in 21-day cultures [36]. We attributed this phenomenon to macrophage endotoxin tolerance. However, increased cell senescence in primary macrophages over time may also contribute to their attenuated cytokine response. This idea is supported by increased senescence seen in BMMΦs over 21-day cultures, even in the persistent presence of LPS stimulation (Figure 4.5).

Conclusions

This study identified important phenotypic changes that macrophages undergo in extended culture that decrease their competence over time, including a decreased ability to proliferate and phagocytose, both integral responses for proper implant surveillance and antimicrobial activity. This finding may explain macrophages' reduced ability to combat infection around biomaterials. Important future work should determine if macrophages become senescent and decrease their ability to phagocytose around implants in vivo. Understanding the mechanisms that predispose implant sites to infection years after device deployment will aid in better addressing this important clinical issue, perhaps also considering that senescent-state macrophages may increase throughout the duration of implantation. This study demonstrated that the commonly employed senescence-associated beta-galactosidase assay labels both quiescence and senescence cells in macrophage cultures, and revealed conditions inducing quiescence but not senescence in cultured immortalized macrophage cell lines. This is yet another difference between primary and immortalized macrophage cultures that produces inequities in their direct comparisons and perhaps their fidelity to macrophage in vivo behavior around implants. Future studies employing this SA beta-gal assay for macrophages should validate it against additional markers of senescence and proliferation. This study also found that, unlike senescent cells that display significantly decreased phagocytosis, quiescent cells have only slightly reduced but insignificantly different ability to phagocytose particles. This important functional measure distinguishes macrophage competence between normal and quiescent and senescent cells in extended culture.

Acknowledgements

This research was supported by National Institute of Health grant R01EB000894. We acknowledge PA Tresco, A Welm, R Hitchcock, and C Terry (all University of Utah, USA) for scientific critique and expert insight.

References

1. Anderson JM. Chapter 4 Mechanisms of inflammation and infection with implanted devices. Cardiovasc Pathol 1993;2(3):33S-41S.

2. Anderson JM. Multinucleated giant cells. Curr Opin Hematol 2000 Jan;7(1):40-47.

3. Chambers TJ, Spector WG. Inflammatory giant cells. Immunobiology 1982 Apr;161(3-4):283-289.

4. Bernatchez SF, Parks PJ, Gibbons DF. Interaction of macrophages with fibrous materials in vitro. Biomaterials 1996 Nov;17(21):2077-2086.

5. Rosengren A, Bjursten LM. Pore size in implanted polypropylene filters is critical for tissue organization. J Biomed Mater Res A 2003 Dec 1;67(3):918-926.

6. Helming L, Gordon S. Macrophage fusion induced by IL-4 alternative activation is a multistage process involving multiple target molecules. Eur J Immunol 2007 Jan;37(1):33-42.

7. Cannon GJ, Swanson JA. The macrophage capacity for phagocytosis. J Cell Sci 1992 Apr;101(Pt 4):907-913.

8. Anderson JM, Defife K, McNally A, Collier T, Jenney C. Monocyte, macrophage and foreign body giant cell interactions with molecularly engineered surfaces. J Mater Sci Mater Med 1999 Oct-Nov;10(10/11):579-588.

9. Jenkins SJ, Ruckerl D, Cook PC, Jones LH, Finkelman FD, van Rooijen N, et al. Local macrophage proliferation, rather than recruitment from the blood, is a signature of TH2 inflammation. Science 2011 Jun 10;332(6035):1284-1288.

10. Darouiche RO. Device-associated infections: a macroproblem that starts with microadherence. Clin Infect Dis 2001 Nov 1;33(9):1567-1572.

11. Murray DW, Rushton N. Macrophages stimulate bone resorption when they phagocytose particles. J Bone Joint Surg Br 1990 Nov;72(6):988-992.

12. Williams C, Aston S, Rees TD. The effect of hematoma on the thickness of pseudosheaths around silicone implants. Plast Reconstr Surg 1975 Aug;56(2):194-198.

13. Anderson JM, Rodriguez A, Chang DT. Foreign body reaction to biomaterials. Semin Immunol 2008 Apr;20(2):86-100.

14. Higgins DM, Basaraba RJ, Hohnbaum AC, Lee EJ, Grainger DW, Gonzalez-Juarrero M. Localized immunosuppressive environment in the foreign body response to implanted biomaterials. Am J Pathol 2009 Jul;175(1):161-170.

15. Litovchick L, Florens LA, Swanson SK, Washburn MP, DeCaprio JA. DYRK1A protein kinase promotes quiescence and senescence through DREAM complex assembly. Genes Dev 2011 Apr 15;25(8):801-813.

16. Korotchkina LG, Leontieva OV, Bukreeva EI, Demidenko ZN, Gudkov AV, Blagosklonny MV. The choice between p53-induced senescence and quiescence is determined in part by the mTOR pathway. Aging 2010 Jun;2(6):344-352.

17. Gary RK, Kindell SM. Quantitative assay of senescence-associated beta-galactosidase activity in mammalian cell extracts. Anal Biochem 2005 Aug 15;343(2):329-334.

18. Cristofalo VJ, Volker C, Francis MK, Tresini M. Age-dependent modifications of gene expression in human fibroblasts. Crit Rev Eukaryot Gene Expr 1998;8(1):43-80.

19. Linskens MH, Feng J, Andrews WH, Enlow BE, Saati SM, Tonkin LA, et al. Cataloging altered gene expression in young and senescent cells using enhanced differential display. Nucleic Acids Res 1995 Aug 25;23(16):3244-3251.

20. Guayerbas N, Catalan M, Victor VM, Miquel J, De la Fuente M. Relation of behaviour and macrophage function to life span in a murine model of premature immunosenescence. Behav Brain Res 2002 Aug 21;134(1-2):41-48.

21. Severino J, Allen RG, Balin S, Balin A, Cristofalo VJ. Is beta-galactosidase staining a marker of senescence in vitro and in vivo? Exp Cell Res 2000 May 25;257(1):162-171.

22. Sebastian C, Herrero C, Serra M, Lloberas J, Blasco MA, Celada A. Telomere shortening and oxidative stress in aged macrophages results in impaired STAT5a phosphorylation. J Immunol 2009 Aug 15;183(4):2356-2364.

23. Papadimitriou JM, Robertson TA, Walters MN. An analysis of the Phagocytic potential of multinucleate foreign body giant cells. Am J Pathol 1975 Feb;78(2):343-358.

24. Williams GT, Williams WJ. Granulomatous inflammation--a review. J Clin Pathol 1983 Jul;36(7):723-733.

25. Kurz DJ, Decary S, Hong Y, Erusalimsky JD. Senescence-associated (beta)-galactosidase reflects an increase in lysosomal mass during replicative ageing of human endothelial cells. J Cell Sci 2000 Oct;113 (Pt 20):3613-3622.

26. Holt DJ, Grainger DW. Multinucleated giant cells from fibroblast cultures. Biomaterials 2011 Jun;32(16):3977-3987.

27. Lawrence T. Macrophages and NF-kappaB in cancer. Curr Top Microbiol Immunol 2011;349:171-184.

28. Deane S, Selmi C, Teuber SS, Gershwin ME. Macrophage activation syndrome in autoimmune disease. Int Arch Allergy Immunol 2010;153(2):109-120.

29. Lynn AD, Kyriakides TR, Bryant SJ. Characterization of the in vitro macrophage response and in vivo host response to poly(ethylene glycol)-based hydrogels. J Biomed Mater Res A 2009 Aug 25.

30. McInnes A, Rennick DM. Interleukin 4 induces cultured monocytes/macrophages to form giant multinucleated cells. J Exp Med 1988 Feb 1;167(2):598-611.

31. Chamberlain LM, Godek ML, Gonzalez-Juarrero M, Grainger DW. Phenotypic non-equivalence of murine (monocyte-) macrophage cells in biomaterial and inflammatory models. J Biomed Mater Res A 2009 Mar 15;88(4):858-871.

32. Jay SM, Skokos E, Laiwalla F, Krady MM, Kyriakides TR. Foreign body giant cell formation is preceded by lamellipodia formation and can be attenuated by inhibition of Rac1 activation. Am J Pathol 2007 Aug;171(2):632-640.

33. Godek ML, Sampson JA, Duchsherer NL, McElwee Q, Grainger DW. Rho GTPase protein expression and activation in murine monocytes/macrophages is not modulated by model biomaterial surfaces in serum-containing in vitro cultures. J Biomater Sci Polym Ed 2006;17(10):1141-1158.

34. Rhoades ER, Orme IM. Similar responses by macrophages from young and old mice infected with Mycobacterium tuberculosis. Mech Ageing Dev 1998 Dec 1;106(1-2):145-153.

35. Kim JB, Han AR, Park EY, Kim JY, Cho W, Lee J, et al. Inhibition of LPS-induced iNOS, COX-2 and cytokines expression by poncirin through the NF-kappaB inactivation in RAW 264.7 macrophage cells. Biol Pharm Bull 2007 Dec;30(12):2345-2351.

36. Holt DJ, Chamberlain LM, Grainger DW. Cell-cell signaling in co-cultures of macrophages and fibroblasts. Biomaterials 2010;31(36):9382-9394.

37. Dimri GP, Lee X, Basile G, Acosta M, Scott G, Roskelley C, et al. A biomarker that identifies senescent human cells in culture and in aging skin in vivo. Proc Natl Acad Sci U S A 1995 Sep 26;92(20):9363-9367.

38. Leenen PJ, de Bruijn MF, Voerman JS, Campbell PA, van Ewijk W. Markers of mouse macrophage development detected by monoclonal antibodies. J Immunol Methods 1994 Sep 14;174(1-2):5-19.

39. Duong LT, Rodan GA. PYK2 is an adhesion kinase in macrophages, localized in podosomes and activated by beta(2)-integrin ligation. Cell Motil Cytoskeleton 2000 Nov;47(3):174-188.

40. Mantovani A, Sozzani S, Locati M, Allavena P, Sica A. Macrophage polarization: tumor-associated macrophages as a paradigm for polarized M2 mononuclear phagocytes. Trends Immunol 2002 Nov;23(11):549-555.

41. Gerdes J, Li L, Schlueter C, Duchrow M, Wohlenberg C, Gerlach C, et al. Immunobiochemical and molecular biologic characterization of the cell proliferation-associated nuclear antigen that is defined by monoclonal antibody Ki-67. Am J Pathol 1991 Apr;138(4):867-873.

42. Gown AM, Jiang JJ, Matles H, Skelly M, Goodpaster T, Cass L, et al. Validation of the S-phase specificity of histone (H3) in situ hybridization in normal and malignant cells. J Histochem Cytochem 1996 Mar;44(3):221-226.

43. Gretzer C, Emanuelsson L, Liljensten E, Thomsen P. The inflammatory cell influx and cytokines changes during transition from acute inflammation to fibrous repair around implanted materials. J Biomater Sci Polym Ed 2006;17(6):669-687.

44. Franceschi C, Bonafe M, Valensin S, Olivieri F, De Luca M, Ottaviani E, et al. Inflamm-aging. An evolutionary perspective on immunosenescence. Ann N Y Acad Sci 2000 Jun;908:244-254.

45. Lloberas J, Celada A. Effect of aging on macrophage function. Exp Gerontol 2002 Dec;37(12):1325-1331.

46. Bassaneze V, Miyakawa AA, Krieger JE. A quantitative chemiluminescent method for studying replicative and stress-induced premature senescence in cell cultures. Anal Biochem 2008 Jan 15;372(2):198-203.

47. Sutton JS, Weiss L. Transformation of monocytes in tissue culture into macrophages, epithelioid cells, and multinucleated giant cells. An electron microscope study. J Cell Biol 1966 Feb;28(2):303-332.

48. Sherwood SW, Rush D, Ellsworth JL, Schimke RT. Defining cellular senescence in IMR-90 cells: a flow cytometric analysis. Proc Natl Acad Sci U S A 1988 Dec;85(23):9086-9090.

49. Lees MP, Fuller SJ, McLeod R, Boulter NR, Miller CM, Zakrzewski AM, et al. P2X7 receptor-mediated killing of an intracellular parasite, Toxoplasma gondii, by human and murine macrophages. J Immunol 2010 Jun 15;184(12):7040-7046.

50. Yegorov YE, Akimov SS, Hass R, Zelenin AV, Prudovsky IA. Endogenous beta-galactosidase activity in continuously nonproliferating cells. Exp Cell Res 1998 Aug 25;243(1):207-211.

51. Sandeep Varma R, Ashok G, Vidyashankar S, Patki P, Nandakumar KS. Anti-inflammatory properties of Septilin in lipopolysaccharide activated monocytes and macrophage. Immunopharmacol Immunotoxicol 2010 Apr 12;doi:10.3109/08923971003739236.

52. Lin NJ, Hu H, Sung L, Lin-Gibson S. Quantification of cell response to polymeric composites using a two-dimensional gradient platform. Comb Chem High Throughput Screen 2009 Jul;12(6):619-625.

53. Yoon WJ, Ham YM, Yoo BS, Moon JY, Koh J, Hyun CG. Oenothera laciniata inhibits lipopolysaccharide induced production of nitric oxide, prostaglandin E2, and proinflammatory cytokines in RAW264.7 macrophages. J Biosci Bioeng 2009 Apr;107(4):429-438.

54. Ulevitch RJ, Tobias PS. Recognition of gram-negative bacteria and endotoxin by the innate immune system. Curr Opin Immunol 1999 Feb;11(1):19-22.

55. Ung DY, Woodhouse KA, Sefton MV. Tumor necrosis factor (TNFalpha) production by rat peritoneal macrophages is not polyacrylate surface-chemistry dependent. J Biomed Mater Res 1999 Sep 5;46(3):324-330.

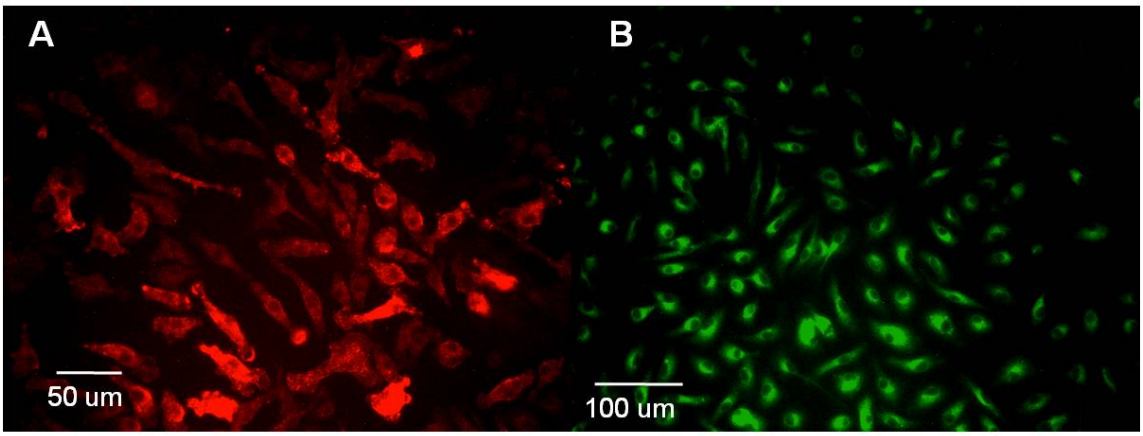

Supplementary Figure 4.1. Representative images of primary BMMΦs labeled with A) F4/80 macrophage maturity marker and B) M2 macrophage marker, CD206 (macrophage mannose receptor). These images indicate strong expression of these two phenotypic markers.

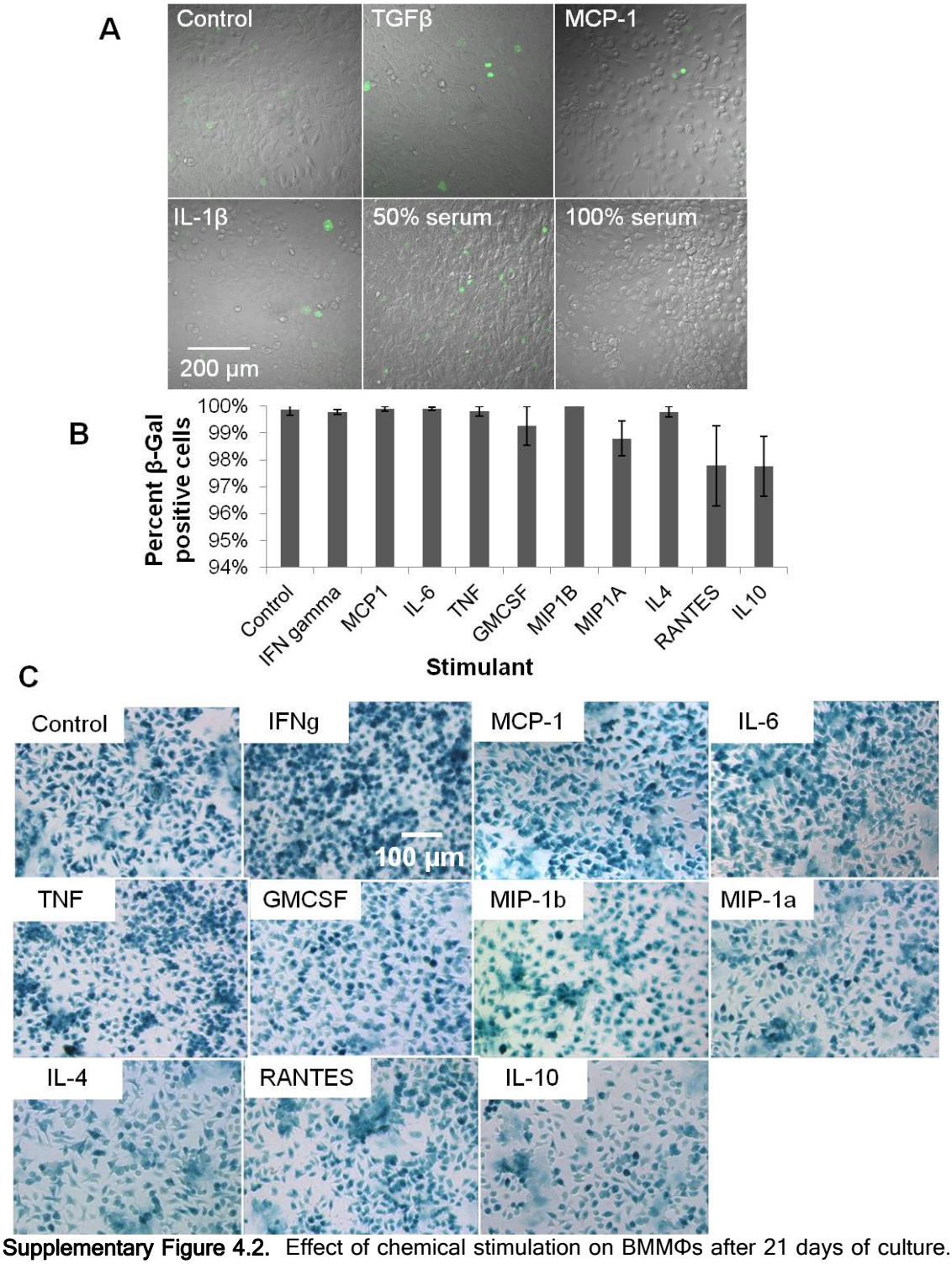

Supplementary Figure 4.2. Effect of chemical stimulation on BMMΦs after 21 days of culture. A) Overlay of brightfield and fluorescence confocal images of Ki-67 staining in cells after mitogen stimulation; B) Percent positive cells for SA beta-gal after cytokine stimulation; C) Color images of SA-beta gal (blue) assays after cytokine stimulation. No significant increases in Ki-67 expression or decreases in SA beta-gal were seen in response to stimulation, suggesting that these cells are senescent. One-way ANOVA with post-hoc Dunnett Multiple Comparisons Test was applied, comparing all conditions with the control. Significance is noted as $p<0.05$* and $p<0.001$ **.

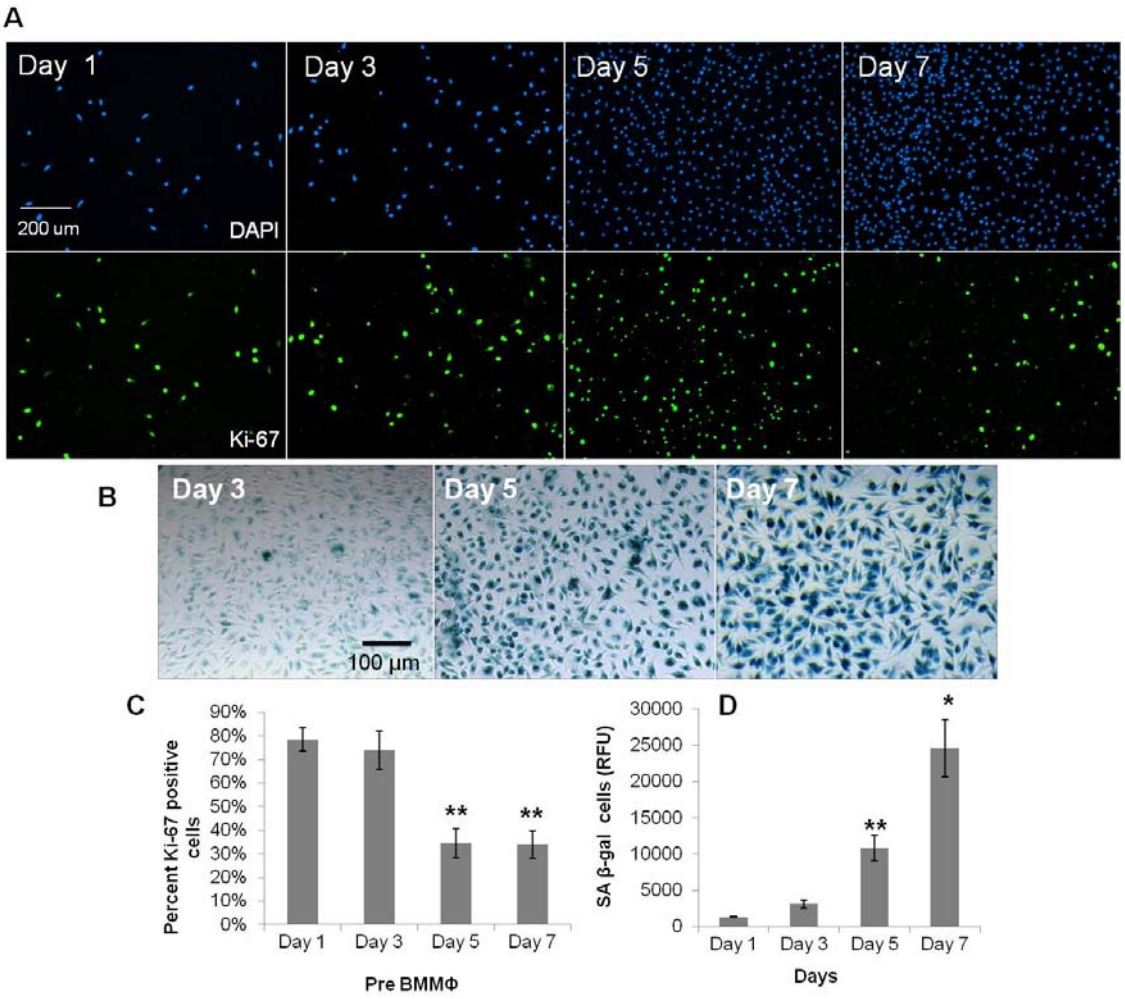

Supplementary Figure 4.3. Proliferative capacity of monocytes and bone marrow cells prior to full differentiation into bone-marrow macrophages during the first 7 days post-harvest. A) Fluorescent images of DAPI and Ki-67 labeling, and B) color images of SA beta-gal expression in predifferentiated BMMΦ cells. C) Percent positive cells for Ki-67. D) SA beta-gal expression using the fluorescent SA beta-gal assay. Decreasing Ki-67 labeling and increasing SA beta-gal staining indicate cellular quiescence. One-way ANOVA with post-hoc Dunnett Multiple Comparisons Test was applied, comparing all days to the day 1 condition. Significance is noted as $p<0.05$ * and $p<0.001$ **.

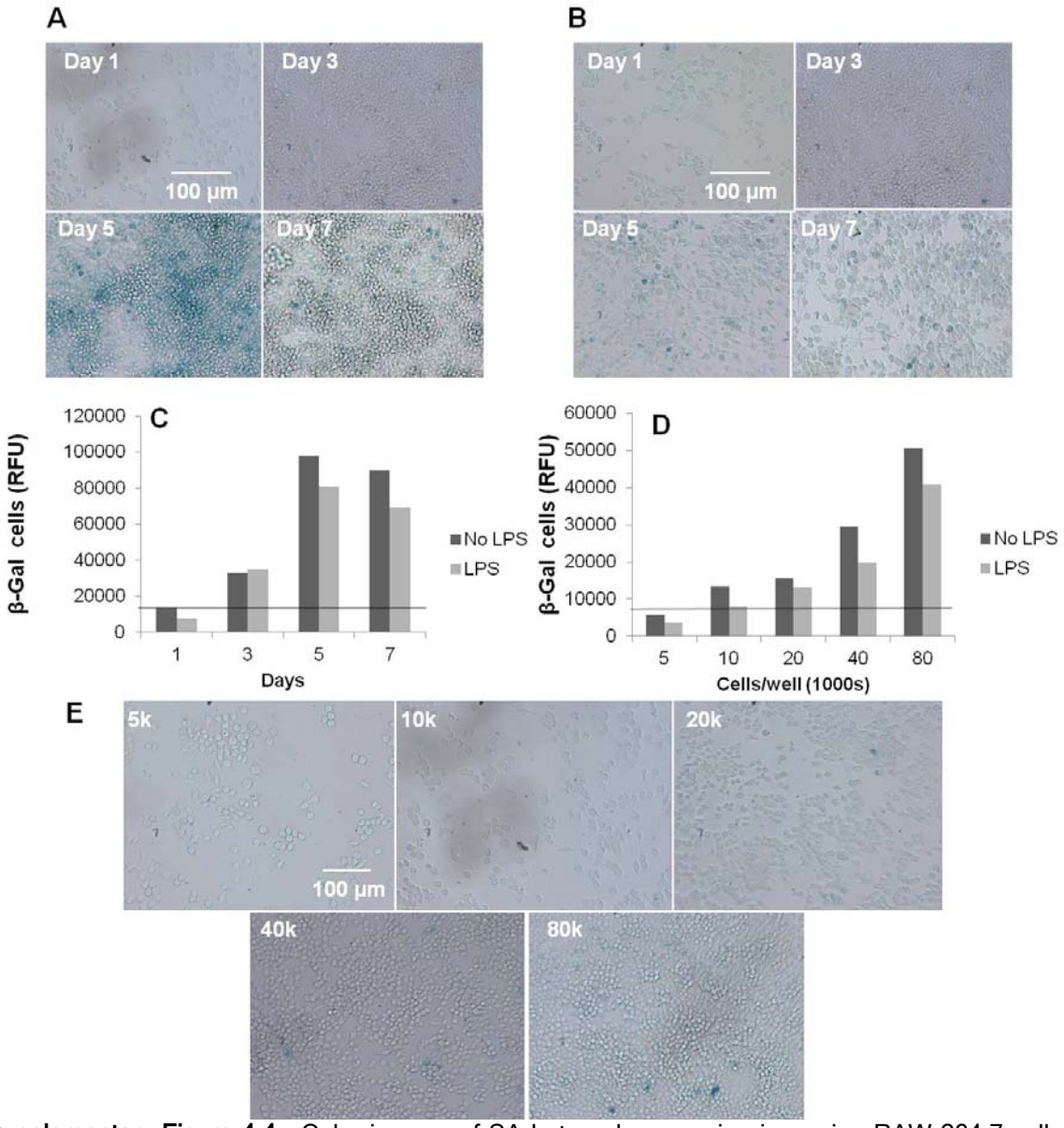

Supplementary Figure 4.4. Color images of SA beta-gal expression in murine RAW 264.7 cells during 7 days of culture: A) without, and B) with LPS stimulation. Graphical representation of fluorescent SA beta-gal C) over 7 days of culture, and D) with increasing confluence in the presence and absence of LPS stimulation; E) color images of SA beta-gal expression in RAW cells with increasing confluence over 24 hours. Positive SA beta-gal staining indicates quiescence in immortalize RAW cells. These data also indicate an ameliorated expression of SA beta-gal in response to LPS stimulation, indicating a decreased quiescence response. Cell lysates from 3 wells of RAW cells were physically combined for each condition prior to employing the fluorescent SA beta-gal assay. Horizontal bar represents the limit of detection for the assay.

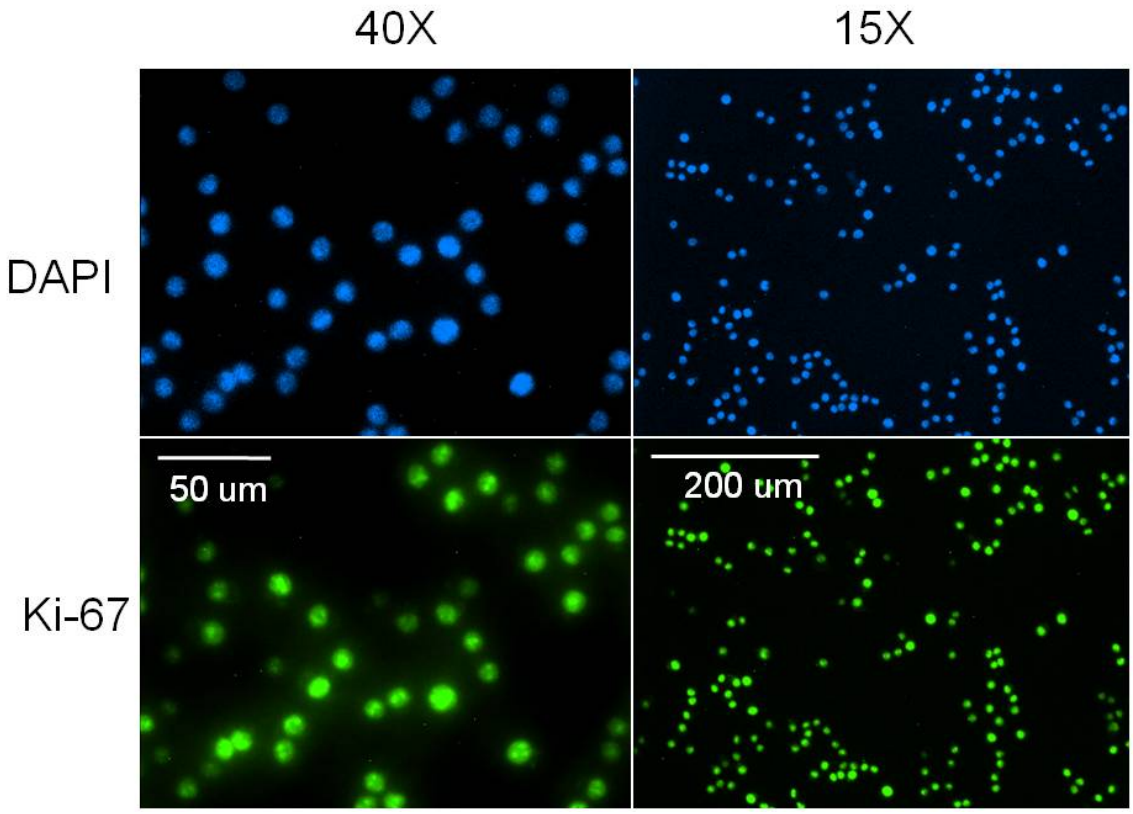

Supplementary Figure 4.5. Fluorescent images of DAPI and Ki-67 labeling in murine RAW 264.7 macrophage cells after 30 passages, signifying no decrease in RAW cell proliferative capacity with increased passages.

CHAPTER 5

SUMMARY AND FUTURE DIRECTIONS

Summary of results

This dissertation sought to address the hypothesis that cultured cells are not representative of in vivo cell behavior and this difference is exacerbated in immortalized cell lines compared to primary cells. The specific impact of this work can be summarized as follows:

Chapter 2 aimed to develop a more representative in vitro model and identify feedback mechanisms that may be necessary to recapitulate in vivo signaling. Data presented there demonstrated that:

- Primary and secondary macrophages are not equivalent in culture as shown by disparate responses to LPS exposure, cultured morphology, and cytokine production.
- Primary macrophages demonstrate endotoxin tolerance with repeated exposure to LPS in culture -- more representative of in vivo responses than secondary macrophages that did not exhibit this tolerance.
- Coculture of macrophages with fibroblasts is more representative of in vivo conditions than monocultures of either macrophages or fibroblasts based on cytokine signaling dynamics seen during coculture that are also seen in vivo but absent from monocultures.

These results were published in *Biomaterials*: Holt DJ, Chamberlain LM, Grainger DW. Cell-cell signaling in co-cultures of macrophages and fibroblasts. *Biomaterials* 2010;31:9382-94

Chapter 3 aimed to establish the existence and mechanism for formation of multinucleated fibroblasts in culture. Data presented there demonstrated that:

- Fibroblasts, like cultured macrophages, can form multinucleated cells in culture.

- Secondary fibroblasts can form multinucleate cells via fusion with other fibroblasts in the presence of secondary macrophage cultures.
- Primary fibroblasts can multinucleate in culture with or without the presence of primary or secondary macrophages, but not due to fusion, but rather senescence-associated nuclear division without cytokinesis.
- Primary multinucleated fibroblasts stain positive for replicative senescence.

These results were published in *Biomaterials*. Holt DJ, Grainger DW. Multinucleated giant cells from fibroblast cultures. *Biomaterials* 2011;32:3977-87.

Chapter 4 aimed to determine the potential macrophages have to senesce in culture. Data presented there demonstrated that:

- Primary macrophages undergo quiescence during high confluence cultures and senesce during longterm culture.
- Secondary macrophages undergo quiescence during high confluence cultures and longterm culture, but do not senesce.
- Senescence is delayed in primary macrophages, and quiescence is ameliorated in secondary macrophages in the presence of lipopolysaccharide stimulation.

These results have been accepted for publication in *Biomaterials* (July 2012)

Impact of this work

The work from this dissertation has further elucidated the in vitro phenotypes of macrophages and fibroblasts, two primary effector cells of the foreign body response. The first study analyzed intracellular signaling between macrophages and fibroblasts and identified what feedback systems resulted in the most relevant signaling patterns. We found that macrophages and fibroblasts in coculture had more representative cytokine secretion patterns of in vivo implant scenarios compared to monoculture. Where current models primarily involve only monoculture to assess biocompatibility of drugs and devices, this work may lead to the formation and adoption of more relevant in vitro models for drug and device testing.

The second study identified the existence of multinucleate fibroblasts. The foreign body response is often characterized by the amount of foreign body giant cells (FBGCs) present. FBGCs are often counted as any multinucleate cell found at the surface of an implant. The presence of multinucleate fibroblasts may confound these results. By identifying the existence of multinucleate fibroblasts, their potential presence can now be accounted for. Additionally, understanding the existence of multinucleate fibroblasts may aid in deciphering their role in various pathologies including, fibrosis, aging, and cancer, where their presence has been postulated.

The third study performed for this dissertation work identified the senescence of macrophages in culture. This phenotypic shift by macrophages could greatly impact their responsiveness in culture. Additionally, though the surfaces of implants are ostensibly coated in hundreds of macrophages indefinitely, if the macrophages are senescent and unable to respond to bacterial colonization, infection could proceed unchecked. Understanding this potential change in macrophage behavior may also enable more appropriate prophylaxis and treatment of infected implants.

Each of these studies have compared the behavior of primary versus secondary derived cells and have identified large disparities between them, with primary cells representing in vivo behavior more accurately than secondary cells. Though secondary cells are commonly employed in culture due to their ease of culture, cost effectiveness, and the lack of ethical concern associated with them, their use may yield misleading results. This work substantiates their variability and suggests use of secondary cells be validated against primary cells and/or in vivo systems.

In general this work has identified unique behavior elicited by both macrophages and fibroblasts in culture. This increased understanding of their behavior in various culture conditions will enable more accurate data interpretation and better experimental design in future studies. This dissertation work has also identified conditions where macrophages and fibroblasts better represent in vivo responses; however, further improvement can be made by adding increased sophistication to in vitro cultures including wounding and 3D growth . A proposal for these in vitro models is described later in this section.

Looking ahead[1]

Though the FBR is a ubiquitous phenomenon, there are ways to ameliorate its deleterious effects on implants; some of these methods are described below:

Genetic targets to impact the FBR

Through the use of knockout (KO) models, potential gene targets that could one day be treated with pharmacological agents or genetic engineering approaches have been identified to ameliorate the FBR.

MCP-1 is an important chemoattractant for macrophages and has been hypothesized to play a role in FBGC formation and the FBR. Kyriakides et al implanted cellulose ester filters and polyvinyl alcohol sponges in MCP-1 KO mice. They found FBGC numbers surrounding the filters were reduced by 75% and the sponges were reduced by 90% within MCP-1-null mice. They also found that the number of nuclei per cell was decreased in MCP-1-null mice. They did however still find an abundance of macrophages even though there were fewer or no FBGCs. Importantly, despite a reduced formation of FBGCs in MCP-1-null mice, capsule formation proceeded normally around the implants [1]. The pleiotropic and redundant nature of the signaling pathways could account for the continued capsule formation, even with a KO of a significant signaling molecule and a subsequent reduction in FBGC formation. This study indicates that MCP-1 would not be a useful target against the FBR.

This same group also looked at the effect thrombospondin 2(TSP2) had upon the FBR. They implanted polydimethylsiloxane (PDMS) into TSP2-null and control mice. After 4 weeks, they found that fibroblasts aggregated on the surface of implants in the TSP2-null mice, rather than as a monolayer, as in the control mice. Interestingly they found the collagenous capsule in the TSP2-null mice was highly vascularized and thicker than that formed in normal mice and consisted of abnormally shaped collagen fibers [2].

---

[1] This section has been adapted in part from the book chapter: Holt DJ, Grainger DW. Host Response to Biomaterials. Second Edition. An Introduction to Biomaterials and their Applications. Hollinger, JO.2011.ISBN-10:143981256X.

Another study added MMP-9 (a matrix metalloproteinase responsible for extracellular matrix remodeling) function-blocking antibodies to a macrophage culture and discovered a reduced ability of macrophages to fuse to form FBGC. This discovery prompted the Kyriakides group to study the effect MMP-9 had upon the FBR. They implanted cellulose ester disks and polyvinyl alcohol sponges into MMP-9 KO mice. After 4 weeks, they identified equal macrophage recruitment between wild-type and MMP-9 null mice. but found that null mice had decreased angiogenesis and increased capsule thickness compared to control animals [3], making MMP-9 a poor target against the FBR.

Plasma proteins such as fibronectin have been shown to modulate inflammatory cell recruitment and activation. Because of this, the Garcia group selected plasma fibronectin as a target to ameliorate the FBR. They implanted fibronectin KO mice with polyethylene terephthalate disks and observed the fibronectin depleted mice had a twofold thicker fibrous collagen capsule compared to control wildtype animals. Additionally, though acute leukocyte recruitment and macrophage numbers were unaltered in the KO mice, the formation of FBGCs was three times higher, indicating fibronectin as a poor FBR target. It has been hypothesized that FBGCs form from frustrated macrophages, [4] and where the absence of fibronectin could perturb macrophage adherence, this KO could induce their fusion to form FBGCs.

SPARC (secreted protein, acidic and rich in cysteine) is a protein that modulates the interaction of cells with the ECM. After 4 weeks, SPARC-null mice implanted with polydimethylsiloxane (PDMS) and cellulose filters displayed significantly reduced vascular density and the associated collagen fibers were smaller, less mature and more uniform compared to wildtype animals. Significantly the thickness of the capsule was decreased in SPARC-null mice compared to wildtype [5], indicating SPARC could be a viable FBR target.

Significantly, though many signals are prominently found in the context of the FBR, their absence has thus far not equated to the absence of the FBR. As mentioned previously, this may be due to the redundancy of the signaling pathways within the body that enable other signaling mechanisms to proceed in the absence of others. Interestingly, KOs of targets that are hypothesized to reduce capsule thickness due to an alteration in the effector cells of the FBR can actually result in thicker capsules. However, the absence of some signals such as SPARC has been shown to reduce capsule thickness and therefore could be used to ameliorate the FBR. Due to the complexity and

overlapping of signaling pathways, complete elimination of a fibrous capsule or localized inflammatory cells surrounding implants may not be achievable through eliminating pieces of signaling pathways. Eliminating entire signaling pathways or major players such as macrophages may provide more promise. Clodronate for example can selectively deplete macrophages, and may be able to mitigate the FBR if applied locally [6]. However, the consequences of eliminating major players may yield more damaging consequences than the FBR.

Increasing porosity to reduce the FBR

To increase implant-associated vascularity and associated transport and perfusion, tissue infiltration, and reduced overall FBR magnitude, biomaterials with controlled pore size and void fractions are often used. Interestingly, Rosognren *et al.* identified porous membranes or filters with pore sizes small enough to prevent macrophage infiltration that exhibited a more pronounced FBR when compared to membranes with pore sizes large enough to enable macrophage infiltration [7]. Additionally, they found that filter-associated capsule formation was correlated with macrophages found outside the filters as opposed to those infiltrating them. Filters with the largest pore sizes had the most macrophages residing in the internal porous structure, and the fewest found to the outside. They also found an increased vascularity within the filters in the larger pore sizes compared to smaller ones. Similar results showing a decreased FBR and increased implant site vascularity are described by Ward *et al.* [8] and Brauker *et al.* [9]. Others have also reported increased vascularity with increased porosity [10-12].

Table 5.1 shows an increase in vascularity adjacent to implants with increased porosity. This trend was seen with various porous polymers including cellulose, PTFE, polyurethane, and acrylic polymers. Macrophage penetration and colonization of the implant pores appears to promote angiogenesis over FBR fibrosis. However, though increased porosity of synthetic material decreases the FBR, macrophage insult and subsequent fibrous encapsulation still occur.

Table 5.1. Comparison of implant pore size, cell penetration, vascularity, and relative FBR. Adapted from Brauker et al, JBMR 1995 29(12) [9], additional references include [7, 8, 13].

Implant Pore Size (μm)	Cell Penetration	Close Vascular Structures	Relative FBR
0.22	No	No	++
0.45	No	No	++
0.6	No	No	++
0.65	No	No	++
0.8	Yes	Yes	+
1	Yes	Yes	+
3	Yes	Yes	+
5	Yes	Yes	+
8	Yes	Yes	+
10	Yes	Yes	+
30	Yes	Yes	+
60	Yes	Yes	+

Elimination of synthetic material to mitigate the FBR

Every synthetic material implanted in the body instigates a FBR [14-16]. Nondegradable solid biomaterials including polymers such as biostable polyurethanes [8], poly(2-hydroxyethyl methacrylate) pHEMA [17], polydimethylsiloxane (i.e., silicone rubber), polyethylene and poly(tetrafluoroethylene) (PTFE, i.e., Teflon®) [9], metals and ceramics are all known to become encapsulated with a largely avascular, highly cellularized fibrotic capsule [2].

Synthetic polymeric biomaterials such as polyurethanes do not actively promote either healing or deter the FBR. They lack intrinsic cell adhesion motifs and nonspecifically adsorb host proteins that can engage inflammatory cells. Despite the array of sophisticated synthesis and fabrication techniques available for synthetic polymers, a thin denatured protein layer on the surface of these polymers leads to encapsulation. Thus, the elimination of synthetic material and the use of natural material may provide the best route to mitigating the FBR.

Degradable materials

Temporary implants such as degradable scaffolds are often fabricated using synthetic degradable materials such as polyesters and polyurethanes [18-20]. Degradable sutures, bone plates and screws, and other orthopaedic devices made of degradable polyesters resolve their FBR

once degraded [21-23]. Several degradable synthetic materials are currently employed in device applications including polyurethane[24], poly(L-lactic) acid (PLLA)[25], copolymers of polylactic and polyglycolic acid (PLGA)[26, 27], and polycaprolactone (PCL)[27-29]. Device degradation significantly impacts the duration of the FBR, with an increase in material degradation rate corresponding to a decreasing FBR [28]. Dogma suggests resolution of the FBR occurs upon the complete disintegration and metabolism of device material byproducts, leaving no interface between tissue and implanted materials. Many times the approach intends for the implanted synthetic structure to be broken down over time by hydrolytic and enzymatic processes at the defect site, providing a temporary template for host cells to conduct repair. While degradation byproducts are designed to be innocuous and readily cleared, accumulation of the most seemingly benign residues can become problematic and reach levels sufficient to induce inflammatory responses and compromise healing[30]. Thus in the context of minimizing the FBR, degradable natural materials may provide the best alternative for bulk implant materials for appropriate applications. For example, collagen gel implants have shown excellent biocompatibility and decreased FBR compared to synthetic degradable materials [31-33].

Summary

The FBR has thus far been an insurmountable problem, but the incorporation of the methods described above, may work to ameliorate and the negative consequences of the FBR to implanted materials and enable their more longterm success. Though due to the complex nature of the foreign body response and redundant signaling pathways, the complete elimination of the FBR may require the complete elimination of anything foreign or synthetic. However, naturally-derived materials still require much optimization for use in many implant applications. Thus there exist distinct directions to focus FBR elimination efforts including, “masking” synthetic material, using pharmacological or genetic approaches to modulate key FBR modulators, or utilizing natural material in medical implants. Importantly some implant applications would be ineligible for use with any one specific strategy, for example glucose sensors and pumps require synthetic material and cannot be made entirely of natural components. Tissue engineering strategies and ultimately organ engineering may provide a solution to some implant scenarios (e.g., replacing

glucose sensors and pumps with a pseudo pancreas), but are infantile in their development and may still suffer from host attack. Thus, the solution to completely resolving the FBR, especially in the immediate future, will likely lie in the combination of multiple approaches elegantly executed.

Next steps

Though coculture of macrophages and fibroblasts provided more representative signaling behavior than monocultures as described in Chapter 2, this model could be improved by addressing missing key in vivo FBR events, including fibrosis, inflammatory cell migration, and cytokine signaling in response to an implant. The incorporation of these events in an in vitro model may be able to provide a more representative in vitro model for studying the foreign body response as well as provide a more relevant platform for device screening compared to current in vitro models that do not address these events. Specific experiments for this future work are proposed below in the preliminary study.

Chapter 3 identified culture conditions and mechanisms by which primary and secondary fibroblasts multinucleate. However, further experiments identifying changes in phenotypic behavior of these cells such as metabolic rates and products, collagen secretion and ability to phagocytose etc. would be valuable as these behaviors may affect the host response to implants in vivo [2, 8, 9, 14-16, 34-40]. Important future work will be to identify if this phenotype exists at the surface of an implant in vivo. Macrophage- and fibroblast-specific markers, (such as F4/80, CD14, CD40, macrophage mannose receptor (MMR), CD11b, and CD18 for macrophages [41, 42] and FSP-1, FGF-1, and FGFR-1 for fibroblasts [43, 44]) could be stained around implants in vivo to determine the precise origin of the multinucleated cells. Macrophages and fibroblasts labeled with long lived intracellular red and green dyes, transfected or obtained from genetically engineered mice to express red and green fluorescent proteins can also be injected/implanted into animal models to determine 1) in vivo fusion or mitosis without cytokinesis and 2) confirm multinucleated cells of macrophage or fibroblastic origin as has been demonstrated previously for fusion experiments [42, 45].

Chapter 4 identified culture conditions by which primary macrophages senesce. Future studies could explore additional conditions by which macrophages senesce, and importantly

determine the Hayflick limit of this cell type. Future work identifying changes in macrophage phenotypic responses due to quiescence and senescence including: phagocytosis, enzyme and cytokine secretion, and external receptor expression would be valuable as these behaviors determine the activity and consequently response of macrophages to both implants and invading pathogens in vivo [40, 46-48]. Macrophage quiescence and senescence in vivo could explain the decreased activity macrophages display over time and may address the risk implants have to become infected years after surgery even when ostensibly coated in hundreds of macrophages. Essential future work would be to identify if this phenotype exists in vivo at implant sites. Tissue sections surrounding implants could be stained for senescence-associated betagalactosidase (SA betagal) expression in surrounding cells. Colabeling experiments could identify colocalization of SA betagal specifically in macrophages, using macrophage-specific markers: F4/80, CD14, CD40, macrophage mannose receptor (MMR), CD11b, and CD18 [41, 42]. Animals could also be inoculated with bacteria such as *Staphylococcus aureus* (commonly employed for rodent infection models [49]) to 1) verify the propensity of the implant to become infected and 2) determine if SA betagal expression could decrease in macrophages over time (indicating senescence rather than quiescence as SA betagal has been shown to be expressed during both resting states in macrophages, detailed in Chapter 4). The injection of fluorescently labeled macrophages using a long lived intracellular dye [42] into a rodent tail vein [50] after bacterial challenge could also determine the recruitment of new macrophages to the implant site in addition to resident macrophages that may be quiescent. Determining the number of active macrophages after bacterial insult (those not expressing SA betagal), could shed light on the mechanism of infection of implants after long periods of times. Multiple time points could be tested to analyze the threshold of time at which infection may become more prevalent, and potentially correlate this with SA betagal expression in implant-resident macrophages.

Preliminary study: improved in vitro cell culture model of the FBR

Though the FBR is a nearly universal response to implanted materials of widely varying properties and has been studied for decades, the precise mechanisms by which it is manifested

are largely unknown. The consequence of not fully understanding this process impedes the development of more successful longterm indwelling devices such as glucose sensors, neural recorders, orthopedic implants and many other longterm devices [51-55]. A greater understanding of the FBR will enable better development of materials and therapies to combat its deleterious effects against implanted material. A highly controllable in vitro model will aid in deciphering this complex phenomenon. Additionally a more representative in vitro model of the FBR will enable: 1) increased fidelity of materials and device biocompatibility testing prior to in vivo implantation, 2) decreased screening costs compared to in vivo studies, 3) more accurate high throughput testing, and 4) increased identification of materials with a dampened FBR.

Current in vitro models of the foreign body response involve culturing macrophages or fibroblasts to confluency on tissue culture polystyrene (TCPS) and then placing the material to be tested on top of the layer of cells [56, 57] or culturing cells on top of the material [58-60]. This rudimentary design is unable to properly recapitulate semblance of a fibrous sheath, cell migration, and changes in cellular phenotype with respect the implant interface as seen in vivo.

Cocultures employing both macrophages and fibroblasts, two primary effector cells of the FBR, yielded promising results, showing feedback mechanisms representative of in vivo conditions (Chapter 2) [61]. However, this model is inadequate to recapitulate fibrosis, ubiquitous to nearly all implanted materials,

A previous model aimed at addressing multiple aspects of the FBR yielded promising results. Reichert et al. cultured a mixed population of the neural cell types known to play a major role in the observed in vivo tissue reactions, such as neurons, astrocytes, and microglia, to confluency, and placed a stainless steel wire over the top of them [62]. In another culture dish, they also addressed tissue wounding occurring in vivo by culturing the cells to confluency and then scraping a portion of them away. They found a measure of gliosis, seen in vivo, was replicated in their system with infiltration of glial cells into the wound area and around the wire, surrounding hypertrophic astrocytes, and a reduced number of neurons. These results indicated that cells in vitro could respond to a device similar to in vivo cellular response.

We established a comparable model to recapitulate integral aspects of the in vivo FBR, consisting of cocultured macrophages and fibroblasts interfaced with a model biomaterial

"implant" on the same size scale as cells. The small scale of the wire readily enabled analysis of interfacial changes between the cells and biomaterial placed in culture. Cell localization, phenotypic alterations and collagen production with relation to the cell-implant interface were assessed. Events comparable to those that occur in vivo adjacent to implants, such as macrophage and fibroblast recruitment and organization [36, 63], altered cellular phenotype including upregulation of macrophage marker CD14, seen in activated macrophages [41, 42] and upregaulation of αSMA, seen in fibrotic fibroblasts [64-67] adjacent to implants were seen. A measure of fibrous encapsulation, prominent surrounding implants in vivo [2, 8, 9, 14-16, 34-39] was noted as demonstrated by increased staining of Sirius Red, a collagen-specific dye. This model may readily enable a better screening process for materials prior to in vivo implantation as well as provide a more accurate model to study the FBR in a controlled in vitro system.

Methods and materials

Primary fibroblasts were harvested from the ear dermal tissue of 3- to 4-month-old male C57BL/6 mice, while monocytes and hematopoietic cells precursor cells were harvested from the bone marrow and differentiated into macrophages using a previously established protocol[7]. Primary fibroblasts (5,000) and macrophages (20,000) were cultured in 96 well plates in physical contact with one another for 10 days. This ratio was selected to prevent the more highly proliferative fibroblasts from overtaking the surface of the well.

Implants were made of stainless steel flat wire (large: 76.2 μm high and 254 μm wide, medium: 25.4 μm high and 76.2 μm wide, and small: 12.7 μm high and 63.5 μm wide). These dimensions were selected so that the implant would be on the same size scale and therefore plane as the cells, and readily enable imaging interfacial changes. The size of these implants is also useful in representing electrodes, leads, and sutures, that are on the same size scale as the implants selected for this study, and commonly implanted in vivo [68, 69].

Brightfield microscope images were taken of live cells. Cells were stained with a green Vybrant® CFDA SE or a red Cell Trace Far Red DDAO-SE long lived intracellular dye in order to distinguish between fibroblast and macrophage populations during coculture. A fluorescently tagged macrophage activation marker, anti-CD14, was added to cultures to determine changes in

activation near the implant interface. Cell nuclei were stained with DAPI. Sirius Red was used to stain cells for collagen production [70].

Results

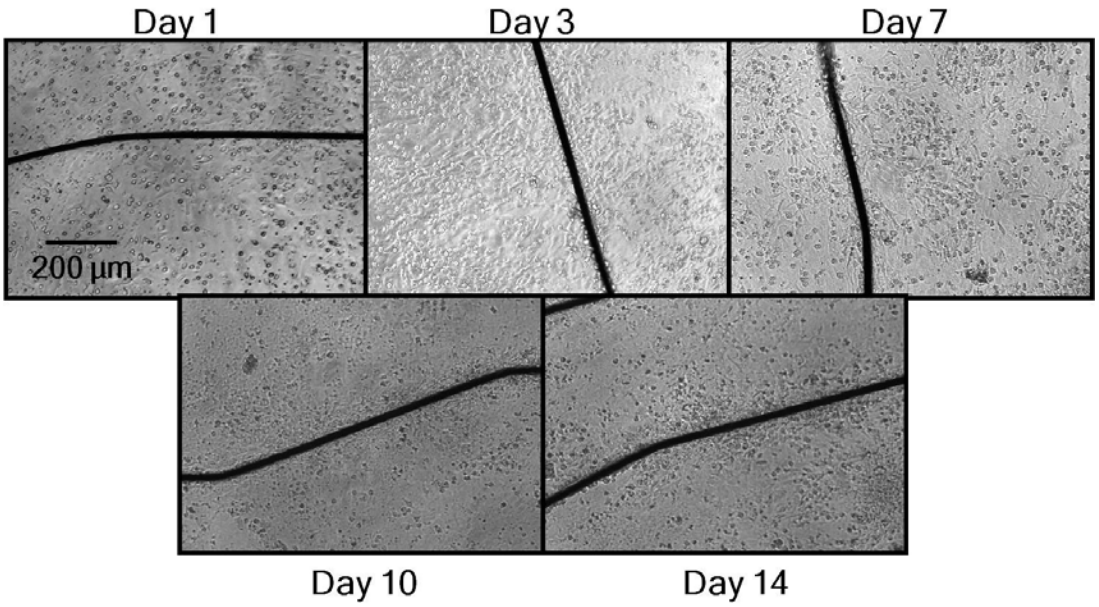

Figure 5.1. Brightfield images of cocultured macrophages and fibroblasts over a period of 10 days (a time required for many aspects of the FBR to develop in vivo [71]). This figure shows increased cell migration to the implant interface over time. Representative images were selected from three independent replicates.

We were able to see migration, localization and distribution of macrophages and fibroblasts adjacent to implant surfaces (Figure 5.1), regardless of implant size (Figure 5.2) at short (Figure 5.6) and longterm (Figure 5.7) culture times, comparable to that seen in vivo [36, 63]. Increased collagen, prevalent in vivo [2, 8, 9, 14-16, 34-39], was detected using the Sirius Red Assay at the interface of the implant in this culture system (Figure 5.3). Also, upregulation of macrophage and fibroblast activation markers, seen in vivo [41, 42, 64-67], were detected in this culture model (Figures 5.4 and 5.5).

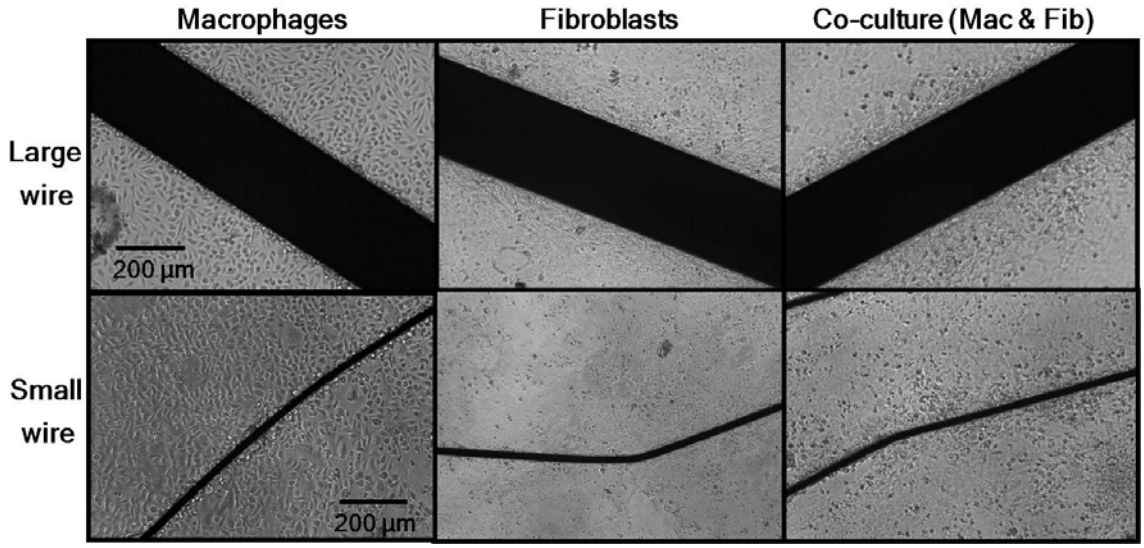

Figure 5.2. Brightfield images of large (top row) and small (bottom row) flat wires in cultures of macrophages only (column 1), fibroblasts only (column 2), and macrophages and fibroblasts in direct contact (column 3) after 10 days of culture. This figure shows increased cell localization near the implant interface regardless of cell type and implant size. Representative images were selected from three independent replicates.

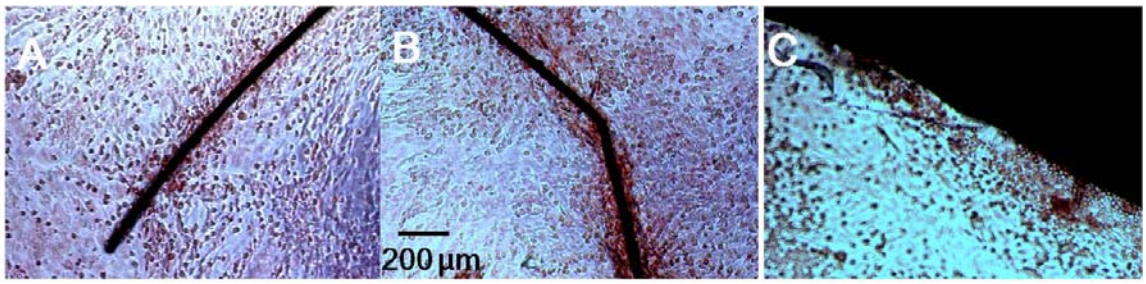

Figure 5.3. Brightfield images of Sirius Red stained (A and B small and (C large flat wires after 10 days of fibroblast and macrophage coculture. This figure shows increased red stain, and therefore collagen produced adjacent to the implant interface. Representative images were selected from three independent replicates.

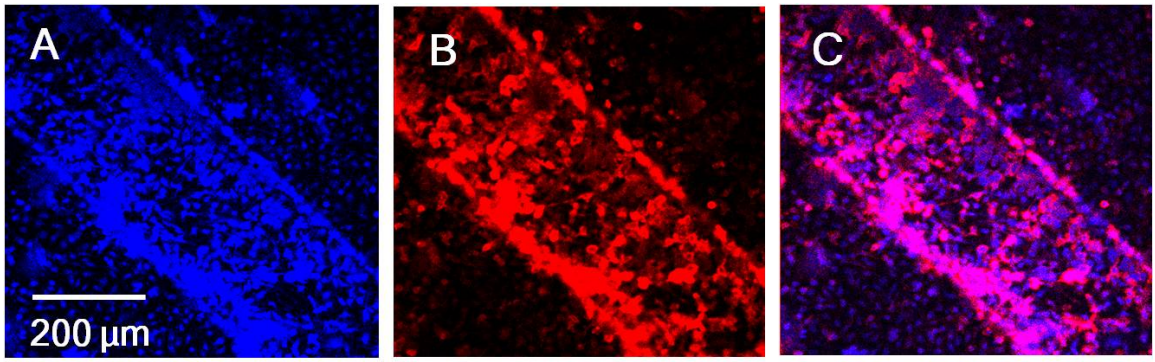

Figure 5.4. Confocal images of A) DAPI, B) macrophage marker–CD-14, and C) an overlay of the red and blue channels. This figure shows increased CD-14 intensity adjacent to the implant compared to distal from the implant. This is due to increased cell number at the implant interface and increased CD-14 expression per macrophage adjacent to the implant (as seen by dim CD-14 staining per macrophage distal to the implant). Representative images were selected from three independent replicates.

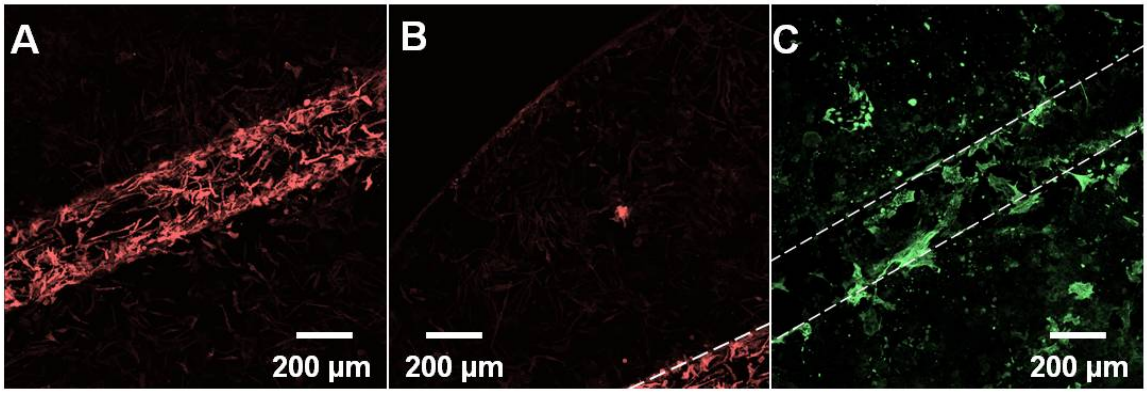

Figure 5.5. Confocal images of anti-CD14 labeling in BMMΦs cultured with a stainless steel wire (A and B). These images show an increased intensity of CD-14 labeling in cells adjacent to an implanted wire. C) α-smooth muscle actin (α-SMA) staining in a mixed population of primary BMMΦs and primary fibroblasts adjacent to an implanted stainless steel wire. Upregulation of CD-14 and α-SMA are both seen in vivo at implant surfaces [41, 42, 64-67]. Representative images were selected from three independent replicates.

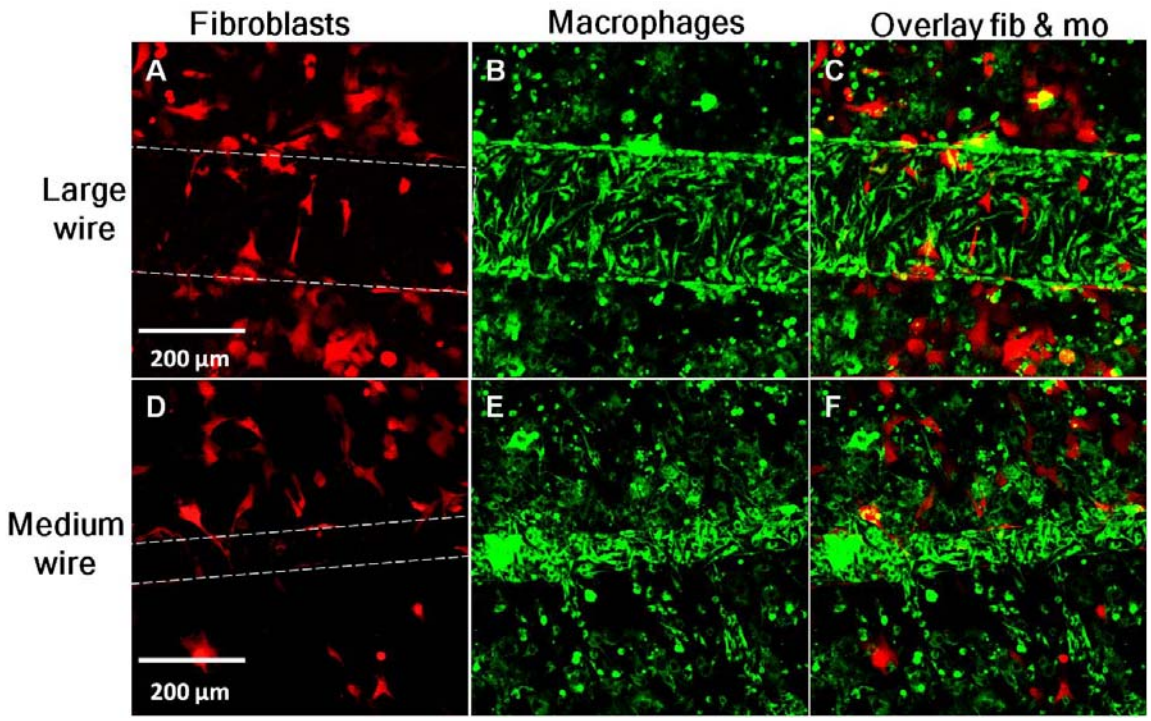

Figure 5.6. Confocal images of a coculture of prelabeled fibroblasts (red, Column 1) and macrophages (green, Column 2) and an overlay (Column 3) of red and green channels surrounding large (Top Row) and medium (Bottom Row) flat wire after 3 days of culture. This image shows a higher affinity for the implant surface in macrophages compared to fibroblasts. This phenomenon is consistent with implants in vivo where macrophages are found 1-2 cell layers thick directly adjacent to implants [36, 63]. Representative images were selected from three independent replicates.

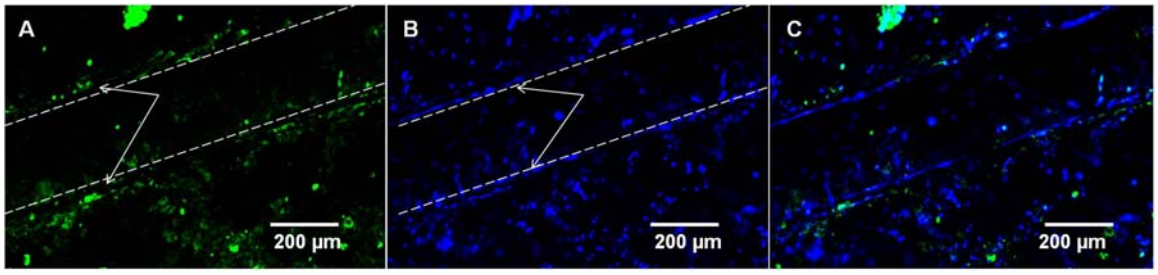

Figure 5.7. Confocal images of cocultured prelabeled fibroblasts and macrophages surrounding large flat stainless steel wire after 7 days of culture. A) Green fibroblast and B) blue macrophage channels are shown. C) Overlay of green and blue channels revealing labeled macrophages and fibroblasts. This image shows macrophages directly adjacent to implants and fibroblasts more distal (both denoted by arrows). This distribution is consistent with in vivo macrophage and fibroblasts organization [36, 63]. Representative images were selected from three independent replicates.

Discussion and future work[2]

We were able to successfully develop and characterize an in vitro model that is able to recapitulate in vivo: migration of FBR-relevant cells (i.e. macrophages and fibroblasts), increased collagen (detected using the Sirius Red Assay at the interface of an implant), increased expression of macrophage and fibroblast activation markers, and distribution of macrophages and fibroblasts adjacent to an implant.

It is difficult to elucidate if cell localization near the implant is due to an active foreign body response or if it is simply due to the presence of a material with increased surface area for cells to attach to. To address this issue, inflammatory cytokines should be stained in situ to determine if an active cytokine gradient is formed in response to the implant.

The increased collagen staining seen in Figure 5.3 may due to increased collagen or simply increased cell density which may be nonspecifically stained with Sirius Red. A collagen specific antibody should be used in situ which will eliminate any misleading nonspecific binding. Confocal reflection microscopy can also be utilized to determine collagen alignment adjacent to the implant surface, as highly organized and dense collagen is seen in vivo adjacent to implant surfaces compared to distally found more disperse and randomly aligned fibrils [72-75].

Though this two-dimensional (2D) model has the potential to improve upon current 2D systems, it is inherently missing critical aspects of the in vivo FBR. 2D systems cultured on rigid TCPS plastic are inherently flawed for several reasons, including the fact that TCPS is a foreign material not found natively within the body and elicits a dramatic FBR when implanted [76, 77]. Furthermore, TCPS is a rigid surface to which cells are not accustomed, and they are never grown as a monolayer or sandwiched in between TCPS and a biomaterial in vivo as they are in current in vitro models. Thus any in vitro model of the FBR will be confounded by the presence of TCPS. Other studies have identified this problem and coat TCPS with collagen, laminin, fibronectin, or other naturally-derived materials in order to better represent the in vivo condition [78-81]. However, these studies 1) often only implement a single adhesion protein, 2) still possess a culture surface more rigid than any in vivo extracellular matrix (ECM) protein (not attached to

[2] A more detailed expansion on this section can be found in the written proposal for Dolly Holt.

solid TCPS), and 3) do not address the intrinsic constraints of 2D cell culture. These constraints are not seen in vivo and may be just as foreign as TCPS, also producing confounding results.

Every implant in the body will create a wound, yet this critical feature is inherently absent from 2D culture. In a 2D system, wounding and subsequent implantation cannot be duplicated, as wounding will merely remove the cells, preventing them from coming into contact with the device. In vivo, though a wound is created, cells remain on all sides of the implant, enabling their subsequent response to that implant. In contrast, a three-dimensional (3D) environment would allow for wounding and subsequent implantation in vitro while the cells are still able to be in contact with the foreign material, similar to the in vivo condition, where a confluent 3D construct can be sliced through (analogous to slicing in vivo) and allow an implant to be placed in the previously wounded area.

Significantly, another missing aspect in 2D in vitro models is the ability to analyze 3D fibrosis, a ubiquitous in vivo phenomenon around most implants. Current models analyze production of TGF-β, procollagen in the media, or even collagen adhered to the plastic tissue culture surface dish, but are not able to recapitulate the 3D collagenous encapsulation that occurs in vivo. In vitro models are known to have incomplete procollagen processing and poor matrix formation compared to in vivo [82]. To combat this, efforts are made to artificially stimulate the environment to increase collagen production. One example of this is known as a “scar-in-a-jar” that adds exogenous dextran sulfate to increase the “molecular crowding” in the Petri dish, resulting in increased collagen production [82]. However, it has been shown that cells grown in 3D produce significantly more ECM than cells in 2D culture [83]. Perhaps this is due to cells being able to grow and behave in their native 3D confirmation. When cultured in a 3D scaffold, FBR-relevant cells will likely be able to naturally produce increased collagen, eliminating the need to stimulate their production artificially.

In vitro models constrained to 2D can only address certain aspects of cell inflammatory signaling and cannot adequately address more complex cellular dynamics such as fibrosis, implant-specific signaling, and 3D localization and phenotypic expression of macrophages and fibroblasts at the implant surface. In vivo, the FBR is marked by localization and phenotypic alterations of macrophages and fibroblasts, increased and highly oriented collagen production,

and increased concentrations and localization of inflammatory cytokines adjacent to implant surfaces. Future studies could address these issues by culturing a mixed population of macrophages and fibroblasts, both critical to the FBR, in 3D naturally-derived scaffolds made of multiple ECM proteins which will: 1) serve to stimulate 3D growth, 2) enable increased ECM production, 3) remove contact of the cells by any foreign material (other than that implanted), importantly 4) enable 3D encapsulation of an implant by cell-secreted ECM and 5) enable actual wounding and implantation more similar to that seen in vivo.

The use of an in vitro model over an in vivo model will still enable highly controlled mechanistic studies that are capable of high throughput testing. Human cells in lieu of animal cells can also be employed with this 3D in vitro model, compared to traditional animal models. Implementation of a more physiologically relevant in vitro model will facilitate more accurate material and device screening for highthroughput biomaterial response testing and provide a more representative yet simple tool to further investigate mechanisms of the foreign body response.

3D cell culture has been proven to produce more accurate and relevant cell morphology and behavior and should allow for a more representative in vitro model of the FBR for fundamental mechanistic studies. Additionally, an improved ability to replicate in vivo cell-cell interactions and responses to a surgical wound and subsequent device implantation should provide a more realistic model for screening the FBR to new biomaterials and to study basic FBR mechanisms.

Additionally, accurate models will need to incorporate proper serum and proper serum levels. Many models continually expose cells to fetal serum. This can produce misleading results due to the presence of perpetual fetal serum that is only seen during 1) fetal development and not adulthood (which most assays intend to model) and 2) acute phase healing that subsides after hemostasis in vivo. A more representative model could be simulated with a low level of serum such as 2% adult serum for the first 24 hours (as has been used in other primary cell culture models [62]), levels found at the in vivo wound site, and would provide the necessary growth factors that have been shown to remain upregulated at implant sites [84-86]. However after acute

stimulation with serum, enriched serum-free media would be most representative of the chronic in vivo scenario.

Due to the complexity of in vivo models and insufficiently representative in vitro models, the FBR remains a poorly understood phenomenon. The scientific community would greatly benefit from a properly designed 3D in vitro model capable of recapitulating in vivo FBR events, currently unattainable with existing 2D models and growth conditions.

References

1. Kyriakides TR, Foster MJ, Keeney GE, Tsai A, Giachelli CM, Clark-Lewis I, et al. The CC chemokine ligand, CCL2/MCP1, participates in macrophage fusion and foreign body giant cell formation. Am J Pathol 2004 Dec;165(6):2157-2166.

2. Kyriakides TR, Leach KJ, Hoffman AS, Ratner BD, Bornstein P. Mice that lack the angiogenesis inhibitor, thrombospondin 2, mount an altered foreign body reaction characterized by increased vascularity. Proc Natl Acad Sci U S A 1999 Apr 13;96(8):4449-4454.

3. MacLauchlan S, Skokos EA, Meznarich N, Zhu DH, Raoof S, Shipley JM, et al. Macrophage fusion, giant cell formation, and the foreign body response require matrix metalloproteinase 9. J Leukoc Biol 2009 Apr;85(4):617-626.

4. O'Neill LA. Immunology. How frustration leads to inflammation. Science 2008 May 2;320(5876):619-620.

5. Puolakkainen P, Bradshaw AD, Kyriakides TR, Reed M, Brekken R, Wight T, et al. Compromised production of extracellular matrix in mice lacking secreted protein, acidic and rich in cysteine (SPARC) leads to a reduced foreign body reaction to implanted biomaterials. Am J Pathol 2003 Feb;162(2):627-635.

6. Danenberg HD, Fishbein I, Gao J, Monkkonen J, Reich R, Gati I, et al. Macrophage depletion by clodronate-containing liposomes reduces neointimal formation after balloon injury in rats and rabbits. Circulation 2002 Jul 30;106(5):599-605.

7. Rosengren A, Bjursten LM. Pore size in implanted polypropylene filters is critical for tissue organization. J Biomed Mater Res A 2003 Dec 1;67(3):918-926.

8. Ward WK, Slobodzian EP, Tiekotter KL, Wood MD. The effect of microgeometry, implant thickness and polyurethane chemistry on the foreign body response to subcutaneous implants. Biomaterials 2002 Nov;23(21):4185-4192.

9. Brauker JH, Carr-Brendel VE, Martinson LA, Crudele J, Johnston WD, Johnson RC. Neovascularization of synthetic membranes directed by membrane microarchitecture. J Biomed Mater Res 1995 Dec;29(12):1517-1524.

10. Salzmann DL, Kleinert LB, Berman SS, Williams SK. The effects of porosity on endothelialization of ePTFE implanted in subcutaneous and adipose tissue. J Biomed Mater Res 1997 Mar 15;34(4):463-476.

11. Andrade SP, Fan TP, Lewis GP. Quantitative in-vivo studies on angiogenesis in a rat sponge model. Br J Exp Pathol 1987 Dec;68(6):755-766.

12. Williams SK, Berman SS, Kleinert LB. Differential healing and neovascularization of ePTFE implants in subcutaneous versus adipose tissue. J Biomed Mater Res 1997 Jun 15;35(4):473-481.

13. Padera RF, Colton CK. Time course of membrane microarchitecture-driven neovascularization. Biomaterials 1996 Feb;17(3):277-284.

14. Anderson JM, Rodriguez A, Chang DT. Foreign body reaction to biomaterials. Semin Immunol 2008 Apr;20(2):86-100.

15. Higgins DM, Basaraba RJ, Hohnbaum AC, Lee EJ, Grainger DW, Gonzalez-Juarrero M. Localized immunosuppressive environment in the foreign body response to implanted biomaterials. Am J Pathol 2009 Jul;175(1):161-170.

16. Zachariou Z. Amniotic membranes as prosthetic material: experimental utilization data of a rat model. J Pediatr Surg 1997 Oct;32(10):1458-1463.

17. Savina IN, Dainiak M, Jungvid H, Mikhalovsky SV, Galaev IY. Biomimetic macroporous hydrogels: protein ligand distribution and cell response to the ligand architecture in the scaffold. J Biomater Sci Polym Ed 2009;20(12):1781-1795.

18. Heijkants RG, van Calck RV, De Groot JH, Pennings AJ, Schouten AJ, van Tienen TG, et al. Design, synthesis and properties of a degradable polyurethane scaffold for meniscus regeneration. J Mater Sci Mater Med 2004 Apr;15(4):423-427.

19. Zdrahala RJ, Zdrahala IJ. Biomedical applications of polyurethanes: a review of past promises, present realities, and a vibrant future. J Biomater Appl 1999 Jul;14(1):67-90.

20. Gogolewski S, Pennings AJ. An artificial skin based on biodegradable mixtures of polylactides and polyurethanes for full-thickness skin wound covering. Die Makromolekulare Chemie, Rapid Communications 1983;4(10):675-680.

21. Gilding DK, Reed AM. Biodegradable polymers for use in surgery – polyglycolic/poly(lactic acid) homo – and copolymers: 1. Polymer 1979;20(12):1459–1464.

22. Eppley BL, Morales L, Wood R, Pensler J, Goldstein J, Havlik RJ, et al. Resorbable PLLA-PGA plate and screw fixation in pediatric craniofacial surgery: clinical experience in 1883 patients. Plast Reconstr Surg 2004 Sep 15;114(4):850-856; discussion 857.

23. Middleton JC, Tipton AJ. Synthetic biodegradable polymers as orthopedic devices. Biomaterials 2000 Dec;21(23):2335-2346.

24. Christenson EM, Dadsetan M, Hiltner A. Biostability and macrophage-mediated foreign body reaction of silicone-modified polyurethanes. J Biomed Mater Res A 2005 Aug 1;74(2):141-155.

25. Lam KH, Nijenhuis AJ, Bartels H, Postema AR, Jonkman MF, Pennings AJ, et al. Reinforced poly(L-lactic acid) fibres as suture material. J Appl Biomater 1995 Fall;6(3):191-197.

26. Wen F, Chang S, Toh YC, Arooz T, Zhuo L, Teoh SH, et al. Development of dual-compartment perfusion bioreactor for serial coculture of hepatocytes and stellate cells in poly(lactic-co-glycolic acid)-collagen scaffolds. J Biomed Mater Res B Appl Biomater 2008 Oct;87(1):154-162.

27. Pietrzak WS, Sarver D, Verstynen M. Bioresorbable implants--practical considerations. Bone 1996 Jul;19(1 Suppl):109S-119S.

28. den Dunnen WF, Robinson PH, van Wessel R, Pennings AJ, van Leeuwen MB, Schakenraad JM. Long-term evaluation of degradation and foreign-body reaction of subcutaneously implanted poly(DL-lactide-epsilon-caprolactone). J Biomed Mater Res 1997 Sep 5;36(3):337-346.

29. Witte F, Calliess T, Windhagen H. [Biodegradable synthetic implant materials : clinical applications and immunological aspects]. Orthopade 2008 Feb;37(2):125-130.

30. McClary KB, Ugarova T, Grainger DW. Modulating fibroblast adhesion, spreading, and proliferation using self-assembled monolayer films of alkylthiolates on gold. J Biomed Mater Res 2000 Jun 5;50(3):428-439.

31. Wallace DG, Rosenblatt J. Collagen gel systems for sustained delivery and tissue engineering. Adv Drug Deliv Rev 2003 Nov 28;55(12):1631-1649.

32. Stuart K, Panitch A. Characterization of gels composed of blends of collagen I, collagen III, and chondroitin sulfate. Biomacromolecules 2009 Jan 12;10(1):25-31.

33. Minami Y, Sugihara H, Oono S. Reconstruction of cornea in three-dimensional collagen gel matrix culture. Invest Ophthalmol Vis Sci 1993 Jun;34(7):2316-2324.

34. Christenson L, Aebischer P, McMillan P, Galletti PM. Tissue reaction to intraperitoneal polymer implants: species difference and effects of corticoid and doxorubicin. J Biomed Mater Res 1989 Jul;23(7):705-718.

35. Desai NP, Hubbell JA. Tissue response to intraperitoneal implants of polyethylene oxide-modified polyethylene terephthalate. Biomaterials 1992;13(8):505-510.

36. Anderson JM. Chapter 4 Mechanisms of inflammation and infection with implanted devices. Cardiovasc Pathol 1993;2(3):33S-41S.

37. Kellar RS, Kleinert LB, Williams SK. Characterization of angiogenesis and inflammation surrounding ePTFE implanted on the epicardium. J Biomed Mater Res 2002 Aug;61(2):226-233.

38. Williams C, Aston S, Rees TD. The effect of hematoma on the thickness of pseudosheaths around silicone implants. Plast Reconstr Surg 1975 Aug;56(2):194-198.

39. Sharkawy AA, Klitzman B, Truskey GA, Reichert WM. Engineering the tissue which encapsulates subcutaneous implants. I. Diffusion properties. J Biomed Mater Res 1997 Dec 5;37(3):401-412.

40. Auger MJ, Ross JA. Chapter 1: The biology of the macrophage. In: Lewis CE, McGee JOD, editors. The Macrophage. Oxford: Oxford University Press, 1992.

41. Chamberlain LM, Godek ML, Gonzalez-Juarrero M, Grainger DW. Phenotypic non-equivalence of murine (monocyte-) macrophage cells in biomaterial and inflammatory models. J Biomed Mater Res A 2009 Mar 15;88(4):858-871.

42. Holt DJ, Grainger DW. Multinucleated giant cells from fibroblast cultures. Biomaterials 2011 Jun;32(16):3977-3987.

43. Lawson WE, Polosukhin VV, Zoia O, Stathopoulos GT, Han W, Plieth D, et al. Characterization of fibroblast-specific protein 1 in pulmonary fibrosis. Am J Respir Crit Care Med 2005 Apr 15;171(8):899-907.

44. Rossini M, Cheunsuchon B, Donnert E, Ma LJ, Thomas JW, Neilson EG, et al. Immunolocalization of fibroblast growth factor-1 (FGF-1), its receptor (FGFR-1), and fibroblast-specific protein-1 (FSP-1) in inflammatory renal disease. Kidney Int 2005 Dec;68(6):2621-2628.

45. Helming L, Gordon S. Macrophage fusion induced by IL-4 alternative activation is a multistage process involving multiple target molecules. Eur J Immunol 2007 Jan;37(1):33-42.

46. DeFife KM, Colton E, Nakayama Y, Matsuda T, Anderson JM. Spatial regulation and surface chemistry control of monocyte/macrophage adhesion and foreign body giant cell formation by photochemically micropatterned surfaces. J Biomed Mater Res 1999 May;45(2):148-154.

47. DeFife KM, Hagen KM, Clapper DL, Anderson JM. Photochemically immobilized polymer coatings: effects on protein adsorption, cell adhesion, and leukocyte activation. J Biomater Sci Polym Ed 1999;10(10):1063-1074.

48. DeFife KM, Yun JK, Azeez A, Stack S, Ishihara K, Nakabayashi N, et al. Adhesion and cytokine production by monocytes on poly(2-methacryloyloxyethyl phosphorylcholine-co-alkyl methacrylate)-coated polymers. J Biomed Mater Res 1995 Apr;29(4):431-439.

49. Donnelly TM, Stark DM. Susceptibility of laboratory rats, hamsters, and mice to wound infection with Staphylococcus aureus. Am J Vet Res 1985 Dec;46(12):2634-2638.

50. Hu J, Verkman AS. Increased migration and metastatic potential of tumor cells expressing aquaporin water channels. Faseb J 2006 Sep;20(11):1892-1894.

51. Wisniewski N, Moussy F, Reichert WM. Characterization of implantable biosensor membrane biofouling. Fresenius J Anal Chem 2000 Mar-Apr;366(6-7):611-621.

52. Murray DW, Rushton N. Macrophages stimulate bone resorption when they phagocytose particles. J Bone Joint Surg Br 1990 Nov;72(6):988-992.

53. Stark GB, Gobel M, Jaeger K. Intraluminal cyclosporine A reduces capsular thickness around silicone implants in rats. Ann Plast Surg 1990 Feb;24(2):156-161.

54. Anderson JM. Mechanisms of inflammation and infection with implanted devices. Cardiovas Path 1993;2(3):33S-41S.

55. McNally AK, Anderson JM. Interleukin-4 induces foreign body giant cells from human monocytes/macrophages. Differential lymphokine regulation of macrophage fusion leads to morphological variants of multinucleated giant cells. Am J Pathol 1995 Nov;147(5):1487-1499.

56. Keong LC, Halim AS. In vitro models in biocompatibility assessment for biomedical-grade chitosan derivatives in wound management. Int J Mol Sci 2009 Mar;10(3):1300-1313.

57. Sun Y, Lacour SP, Brooks RA, Rushton N, Fawcett J, Cameron RE. Assessment of the biocompatibility of photosensitive polyimide for implantable medical device use. J Biomed Mater Res A 2009 Sep 1;90(3):648-655.

58. Peschel G, Dahse HM, Konrad A, Wieland GD, Mueller PJ, Martin DP, et al. Growth of keratinocytes on porous films of poly(3-hydroxybutyrate) and poly(4-hydroxybutyrate) blended with hyaluronic acid and chitosan. J Biomed Mater Res A 2008 Jun 15;85(4):1072-1081.

59. Schutte RJ, Parisi-Amon A, Reichert WM. Cytokine profiling using monocytes/macrophages cultured on common biomaterials with a range of surface chemistries. J Biomed Mater Res A 2009 Jan;88(1):128-139.

60. Rhie JW, Han SB, Byeon JH, Ahn ST, Kim HM. Efficient in vitro model for immunotoxicologic assessment of mammary silicone implants. Plast Reconstr Surg 1998 Jul;102(1):73-77.

61. Holt DJ, Chamberlain LM, Grainger DW. Cell-cell signaling in co-cultures of macrophages and fibroblasts. Biomaterials 2010;31(36):9382-9394.

62. Polikov VS, Block ML, Fellous JM, Hong JS, Reichert WM. In vitro model of glial scarring around neuroelectrodes chronically implanted in the CNS. Biomaterials 2006 Nov;27(31):5368-5376.

63. Bernatchez SF, Parks PJ, Gibbons DF. Interaction of macrophages with fibrous materials in vitro. Biomaterials 1996 Nov;17(21):2077-2086.

64. Tomasek JJ, McRae J, Owens GK, Haaksma CJ. Regulation of alpha-smooth muscle actin expression in granulation tissue myofibroblasts is dependent on the intronic CArG element and the transforming growth factor-beta1 control element. Am J Pathol 2005 May;166(5):1343-1351.

65. Arena S, Fazzari C, Implatini A, Torre S, Villari D, Arena F, et al. Dextranomer/hyaluronic Acid copolymer implant for vesicoureteral reflux: role of myofibroblast differentiation. J Urol 2009 Jun;181(6):2695-2701.

66. Lossing C, Hansson HA. Peptide growth factors and myofibroblasts in capsules around human breast implants. Plast Reconstr Surg 1993 Jun;91(7):1277-1286.

67. Campbell JH, Efendy JL, Han C, Girjes AA, Campbell GR. Haemopoietic origin of myofibroblasts formed in the peritoneal cavity in response to a foreign body. J Vasc Res 2000 Sep-Oct;37(5):364-371.

68. Polikov VS, Tresco PA, Reichert WM. Response of brain tissue to chronically implanted neural electrodes. J Neurosci Methods 2005 Oct 15;148(1):1-18.

69. Setzen G, Williams EF, 3rd. Tissue response to suture materials implanted subcutaneously in a rabbit model. Plast Reconstr Surg 1997 Dec;100(7):1788-1795.

70. Williams EJ, Benyon RC, Trim N, Hadwin R, Grove BH, Arthur MJ, et al. Relaxin inhibits effective collagen deposition by cultured hepatic stellate cells and decreases rat liver fibrosis in vivo. Gut 2001 Oct;49(4):577-583.

71. Gretzer C, Emanuelsson L, Liljensten E, Thomsen P. The inflammatory cell influx and cytokines changes during transition from acute inflammation to fibrous repair around implanted materials. J Biomater Sci Polym Ed 2006;17(6):669-687.

72. Brodsky B, Ramshaw JAM. Collagen organization in an oriented fibrous capsule. International Journal of Biological Macromolecules 1994;16(1):27-30.

73. Prantl L, Schreml S, Fichtner-Feigl S, Poppl N, Eisenmann-Klein M, Schwarze H, et al. Clinical and morphological conditions in capsular contracture formed around silicone breast implants. Plast Reconstr Surg 2007 Jul;120(1):275-284.

74. Brown BG, Fry DL. The fate and fibrogenic potential of subintimal implants of crystalline lipid in the canine aorta. Quantitative histological and autoradiographic studies. Circ Res 1978 Aug;43(2):261-273.

75. Pickering JG, Boughner DR. Quantitative assessment of the age of fibrotic lesions using polarized light microscopy and digital image analysis. Am J Pathol 1991 May;138(5):1225-1231.

76. Liu WF, Ma M, Bratlie KM, Dang TT, Langer R, Anderson DG. Real-time in vivo detection of biomaterial-induced reactive oxygen species. Biomaterials 2011;32(7):1796-1801.

77. Jay SM, Skokos EA, Zeng J, Knox K, Kyriakides TR. Macrophage fusion leading to foreign body giant cell formation persists under phagocytic stimulation by microspheres in vitro and in vivo in mouse models. J Biomed Mater Res A 2010 Apr;93(1):189-199.

78. Fan JM, Ng YY, Hill PA, Nikolic-Paterson DJ, Mu W, Atkins RC, et al. Transforming growth factor-beta regulates tubular epithelial-myofibroblast transdifferentiation in vitro. Kidney Int 1999 Oct;56(4):1455-1467.

79. Inouye K, Kurokawa M, Nishikawa S, Tsukada M. Use of Bombyx mori silk fibroin as a substratum for cultivation of animal cells. J Biochem Biophys Methods 1998 Nov 18;37(3):159-164.

80. Nathan CF. Respiratory burst in adherent human neutrophils: triggering by colony-stimulating factors CSF-GM and CSF-G. Blood 1989 Jan;73(1):301-306.

81. Gilchrest BA, Nemore RE, Maciag T. Growth of human keratinocytes on fibronectin - coated plates. Cell Biol Int Rep 1980 Nov;4(11):1009-1016.

82. Chen CZ, Peng YX, Wang ZB, Fish PV, Kaar JL, Koepsel RR, et al. The Scar-in-a-Jar: studying potential antifibrotic compounds from the epigenetic to extracellular level in a single well. Br J Pharmacol 2009 Nov;158(5):1196-1209.

83. Webb K, Li W, Hitchcock RW, Smeal RM, Gray SD, Tresco PA. Comparison of human fibroblast ECM-related gene expression on elastic three-dimensional substrates relative to two-dimensional films of the same material. Biomaterials 2003 Nov;24(25):4681-4690.

84. Schutte RJ, Xie L, Klitzman B, Reichert WM. In vivo cytokine-associated responses to biomaterials. Biomaterials 2009 Jan;30(2):160-168.

85. Leibovich SJ, Chen JF, Pinhal-Enfield G, Belem PC, Elson G, Rosania A, et al. Synergistic up-regulation of vascular endothelial growth factor expression in murine macrophages by adenosine A(2A) receptor agonists and endotoxin. Am J Pathol 2002 Jun;160(6):2231-2244.

86. Lau TM, Affandi B, Rogers PA. The effects of levonorgestrel implants on vascular endothelial growth factor expression in the endometrium. Mol Hum Reprod 1999 Jan;5(1):57-63.

APPENDIX

STANDARD OPERATING PROCEDURES

Protocol: 3T3 cell culture
Dolly Holt
Date Entered: 03-7-2012

- Complete Media
    - DMEM high glucose + L glutamine
    - + 10% FBS
    - + 1% antibiotic/antimycotic
- Place 10 ml of complete media in a T75 flask and place in incubator to prewarm for 10 min
    - Spray with 70% ethanol and place in sterile hood
- Thaw a cryovial of 3T3s in a 37 °C water bath (this will only take a couple of minutes)
- When the vial is nearly thawed, remove from water bath, dry off, spray with 70% ethanol and place in hood.
- Using a 5 ml pipette, transfer contents of vial into T75
- Remove some of the media in the T75 and add it to the cryovial to remove any residual cells
    - Repeat this a couple of times until you feel you have removed all of the cells
- Place T75 in incubator and allow cells to adhere. This may take 2-5 hours.
- After cells have adhered, prewarm complete media and replace media above cells
    - The purpose of this is to remove residual DMSO that was in the frozen cells
- Replace T75 in incubator
- Cells will take 3-4 days to reach confluency

Passaging

- When cells are 80% confluent they need to be passaged
    - This occurs when what appears to only be 20% of the area of the T75 is still available for cell growth
- Fibroblasts are not contact inhibited, so they will begin to grow over the top of one another if they become more than 100% confluent.
    - Once they begin to grow on top of one another, they may change their phenotype, so it is important to keep a close watch on these cultures
- To passage the cells, aspirate off the media, and add 3 ml of TryplE in a T75 flask, just enough to cover the cells
- Watch the cells under the microscope, in about 5 minutes they will begin to ball up.
- Before they have completely detached you can carefully return the T75 flask to the incubator (being careful not to hit it on anything as that will knock the cells off) and gently remove as much TryplE as possible. Don't tilt the flask, just remove the media from the top.
- Add 5 ml complete media and using the pipette, gently wash the cells from the bottom of the flask.
- Once they are all detached, transfer 10% of the volume (500 ul) into a new flask and add 10 ml of complete media.
    - You may use the remaining cells for experimentation by using them directly or plating them into a 96-well plate for example.
- Place T 75 in 37 °C incubator with 5% supplemental carbon dioxide
    - Cells will take 4 days to reach confluency.
    - You may always add more cells to reach confluency faster. Be careful when adding fewer cells, if you add too few, the cells will never become confluent, but will grow in small clusters and become quiescent. If this happens, you may still passage them and plate them at a higher density to stimulate them to grow, but you have now affected their phenotype.
- The passaging technique described can take some practice, so if you feel more comfortable, you can add the TryplE, place it in the incubator at 37 °C and wait until all of

the cells have become completely detached. You can knock the flask on the counter to dislodge the cells

- Add a greater amount of complete media than TryplE (eg 5 ml). Complete media has antitrypsin that will inhibit the function of the enzyme.
- Use a pipette to gently rinse the remainder of the cells from the bottom of the flask.
    - Theoretically, your cells should be fine with residual triple, but if they are not behaving properly, you may want to remove any residual TryplE by adding the cells to a 15 ml conical tube and centrifuging them at 500 rcf for 5 min, aspirating the supernatant, and resuspending the pellet in complete media.
        - Centrifuging can be damaging to cells, so you can also plate them, and after they are adhered (a couple of hours), then you can replace the media with complete media (just as was done to remove the DMSO)
- Transfer 10% of the volume to a new T75 flask and add 10 ml of complete media
- Place T 75 in 37 °C incubator with 5% supplemental carbon dioxide

Protocol: ASC Isolation
Updated: 12.29.08
Author: Dorthyann Isackson
References: (Torres, Rodrigues et al. 2007), (Zuk, Zhu et al. 2001), (Prichard, Reichert et al. 2007) (Bjorntorp, Karlsson et al. 1978)

ASC Isolation

Adipose Compartments:

- Rabbit: dorsomedial behind cranium on shoulder region
- Mouse: epididymal, inguinal (iliac region) and neck region
- Rat: inguinal (iliac region) and epididymal

Tissue Harvest:

Materials:

- scissors
- Sterile PBS
- Sterile Falcon Tube or container for adipose

Method:

- Under sterile conditions, make small incision (~1 cm) over adipose compartment
- Gently extract adipose tissue from epididymal fat pad
- Place adipose in sterile PBS
- Wash extensively in sterile PBS to remove residual blood
- Mince adipose with sterile razor blade.

Tissue Digest:

Materials:

- Collagenase, Type I (1 gram, Invitrogen, Cat No. 17100017)
- Sterile PBS
- DMEM w/10% FBS, 1% antibiotic/antimycotic
- 160 mM NH_4Cl
- T-75 tissue culture flask

Method:

- Digest tissue ECM in is 0.2% Collagenase Type I (2 mg/ml) in PBS at 37°C for 45 minutes in agitating water bath
- Neutralize enzyme digest with equal volume of DMEM w/10% FBS and 1% anti/anti
- Centrifuge at 1200g for 10 min at RT
- Discard supernatant, resuspend pellet in 160 mM NH_4Cl, incubate at RT for 10 min to lyse RBCs (optional)
    - 160 mM NH_4Cl
        - .160 Mol/L x (0.5 L) = 0.08 mol x (53.45 g/mol NH_4Cl) = 4.28 g NH_4Cl + 500 ml sterile PBS
- Centrifuge at 1200g for 10 min at RT
- Discard supernatant, resuspend in DMEM/F-12 (1:1) w/10% FBS and 1% antibiotic/antimycotic
- Plate suspension in T-75 tissue culture flask and expand cells in culture until 90% confluent

Plating and Cell Expansion:

Materials:

- DMEM/F-12 (1:1) w/10% FBS and 1% antibiotic/antimycotic

- T-75 tissue culture flask (or desired plating container)
- Trypan blue
- Hemacytometer

Method:

- Change media 24 hrs after plating, then change media every 2-3 days thereafter
- Determine cellular viability and numbers at time of passage by trypan blue exclusion and hemacytometer cell counts
- Passage cells repeatedly after achieving a density of 75%-90% (~5 days in culture) until passage 8

* Alternative is 0.2% Collagenase (2 mg/ml) as last noted in lab book (Book 1, page 126-127) to decrease collagenase solution volume and increase collagenase concentration.

Bjorntorp, P., M. Karlsson, et al. (1978). "Isolation and characterization of cells from rat adipose tissue developing into adipocytes." J Lipid Res **19**(3): 316-324.

Prichard, H. L., W. M. Reichert, et al. (2007). "Adult adipose-derived stem cell attachment to biomaterials." Biomaterials **28**(6): 936-946.

Torres, F. C., C. J. Rodrigues, et al. (2007). "Stem cells from the fat tissue of rabbits: an easy-to-find experimental source." Aesthetic Plast Surg **31**(5): 574-578.

Zuk, P. A., M. Zhu, et al. (2001). "Multilineage cells from human adipose tissue: implications for cell-based therapies." Tissue Eng **7**(2): 211-228.

Protocol: BMMΦ Media Details
Dolly Holt 03-31-2011
Reference(s): Orme lab protocols

Part I. L929 conditioned media

Purpose: To define a procedure for L-929 Conditioned Media. L-929 cells secrete growth factors needed for macrophage growth (M-CSF/GM-CSF). The supernatant of L-929 cells is used for L-929 conditioned media.

Materials:

- RPMI Medium 1640 (+ L-glutamine) with 10% heat inactivated FBS and 1% antibiotic/antimycotic
- Sterile T175 flask
- Pipettes and pipettman
- Micropipettes and micro-pipettor

Procedure:

- L-929 cells from ATCC are grown up at $4.7x10^5$ cells total. Cells are allowed to grow for 7 days or until confluent. On day 7 collect the supernatant and filter through a 0.45 µm Nalgene filter. You can centrifuge the supernatant for 10 minutes, 1000 rpm, at 4°C prior to filtering to remove any large debris. This will make the filtering go faster. Then label and freeze at -20°C in 50 ml aliquots.

Part II. BMMO Media

BMMO Media (total 500 ml)

- 10% (50 ml) Hi (heat inactivated) FBS
- 10% (50 ml) L929 cond Media
- 1% (5 ml) HEPES
- 1% (5 ml) Antibiotic/antimycotic
- 1% (5 ml) MEMS non essential amino acids
- 1% (5 ml) Na Pyruvate
- In high glucose DMEM + L-Glutamine

  *Be sure to remove the same volume of liquid you are going to add back in so that your concentration is accurate (i.e. you are going to add in 120 ml, so remove 120 ml of DMEM before you begin).

SOP for Flow Cytometry Portion of CBA Assay
Prepared by Dolly Holt
06/18/2008

Prior to CBA

- Collect media from cells and store at -80 deg C until all samples have been collected.
- Once all samples are collected, thaw media aliquots and vortex to mix contents.
- Spin at 500 rcf for 5 minutes
- Remove 50 µl to be used in the CBA assay

Before you go to the Cytometry lab:

- Bring set up beads, P1000 and p10 pipette, tips for pipettes

Once you get to the lab

1. Log in at one of the FACSCANs
2. Double-Click Rainbow
    a. FACSCAN 2: File->import settings-> BD Applications->temp data-> Grainger-> CBA->CBA Settings 040407
    b. FACSCAN 1: File->import settings->BD Applications->temp data-> Grainger-> CBA->CBA Settings Mac-> CBA Settings 040407
3. Double-Click Cell Quest
    a. FACSCAN 2: File->open-> BD Applications->temp data-> Grainger-> CBA->CBA Acquisition 061307 (or most recent data file)
    b. FACSCAN 1: File->open-> BD Applications->temp data-> Grainger-> CBA->CBA Settings-> CBA Acquisition 061307 (or most recent data file)
    c. Acquire->Connect to Cytometer (If it will not connect it is because the computer needs to be turned on either before or after the flow cytometer)
    d. Cytometer->instrument settings->open-> BD Applications->temp data-> Grainger-> CBA->CBA Acquisition 061307 (I think it might be settings 040407) (or most recent data file)-CLICK SET!!->done
    e. Acquire->Acquisition and Storage-> 300 Xs # of Analytes = # of Events to collect of gate G1=R1
    f. Acquire->Parameter Description->Folder->Select folder ex. 02052008->Select->File (rename the prefix and set the number to start counting at 1)->OK
    g. In Rainbow Preference Dialog Box->update 4/5 color settings->Choose Base Directory-> Select the folder that the files are being saved to ex. 02052008 in CBA in Grainger -> Choose->OK
    h. Acquire->Counters
        i. Must unclick the setup to save! (Now your 1st sample will show up in the directory heading).
        ii. If you have set your events properly it will stop once the # of events is collected, save, and automatically move to the next sample in the directory
        iii. If for whatever reason you need to stop earlier or manually->click pause and save.
    i. Turn the knob on the cytometer to run and high, make sure that the light that said “Standby” when the knob was at standby now says “Ready”.
    j. Run Test Beads to locate clusters. Bead A9 should be in the upper right corner
    k. Run 0 standard and make sure you see all 6 clusters. The FL2 histogram should be around 0.
    l. In Rainbow Preference Dialog box->decrease or increase the FL4 or FL5 voltage settings to see all of the beads ex. 6 clusters
    m. In Rainbow Preference Dialog Box->Adjust compensation to resolve the bead clusters if they are too close together.
4. Shutting Down

a. When you are finished, wash the cytometer with water, don't need the Bleach Water
    i. Make sure the cytometer says "Run". Fill water to top line and flush with the cytometer arm open until the line reaches the bottom line.
    ii. Let the cytometer run for 5 min with the arm closed.
    iii. Turn the cytometer to "standby"
b. Shut down programs, Log off, if you are the last to use the cytometer turn it off

Tips

c. Press the apple key +1,2,3,4 to see all of the counters and parameters, etc. (also found under acquire)
d. You can always open a previous acquisition file and that will give you the same settings in Cell Quest as was used before. Cytometer->instrument settings->open->select downstream data file ex. 5-> open->SET!->done
    i. Select a downstream data file because it usually takes the first couple to get totally set.
e. If the cytometer is "not ready" the buffer and waste containers may need to be emptied.
    i. Open the door at the front of the cytometer, click the switch to vent.
    ii. Pull out the waste container and dump down the sink, fill up with 200 ml of bleach (located below the sink) to make a 10% Bleach solution when it is full up to 2 Liters.
    iii. Unscrew the lid of the storage buffer and refill with buffer (distilled water) to the line.

Cell culture notes

- Always avoid making bubbles. Bubbles have very high surface tension and if they come into contact with the cells will disrupt the membrane and kill them.
- To avoid bubbles, always keep your tip submerged and never add all or remove all of the liquid when mixing, transferring etc.
- When you add media to a flask, invert the flask so that you are adding the media to the roof. This will ensure that you do not accidently rinse any of your cells off as well as ensure that any bubbles you produce will stick to the roof, rather than floating in the media when you turn the flask upright.
- Centrifuging is very damaging to cells, spinning, the pellet, resuspending, it all causes a lot of cell death, so avoid it whenever possible.
    - Ways to avoid it are to let the cells adhere before rinsing them
    - Always use volulmes less than what you need so that media can be added rather than having to be removed
        - This is relevant when you are isolating BMMOs, use as little media as possible to rinse the bone marrow
        - When passaging, add less media than the amount you will ultimately need so that you can add media rather than having to spin.
- Always be gentle when pipetting cells and use the largest bore hole possible. This will reduce the sheer force applied to the cells that can lyse them.
- Cells can be very stable even at room temperature, the key is to prevent stark changes in temperature. For example, if your cells are at 37 deg c then you want to add 37 deg C media. If your cells have been in the hood for a long time and are now at room temperature, then it is better to add room temperature media.
- Cells will die in the absence of media almost instantly. Make sure that you only remove the media from a small portion of wells, or even one at a time when you are first learning. The cells can take up to a day to die from drying out, so you may not know immediately if you let them dry out. As you get faster, you can remove media from several wells at a time, but always be mindful of how quickly the liquid can evaporate.
- Cells can tolerate, but do not do well in cold media, so avoid this. Though if you want to prevent receptor mediated endocytosis, then you can keep your cells at 4 deg C.
- Cells can survive for at least 2 hours and up to 2 days, depending on the cell type, in PBS plus calcium/magnesium.
- PBS without calcium/magnesium will prevent cells from using their integrins, that keep them stuck to the surface
    - This is beneficial if you want to gently remove them from a surface, but if you want them to stick, then you must ensure that you have PBS with calcium/magnesium.
- To maintain proper aseptic technique, always make sure your tip never comes in contact with anything. If in doubt get a new one.
- Always replace lids immediately after adding or removing media. This will increase your sterility as well as prevent you from accidentally adding waste for example into your fresh media bottle.
- Media will lose its shelf life the more it is warmed. If your bottle has a lot of media in it, it may be beneficial for you to remove 50 ml and place it into a conical tube. This way you can heat your media faster and can leave your stock at 4 deg C.
    - Another trick is to add cold media to your flask and place your flask in the incubator to warm, rather than warming your media and adding it to the flask (i.e. for passaging etc).
- If you are using media out of a 500 ml bottle, you must make sure it is as sterile as possible. If it gets contaminated, everyone's experiments that use that media will get contaminated. Because of this it should be the last lid removed and the first lid replaced.
- Try to hold lids facing down when working if possible. If you must set the lid down, make sure the open container and the lid are placed toward the back of the hood and away from your arms, as bacteria can fall from your arms as you pass over the top

- Also make sure your lids are placed facing upward, as it is the edge of the lid that can gather the most contamination.
- When spraying vessels off with ethanol to place in the hood, make sure the lid gets the most attention as that is the area that is most likely to cause contamination.
- With antibiotics/antimycotics you can get away with bad cell culture technique, but it is good to have good practices so that if you cannot use antibiotics that your cells will still remain sterile.
- If something is contaminated, dispose of it immediately and use ethanol and/or bleach to wipe down any surface it has come in contact with.
- Before you begin using cells, you can practice with empty containers and then secondary cells before primary cells to ensure you get down proper technique.
- When you are beginning, you must train yourself to always be AWARE. Be aware of where your tip is, be aware of your hands and arms moving over an open container.
- Learn to be efficient. Work smartly and quickly, this will increase the chances your cells have of remaining viable.
- Never be rushed however, when you are rushed, you are more likely to make a mistake.
- Mistakes can kill your cells and affect your results, and can take weeks and many experiments to decipher the problem.

Reference: Orme Laboratory Standard Operating Procedure
Modified: Dolly Holt 03-12-2012

Cell Counting/Viability Using a Hemacytometer

Purpose: To define a procedure for proper use of a hemacytometer for obtaining an accurate count of cells in a suspension used in laboratory procedures. A hemacytometer consists of a thickened glass slide into which a small chamber has been cut to allow for the introduction of cells to be counted. The floor of the chamber is divided (etched) into nine sections; usually only the four corner sections are used in cell counting. With a coverslip in place each square of the hemacytometer represents a total volume of 0.1 mm or 10^{-4} cm. 1 cm^3 is approximately equivalent to 1 ml, the cell concentration per ml (and the total number of cells) can be determined. (Hemocytometers require special coverslip, it is not good to use "any" coverslip)

Trypan Blue: Trypan Blue is a dye that enables easy identification of dead cells. Dead cells take up the dye and appear blue with uneven cell membranes. By contrast, living cells repel the dye and appear refractile and colorless.

Materials:

- Hemacytometer and coverslip for Hemacytometer
- 70% ETOH
- Kim-wipes
- Micropipettors and tips
- Cell solution to count

Procedures:

1) Prepare a hemacytometer for use
    a. Carefully clean all surfaces of the hemacytometer and coverslip using 70% ETOH and a Kim-wipe.
    b. Dry with a kim-wipe
    c. Center coverslip on the hemacytometer.
2) Prepare a cell suspension.
    a. Remove cells from surface of culture dish
    b. Gently mix to create a homogenius suspension
    c. Remove 10 µl of cells and place into a small microfuge tube
    d. Add 10 µl of Trypan blue and gently mix.
        i. This will give you a dilution factor of 2 (see formula below)
    e. Allow mixture to sit for 2-3 minutes to allow absorption of dye, however, cells must be observed within 5 minutes or living cells will also take up dye.
    f. If you choose to not use trypan blue, you do not need to account for a dilution factor
3) Pipette 10 µl of the cell suspension (with or without Trypan blue) into one of the two counting chambers.
    a. Make sure suspension is well mixed.
    b. Place 10 µl pipette tip into notch at bottom of hemocytometer.
    c. Fill the chambers slowly and steadily, allow capillary action to spread the cell suspension over the surface of the hemocytometer.
    d. Avoid injecting bubbles into chambers.
    e. Do not overfill or underfill chambers. (overfilling will raise the coverslip and allow cells to migrate giving an inaccurate count).
4) Count the cells.
    a. Allow cell suspension to settle for at least 10 seconds.
    b. Count the cells in each of the four 1 mm^2 corner squares labeled A thru D in Figure 1.
        i. DO count the cells touching the top or left borders

ii. DO NOT count the cells touching the bottom or right borders.

5) Determine the cell count.
   a. Calculate the total cells counted in the four corner squares.
      i. if more than 10% of the cells counted appear to be clustered, carefully remix the original cell suspension and repeat steps 2 through 4.
      ii. The most reliable concentration of cells to count is 50-100 per A-D square. You can dilute or concentrate the cells to get within this range.
      iii. If you are counting bacteria, hemopoeitic cells or other small cells, you may use the center square and count 5 of the little squares (down the diagonal), average them, multiply them by 25 and you will come up with the same area you would have if you averaged the cells in the four corners.
   b. Calculate the cell count using the equation:
      i. **Cells/ml = (n) x 10^4 x dilution factor**,
      where n = the average cell count per square of the four corner squares counted.
      ii. From this number, you can determine total cells in suspension by multiplying by the total volume of the suspension.
6) Percent Viability
   a. Count all cells. (from same squares)
   b. Count unstained cells. (from same squares)
   c. Calculate viability using the equation:

% Cell Viability = <u>number of unstained (living) cells x 100%</u>
Total cells counted (stained + unstained)

Figure 1

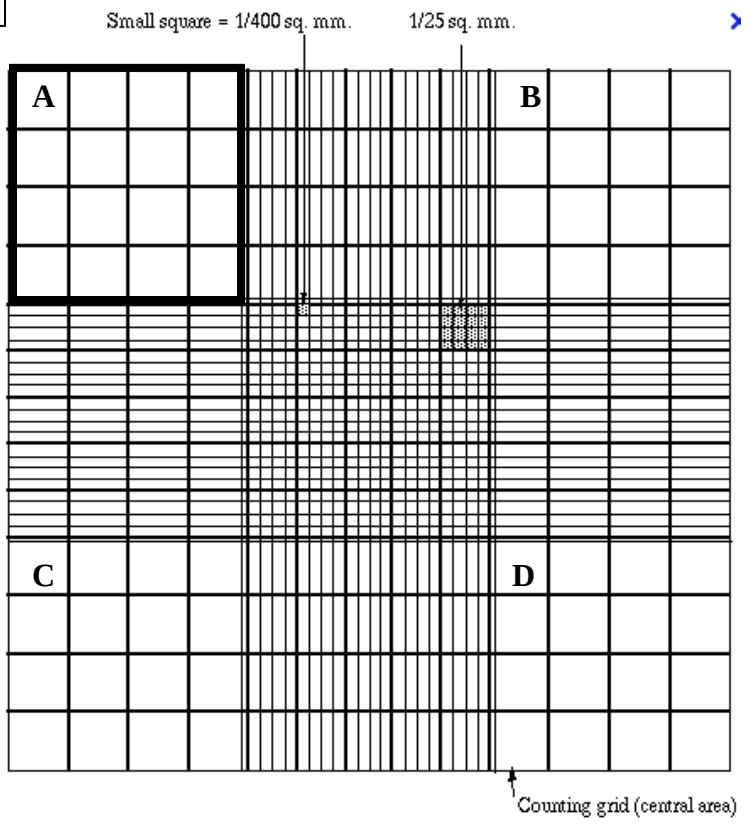

Protocol: Heat Inactivation of FBS Name: Lisa Chamberlain
Date Entered: 20080527
Reference(s): Orme lab protocols
Modified: Dolly Holt 03-31-2011

Preparation of Heat-inactivated FBS: required to inactivate compliment proteins

Components:

- Fetal Bovine Serum (aliquot or bottle)
- 56° C water bath
- Thermometer

1. Thaw FBS (4°C over the weekend is best, but 37°C will work if you are in a hurry)
2. Heat water bath to 56° C and start it shaking.
3. Keep an eye on the water bath temperature. Periodically check the temp (every 5-10 minutes) with a thermometer. Adjust temperature setting until it stabilizes at 56° C.
4. Place FBS in water bath. If using tubes, support them somehow so they're not floating (in a beaker or a float)
5. Feel the tubes and when they feel close to 56°C, then start the timer.
6. Incubate FBS at 56° C for at least 30 minutes. FBS can incubate as long as an hour, but this is not necessary.
7. Label and/or aliquot heat inactivated FBS as HI-FBS and store at -20° C

Make sure the temperature is not above 56° C, and that the FBS doesn't incubate for more than an hour. If the FBS is at high temperature for too long, proteins will denature and fall out of solution making the FBS unusable.

Protocol: Immunocytochemistry
Name: Dolly Holt
Date Entered: 03-7-2012
Reference(s): Hitchcock and Tresco lab protocols

Components
- PBS+Ca^{+2}/Mg^{+2} (Invitrogen) Ph 7.4
- PBS- Ca^{+2}/Mg^{+2} (Invitrogen) Ph 7.4
- Plate shaker
- Antibodies
- 4% PFA (paraformaldehyde)
- Goat block

Immunocytochemistry staining: staining for RAW and BMMOs with Ki-67 antibody

- Remove media above cells
- Rinse 2X with PBS+Ca^{+2}/Mg^{+2} (Invitrogen) Ph 7.4
- Add 4% PFA (paraformaldehyde) to cells
- Incubate for 20 min at room temperature
- Rinse 2X with PBS+Ca^{+2}/Mg^{+2} Ph 7.4
- Add block solution (4% goat serum plus 0.1% triton-X 100, Invitrogen) for 1 hour, RT (room temperature), on shaker plate
- Add primary antibody (diluted in block) incubate for 1 hour, RT, on shaker plate or 4°C overnight
    - Overnight provides a slow and controlled binding that will decrease background, it is the better option if you have time.
    - Add just enough to cover the well (eg. 50 µl in a 96-well plate)
- Wash 3X in PBS (15 min soaks if you need to reduce background)
- Add secondary antibody (diluted in block) for 1 hour, RT, on rocker
- Counterstain with DAPI (optional)
- Wash 3X in PBS (15 min soaks if you need to reduce background)
- Store in PBS at 4°C in dark and/or covered by tinfoil

Primary Antibody
- Ki-67 1:50 dillution for BMMO and RAWs
- Primary anti-mouse Ki-67 (IgG_1, Novacastra, Buffalo Grove, USA, product No. NCL-L-Ki67-MM1) obtained from Tresco lab.
- phospho-histone H3 1:100 for BMMO
- phospho-histone H3 (Cell Signaling Technology, Danvers, USA)

Secondary Antibody
- IgG_1 goat anti-mouse 1:500 for BMMOs; 1:2000 for RAWs
- Secondary IgG_1 goat-anti-mouse antibody conjugated to Alexa 488 (Invitrogen)

Nuclei Counterstain
- DAPI: 21,000 NM in PBS (from our stocks made in 2007, normally you use a much lower concentration, but I think our stocks were diluted improperly to begin with)
- 4',6-diamidino-2-phenylindole (DAPI, Invitrogen) according to manufacturer's instructions prior to imaging.

- Optimal antibody concentrations (if preconjugated to a fluoriphor is listed as the color)
- Antibody, color, dilution
- Primary Antibodies
    - vimentin red 1:50

    - CD14 red 1:100
    - F4/80 red 1:100
    - CD40 green 1:50
    - CD11b green 1:75-1:100
    - MHC I green 1:100
    - MHC II green 1:100
    - MCP-1 red 1:50
    - MIP-1 alpha not dye conjugated 1:100
    - Col-1 (from HIro) no color 1:100-1:75
    - Alpha-SMA no color 1:1000-1:800
- Secondary Antibodies
    - IgG (Rabbit) green 1:2000
    - IgG2a (Rabbit) green 1:2000
- Notes
    - Use the lowest concentration of primary and secondary antibodies possible in order to reduce background
    - Obtain secondary antibody from the host species used to create the primary antibody
    - Use a serum block from the species from the host used to create the secondary antibody
    - Example
        - primary antibody = rabbit antimouse MIP-1alpha
        - secondary antibody = goat anti-rabbit IgG
        - Block serum = goat
    - Blocking in species (host) used to create the secondary antibody is beneficial because it will be more likely to not crossreact with its host proteins (because if it did, it would create an autoimmune disease) and thus it will reduce the nonspecific binding of the secondary antibody.
    - I have heard to use twice the concentration of secondary antibody as primary, because there are two binding sites. However, from my own experience, I have needed almost 10X less secondary and primary because of too much background caused.
    - H & L means heavy and light chain. Secondary antibodies will have this designation because they will bind all IgGs (IgG1, IgG2a, etc). H & L is convenient because you can use 1 for many applications, however it will increase your backround as it is nonspecific. A IgG1 will be more specific and will decrease your background. However if you don't have background problems, then H&L will be fine for your application.
    - Increasing rinse time will reduce background and nonspecific binding. This is especially important when using H&L secondary antibodies.
- Controls
    - Always do just a secondary antibody control. This is to ensure that the signal you see is due to the specific primary antibody binding
    - In order to control for non-specific primary antibody binding, you must have an isotype control (i.e. an IgG antibody shape that doesn't recognize anything). You would need an isotype control for each isotype (eg. IgG1, IgG2a, IgG, etc). You also need to make sure this isotype control is from the same host, but has no known reactivity.
        - Example: primary rabbit antimouse MIP-1a (IgG). The isotype control would be rabbitt IgG.
        - Look to see if there is nonspecific binding of the rabbitt igG isotype control. Use it in the same concentration as you use the functional primary antibody.

Protocol: L929 culture and conditioned media
Dolly Holt 03-31-2011
Reference(s): Orme lab protocols
Edited 4/01/03 JMH
Modified by MGJ 03-18-04
Modified by DJH 02-06-12

L-929 (CCL-1) Fibroblast Support Protocol: Initiation of Cell Line

Purpose: To define an SOP for preparation of L-929 cells. L-929 cells secrete growth factors needed for macrophage growth (M-CSF/GM-CSF). The supernatant of L-929 cells is used for L-929 conditioned media.

Time Frame: 30 min

Materials:

- Cryovial of ATCC L929 fibroblasts, or from our liquid nitrogen stocks
  - Make sure to cross off the vial of cells you remove from the stocks list
  - Also if there are less than 3 vials of cells, it is your responsibility to make more frozen stocks using the vial you remove.
- Complete RPMI Media = RMPI Medium 1640 (+ L-glutamine) with 10% HI FBS and 1% antibiotic/antimycotic
- 1 T75-cm^2 tissue culture flask
- Clean 37^{o}C water bath
- Pipettman and Pipettes
- Pipette-box
- Clean hood

Procedure:

1) Add complete RPMI media T75 and place into incubator for 10 min to reach 37 deg C
2) Thaw one cryovial of cells at a time by dipping bottom ¾ of cryovial in a 37^{o}C water bath and swirl gently for 1-2 minutes until thawed (>3 minutes may damage cells).
3) Wipe cryovial dry then and rinse with 70% Ethanol, note the color of the solution. (ideally, it should be pink)
4) In a clean hood gently resuspend the cells in the cryovial before transfer. Add fresh media to the cryovial to rinse and remove any remaining cells
5) In a clean hood, do one of the following:
   a. Transfer thawed cells into a T75-cm^2 tissue culture flasks containing 10 ml of pre-warmed RPMI medium (prepared in step 1). Gently rock flask to disperse cells.
      i. Allow the cells to adhere for a couple of hours, then replace the media with fresh pre-warmed complete RPMI media to remove residual DMSO
   b. Transfer thawed cells to a conical tube filled with 10 ml of 37^{o}C complete RPMI media. Gently resuspend.
      i. Centrifuge at 500 rcf for 5 min.
      ii. Remove supernatant, be careful not to disrupt the cell pellet.
      iii. Pull 5 ml of RPMI media from the T-75 flask (prepared in step 1) and add to the conical tube and resuspend the pellet. Then transfer all of the contents of the conical tube into the T-75 flask.

6) Place culture flask in 37^{o}C incubator with 5% CO_2, 90% Humidity

7) Change the media every 2-3 days after that while examining them daily. Continue feeding cells until 80% confluent.

*Removal/addition of media is done on the roof of the flask as opposed to directly on top of cells to avoid damage to cells. This is done by turning the flask upside down and adding the media. This will also serve to leave any bubbles on the roof, rather than in contact with the cells, as bubbles can disrupt cell membranes.

8) Clean hood with 70% ETOH when finished.

9) Replace media every 2-3 days until 90% confluent

If cells are:	Then feed them:
< 25% confluence	1 ml per 5 cm^2
25-45% confluence	1.5 ml per 5 cm^2
> 45% confluence	2 ml per 5 cm^2

10) Cells need to be passaged after they are 90% confluent
    a. Remove media
    b. Rinse cells with calcium/magnesium-free PBS (optional, this will just speed up the process)
    c. Add just enough TryplE to cover the cells (3 ml for T-75)
    d. Place T-75 on scope and when cells begin to ball-up, remove 2 ml o f TrypleE (optional, you can leave all 3 mls, but it may be healthier for cells to remove any excess).
        i. You can also place flask in incubator for 3-5 min to speed the detachment process
    e. Once cells have detached, add an equal volume of complete media (media with FBS, FBS has anti-trypsin which will stop the action of the trypsin enzyme)
    f. Using a 5 ml pipette, rinse the bottom of the flask with the media to remove cells (be careful to avoid creating bubbles).
    g. Place 10% of the volume of cells to a new flask and add sufficient complete RPMI media (eg. enough media to bring the volume to 10 ml in a T75 flask). Cells will become confluent in 3-4 days.

Conditioned media

11) After the cells are 80% confluent, they can be passaged and expanded in several T-150 flasks. 10 T-150s is a good number of conditioned media stocks.

12) Add 49 ml of complete RPMI media to 10 T-150 and place in incubator to pre-warm.

13) Add 1 ml of cell suspension (from passaging) to each of the 10 T-150 flasks.

14) Allow cells to grow for 3 days after they become confluent. Do not replace media.
    a. L-929 cells from ATCC are grown up at $4.7x10^5$ cells total.

15) After the time required for step 14, collect the supernatant, centrifuge supernatant for 10 minutes, 1000 rpm, at 4^oC or filter through a 0.45 µm Nalgene filter (Filtering will take out any small celluar debris and is best, but if no filter is available, centrifuging will remove any contaminating viable cells)
16) Freeze at -20^oC in 50 ml aliquots.

**Do not fill the TC flacks above neck line with media, can cause contamination issues.

Protocol: Long-lived intracellular stains
Dolly Holt
Date Entered: 03-7-2012
Cell Trace Far red taken from Invitrogen tech support

green Vybrant® CFDA SE Cell Tracer Kit

- Used according to manufacturer's instructions

Cell Trace Far Red

- Prepare a stock solution (1-10 mM in DMSO)
    - Add 9.89 µl DMSO to 1 vial of Red cell tracer
- Working concentration
    - Dilute stock solution in PBS (or media without phenol red)
- Add working concentration to cells and incubate cells for 30 minutes at 37 °C
- Wash 2X in PBS
- Use no greater concentration than 1 million cells in 1 ml of working concentration of Red cell tracer)
- Green dye gets into nucleus, red dye doesn't
- Both dyes in stock solution remain stable when frozen for several months without needing to create new stock solutions
- Ideal dye concentrations
    - Secondary 3T3 fibroblasts
        - 10 µM Red
        - 10 µM Green
    - Secondary RAW 264.7 macrophages
        - 7 µM Red (though this is dim, it is cytotoxic to increase the concentration)
        - 5 µM Green
    - Ideal fusion conditions for secondary cells
        - 10,000 RAWs and 20,000 3T3s per well of 96-well plate
    - Primary Fibroblasts
        - 3 µM Red
        - 7 µM Green for co-culture
        - 10 µM Green when need it to last a long time in monoculture
    - Primary Macrophages
        - 3 µM Red
        - 5 µM Green for co-culture
        - 10 µM Green when need it to last a long time in monoculture
    - Get the greatest cell viability when cells are seeded in a small enough dish to stain while adherent and then passaged after staining, rather than in suspension.
        - Even 100 mm Petri dishes only require 3 ml of dye solution
    - 10 µM = 1 µl of dye stock in 1000 µl
    - 7 µM =0 .7 µl of dye stock in 1000 µl
    - 5 µM = 0.5 µl of dye stock in 1000 µl
    - 3 µM = 0.3 µl of dye stock in 1000 µl
- At the end of the experiments cells were fixed in 4% paraformaldehyde for 20 minutes at room temperature
- Counterstained with 4,6-diamidino-2-phenylindole (DAPI) (according to manufacturer's instructions.

Protocol: Mouse Sacrifice
Dolly Holt
Date Entered: June 2, 2008
Reference(s): Orme lab and Lisa Chamberlain protocols

Mouse Sacrifice

To use this protocol you must:

- Be listed on an IACUC protocol for mouse sacrifice (or be supervised by someone who is)
- Have access to animal facility of BPRB with fingerprint and authorized University Card (or be supervised by someone who is)
- Be wearing long pants and closed-toed shoes

You will need:

- Small black plastic trash bag from cleaning closet (west side of hallway in animal facility)
- Mice in the animal facility under your IACUC protocol number
- Any supplies necessary for further dissection/collection at necropsy prepared and ready

1. Mice are held in a clean room (passcode is 1-2-3-4-5 or hold card on reader until turns until it turns green)
    - Put on a lab coat (on hook of door, or if none available on cart in hall) and gloves (on cart), step soles of both shoes into sanitizing bucket before entering.
    - If using all mice in a cage, proceed to dirty room (dish room, passcode 1-2-3-4-5, step 2) for sacrifice. If using less than the number of mice in a cage (5):
        - Prepare a new cage (from components on the side of the laminar flow hood)
        - Place cage of mice (labeled with your IACUC protocol number) in laminar flow hood, and transfer required number of mice to new cage.
        - Replace labeled cage to racks.
        - Exit the room with your mice and put the lab coat back on its hook.
2. Enter the Dirty Room (Third room down from the entrance, passcode is 1-2-3-4-5)
    - Place the container with the mice near the sink and prep the CO_2 chamber
    - The CO2 chamber is located against the wall next to the sink
    - The star-shaped valve should already be turned on. Turn the smallest valve located nearest to the hose until you can barely hear air flowing.
    - Allow the CO2 to run for 5 minutes and then turn the gas off.
    - Allow the CO2 to settle for 5 minutes. This creates a 1-2 inch layer of 95% CO2, and will allow for faster, more humane killing of the mice.
    - Gently transfer mice one at a time into the CO2 chamber (try not to disrupt the CO2 layer)
    - Allow the mice to remain in contact with the CO2 for at least 2-3 minutes (Mice should become unconscious within the first 20 seconds, but will show signs of gasping).
    - One minute after mice stop gasping, pinch their tail to ensure they are dead. Once mice are dead, place them in the black garbage bag and bring to lab where the necropsy will take place.

Microscope Features

Light through top (phase contrast) (Dia something):

Condesor: There are phase filters and aperture in order to change the light's properties

Phase: use PH1 with phase 1 objective and PH2 with phase 2 objective

- Use aperture for fluorescence so that you have maximum light (you do not need phase unless you are overlaying a brightfield image)
- You can use aperture for color images or if you want shadows, you can use phase as well

Camera knobs: black knobs on the right of the scope 1-eyes only, 2-R80(right camera and eyes), 3-Aux(left camera and eyes), 5-camera only. Using 1 camera only will give a brighter image than 3.

Small metal knobs- used to adjust the phase to make sure it is centered: turn the bar up to close and make sure the hexagon is focused and centered using the small metal knobs.

Large Metal knobs – already locked in place, but you would turn the spinner on 0 to B and then move the lighted circle into the middle of the black circle.

Yellow filter-make the color more blue than yellow, easier on eyes

1.5 magnification-black knob on right side will increase magnification : by 1.5*40X (or whatever objective you are looking through)

Gridlines-switch black knob in front bottom to put a grid on the field of view

Phase objectives: Use the phase of the objective to rotate the phase of the scope to match if need contrast images (ex with live clear cells) (phase contrast)

- The silver 40X objective lens is for color, the black 40 X lens is for phase
- You can adjust for the thickness of the cover slip by rotating the center portion of the objective on the expensive 40X and 60X.

A: Use the A (aperture) empty when looking at colored images n(brightfield). Can adjust the amount of light that gets through with the slide bar on the A.

Oil Immersion lens: gently let lense paper absorb excel oil, can clean more thoroughly with a cutip if using less often than once a week. You don't want excess oil to dry on the lens

DIC- for DIC, you can remove the slider phase (right hand back, black slider with what looks like a filter). Match this up with the phase (by the small silver knobs) so that when they are stacked the light goes away and the filters turn black (extinction). Slide both phase filters in place. Normal phase leave both of them on their empty slots.

Fluorescence (light through bottom (through objectives) Epifluorescence

There are the same adjustments for the fluorescence as there are for the brightfield. Located on the left and to the back.

Filters: can decrease the amount of fluorescence by applying a filter (located on the right and to the back)

Microscope Function

Basic Microscope function:

- For Brightfield: turn on 1-5 in that order (turn on the left camera for black and white and fluorescence and the right camera for colored pictures)
- Make sure the knob is turned to the correct camera (Aux for black and white camera on left and R for color camera on right)
- Open Metamorph- control panel-click dapi-click bright field-click show live
    - If all you see is white then you need to turn the light down
    - If you see pixilation then you need to turn the light up
    - Click "stop live feed" if you need to "set save" or open any other programs on the PC. This takes up a lot of CPU.
        - MAKE SURE YOU STOP LIVE BEFORE YOU EXIT METAMORPH. It will always freeze your computer.
- Click "Set Save" to pick a folder to save your images to. Rename the file to be what the well is_1. Now every time you take a picture the file name will change to _2 etc.
    - To save the images to your folder click the save live
    - If you want to rename images as you take them, simply click capture and save the images one by one.
- When you are finished, Click the "stop live feed", close Metamorph, turn off 1-5 in reverse order. If the fan is not too hot, put the cover back on, if it is too hot then put the cover on all but the fan.
- Log out of the computer.

Fluorescence

- For fluorescence: turn on 0-5 in that order
- Focus your sample using brightfield and snap images to compare with fluorescence
- Change the filter wheel to represent the appropriate fluorescence
    - DAPI-Blue #4 M
    - FITC-Green #2 B
    - TRITC/CY3- Orange #3 G (Rhodamine)
    - CY5- Red #4
- Click on the appropriate fluorescence in Metamorph
- Normally the exposure is 20 ms, you can increase this to 200 ms to see your fluorescence and be able to pan easily, increase the exposure to 2000 ms or higher to get better resolution.
- Increase the gamma to increase the signal as necessary
- Normally the binning is 2, but you can change it to 4 to get increased fluorescence sensitivity (however the size of the image will decrease by 50% by increasing the binning)
- Turn off the light (both room and/or microscope)
- Select Show Live
- Look at your well plate to make sure you can see a laser light
    - If you don't see any fluorescence the laser light may not be on. Keep clicking it or stop live feed and click until it comes on
- Take images the same as with bright field
- Images will be black and white in Irfanview. You must apply false color.
    - Select overlay images->select blue and then select the image that should be blue etc.->hit apply and save as overlay image.
    - Select the false color button and resave

Color

- Turn on color camera (the camera to the right of the scope)
- adjust knobs to lower right of microscope (Aux80 means the left camera has 80% light and L100 means the left has 100% of light). Choose R80
- Open Q Capture (blue icon) for color cam
- Select acquire
- select a square on the picture that should be white and select “white balance”
- If this doesn’ work, then you will manually have to adjust the color balances
- Always keep your original picture open to use as a reference to ensure all subsequent pictures have similar color balances (i.e. don’t begin to develop a green or blue hue each time you take a new image)
- to take a picture: select “aquire” then “snap” then under file “save as”

The Yan Lab by Mei Zhang
7/17/2012
Obtained from Dorthyann Isackson

Oil Red O Staining for Cultured Cells

1. Culture and treat cultured cells in tissue culture plate as needed (see other protocols).
2. Take the plate (35-mm) out of incubator and remove the medium.
3. Add ~2 ml of PBS to wash the cells and remove PBS completely.
4. Add 2 ml of 10% formalin (RT) and incubate for 10 min at RT.
5. Discard formalin and add 2 ml fresh formalin. Incubate for at least 1 hour, or longer (Cells can be kept in formalin for a couple of days before staining. Wrap with parafilm and cover with aluminum foil to prevent cells from drying).
6. Remove formalin with a pipette.
7. Wash cells with 2 ml of ddH2O twice.
8. Wash cells with 2 ml of 60% isopropanol for 5 min at RT.
9. Let the cells dry completely at RT. If possible, use a hairdryer to dry.
10. Add 1 ml of Oil Red O working solution and incubate at RT for 10-20 min.
11. Remove Oil Red O solution and **immediately** add ddH2O. Wash the cells 4 times with ddH2O.
12. Acquire images under the microscope for analysis.
13. Remove all the water and let dry.
14. Elute Oil Red O dye by adding 1 ml of 100% isopropanol and incubate for 10 min with gently shaking.
15. Pipet the isopropanol with Oil Red O up and down several times to ensure that all Oil Red O is in the solution.
16. Transfer the solution to a 1.5-ml eppendorf tube.
17. Measure OD at 500 nm using100% isopropanol as blank.

Reagents

1. Oil Red O Stock: Sigma (Cat# O-0625), FW 408.5. Weigh 0.35 g Oil Red O and put in 100 ml of isopropanol. Stir O/N, filter (0.2 μ) and store at RT.
2. Oil Red O Working Solution: Mix 6 ml of Oil Red O stock solution with 4 ml of ddH2O. Let sit at room temp for 20 min followed by filtering (0.2 μ).
3. 10% Formalin in PBS: Dilute 27 ml of formalin stock solution (37%, Merck, Cat# K36658003) in 63 ml of ddH2O and 10 ml of 10X PBS.
4. 100% Isopropanol (Merck, Cat# K36543834)
5. 60% Isopropanol: Mix 6 ml of 100% Isopropanol with 4 ml of ddH2O.

Summary

Sudan III, Oil red O and Sudan black are lysochromes (fat soluble dye) predominantly used for demonstrating triglycerides in frozen sections. Oil Red O has largely replaced sudan III and sudan IV as it is much deeper red in color, and consequently more clearly visible.

Originally written by Lenka Janderova

Protocol: Primary Fibroblast Harvest
Dolly Holt
Date Entered: 03-7-2012
Reference(s): Diaz M, Watson NB, Turkington G, Verkoczy LK, Klinman NR, McGregor WG. Decreased frequency and highly aberrant spectrum of ultraviolet-induced mutations in the hprt gene of mouse fibroblasts expressing antisense RNA to DNA polymerase zeta. Mol Cancer Res. 2003 Sep;1(11):836-47

Primary fibroblast media

- 10% FBS
- 1% antibiotic/antimycotic
- 1% HEPES
- 1% Sodium Pyruvate
- 1% MEMs nonessential amino acids

Primary fibroblast isolation

- Prepare two 30 mm Petri dishes: 1 with 70% ethanol and 1 with sterile PBS
    - Remove mouse ears
    - Snip mouse ears before long-hair begins
    - Dip in 70% ethanol for 1-5 min
    - Wash in sterile PBS
- Use the lid or the base of a 30 mm Petri dish for each set of mouse ears (2 ears per mouse)
- Sterilize a razor blade by soaking in 70% ethanol and rinsing with PBS. To be extra cautions, spray with ethanol and UV in hood for 20 minutes on each side (though with just soaking in ethanol and rinsing with PBS, I never had contamination issues).
- Take autoclaved forceps and sterilized razor blade and mince ears into as small of pieces possible. Note: the number of fibroblasts obtained will be directly proportional to how small of pieces you mince at this stage.
    - Incubate minced tissue in 4 mg/ml collagenase Type I (though probably, most collagenases will work, eg Type IV works) in incomplete DMEM for 2 hours in 37°C shaking water bath.
    - Use 2-3 ml of collagenase solution per set of ears
- After the incubation period disperse cells with sterile pipette, or vortex briefly
- Filter cells with 70 µm filter to remove debris. Add 3 ml complete media to wash filter to ensure all cells are obtained.
- Collect filtrate and spin at 500X g (rcf) for 5 min
- Aspirate media
- Resuspend pellet in pre-warmed DMEM with 10% FBS and 1% Penn/strep and fugazone (antibiotic/antimycotic).
- Plate cells in DMEM with 10% FBS and 1% Penn/strep and fugazone, 1% HEPES, 1% Non essential MEMs, and 1% NaPyruvate
    - Can plate cells in a T75 flask to be confluent in 6-7 days or in a T25 flask or 6-well plate to be confluent in 3 days.
- Next day, change media to remove non-adherent debris
- For co-culture with BMMOs, 1X10^7 BMMOs to 100 mm Petri dish to ensure 80% confluency by day 7, so that both cell types can be placed into an experiment by day 7.

Protocol: 3T3 cell culture
Date Entered: 03-7-2012
Name: Dolly Holt

- Complete Media
    - DMEM high glucose + L glutamine
    - + 10% FBS
    - + 1% antibiotic/antimycotic
- Place 10 ml of complete media in a T75 flask and place in incubator to prewarm for 10 min
    - Spray with 70% ethanol and place in sterile hood
- Thaw a cryovial of RAW 264.7 cells in a 37 °C water bath (this will only take a couple of minutes)
- When the vial is nearly thawed, remove from water bath, dry off, spray with 70% ethanol and place in hood.
- Using a 5 ml pipette, transfer contents of vial into T75
- Remove some of the media in the T75 and add it to the cryovial to remove any residual cells
    - Repeate this a couple of times until you feel you have removed all of the cells
- Place T75 in incubator and allow cells to adhere (~2 hours or less)
- After cells have adhered, prewarm complete media and replace media above cells (add 15-20 mls)
    - The purpose of this is to remove residual DMSO that was in the frozen cells
- Replace T75 in incubator
- Cells will take 3-4 days to reach confluency
- These cells are highly metabolically active and their media will turn acidic very quickly. Keep a close eye on them to either passage or replace their media every few days.

Passaging

- When cells are 80% confluent they need to be passaged
    - This occurs when what appears to only be 20% of the area of the T75 is still available for cell growth
- RAws are not contact inhibited, so they will begin to grow over the top of one another if they become more than 100% confluent.
    - Once they begin to grow on top of one another, they may change their phenotype, so it is important to keep a close watch on these cultures
- These cells only need to be scraped to be passaged
- Spray T75 flask and rubber scraper and place in hood
- Scrape of the bottom of the flask, much like you would with a squeegee on a car window. Hold the flask at an angle and you should be able to see where the flask turns clear after the cells have been removed. This way you can ensure you've gotten them all. Keep the bottom of the scraper flat and move gently to avoid creating bubbles.
- Use a 5-10 ml pipette to gently mix the cells, and transfer 10% into a new flask. You can use the remaining cells for experimentation.
- Place T 75 in 37 °C incubator with 5% supplemental carbon dioxide
- Cells will become confluent in 3-4 days.

Protocol: Senescence and BCA Assays
Name: Dolly Holt
Date Entered: 03-7-2012

Components

- PBS+Ca^{+2}/Mg^{+2} (Invitrogen) Ph 7.4
- PBS -Ca^{+2}/Mg^{+2} Ph 7.4
- Plate shaker
- 70% glycerol in DI water
- Respective assay components

Senescence and BCA Assays for macrophages: Qualitative and quantitative SA beta-gal assays

Colorimetric Senescence Assay

- A colorimetric assay for senescence-associated beta-galactosidase (SA beta-gal) used as a labeling kit (Cell Signaling Technology, Danvers, USA) was used according to manufacturer's instructions [1].
- This commonly employed assay [2] labels fixed cells positive for SA beta-gal with a blue precipitate and allows for subsequent visualization of percent positive cells (imaging described below).
- Add just enough senescence stain to cover the well (eg 50 µl per well of a 96 well plate)
- Fresh senescence stain should be made prior to each experiment
- Incubate samples at 37°C for 24 hours and stain was removed
- Store samples in 70% glycerol in DI water at 4°C

Quantitative fluorescence-based SA beta-gal assay

- A second quantitative fluorescence-based SA beta-gal assay, was employed according to a previously established protocol [2] and requires cell lysis and subsequently measures the relative fluorescence of total SA beta-gal in the culture well, rather than distinct of SA-positive cells.
- Samples were obtained and stored at at 4°C until all samples were collected
- Samples were thawed and vortexed vigorously for 30 sec
- Samples were centrifuged for 5 min at 20,000 rcf at 4°C
- 50 µl of supernatant was added to 50 µl of reaction buffer (according to the protocol referenced above).
- Samples were then incubated for 3 hours at 37°C
- Plates were read on the Biotech plate reader
    - Excitation 360 nm, emission 465 µs, integration, gain 46
    - Protocol is listed under Dolly's protocols and is entitled "Senescence"
- Normalized fluorescence divided by total protein in µg of cells in each well
- Control used was the lysis buffer (from protocol referenced above) + reaction buffer
- Important: stop solution for senescence assay is not required, you actually get more accurate readings, but you must read it on the plate reader shortly after completing the assay. If you are going to wait a long time before reading then you must use the stop solution.

BCA Assay

- Cell density was approximated using cell-derived protein content from each culture well detected by the microBCA assay (Pierce Thermo Scientific, USA) used according to manufacturer's instructions.
- Samples were thawed, vortexed, and centrifuged along with those samples used in the quantitative senescence assay described above.
- 20 µl of sample supernatant + 130 µl PBS -Ca^{+2}/Mg^{+2} = 150 µl of diluted lysate
- Control = 20 µl of lysis buffer + 130 µl PBS -Ca^{+2}/Mg^{+2}

- 150 µl of diluted lysate was added to 150 µl of working reagent (described in manufacturer's instructions for BCA assay)
- Plate was added to shaker plate for 30 seconds
- Plate was covered and incubated at 37°C for 2 hours
- Plate was allowed to cool to room temperature
- Plate was read using Biotech plate reader at an absorbance of 562 nm

References

1. Severino J, Allen RG, Balin S, Balin A, Cristofalo VJ. Is beta-galactosidase staining a marker of senescence in vitro and in vivo? Exp Cell Res 2000 May 25;257(1):162-171.
2. Gary RK, Kindell SM. Quantitative assay of senescence-associated beta-galactosidase activity in mammalian cell extracts. Anal Biochem 2005 Aug 15;343(2):329-334.

April 2010
Author: Claudia
Modified: Dolly Holt
SOP: WEASEL

Analyses of the CBA-data measured with a flow cytometer (FacScan, Becton Dickinson)

- Open WEASEL (unlicensed) (just click okay when it asks you to register)
- Drag first file into open space
- Move file over to the right using arrows
- Minimize that window
- Display->dot plot
- Select FL 4 -X-axis vs. FL 5 -Y-axis->enter or okay or whatever
- Enlarge chart/graphic. You should see dot clusters on the right upper side of the graphic that represent the beads of different cytokines. The position of the different cytokine clusters is noted on the bead vials.
    - ex. Cytokine X: B7
    - A9 is located in the upper right-hand corner, the numbers go from right to left in descending order and the letters go from top to bottom in ascending order
    - Ex. A5 A6 A7 A8 A9
      B5 B6 B7 B8 B9
      C5 C6 C7 C8 C9
    - Common Bead positions for mouse
        - TNF
        - MCP-1
        - IL-6
        - MIP-1a
        - MIP-1b
        - RANTES
- Right click on dot plot->create region->draw region, name region, say okay
    - Draw a polygon around the clusters with the mouse by clicking to start and finish a line creating a circle
    - If there is an error, just start again by clicking on the “start again”
    - Determine region for every cytokine
- Right click on dot plot->gates->create a gate->select the region you just created->say okay
- Display->Histogram->select first file in sequence
    - Deselect all parameters expect FL 2 – X-axis versus count y-axis
    - Ok
- Right click on histogram->select gates->select gate you made for the region you created
    - Look to make sure the histogram changes to be smaller when you gate it
- Right click on histogram->set stats list-> check 1) cells, 2) mean, and 3) Read all files in sequence->okay
    - The statistics should appear underneath the histogram and should list all of the files for the CBA in a column
    - The cell # represents how many beads were counted for each sample
    - You can now copy the statistics into excell
- Repeat for all cytokine bead clusters.
    - Hint: It is better to do one cytokine at the time if you have a large amount of data. Otherwise you can do all of the cytokines simultaneously by selecting the appropriate regions.

Lisa Chamberlain 05/08/2007 (reference ATCC website 2007) modified by Dolly Holt 03-31-2011

Thawing/Bringing Up Cells

Components:

- Complete media for cell line being thawed
- New flask
- Centrifuge Tubes
- Centrifuge
- Hood and Incubator

All cell culture reagents and tools should be sterilized before placing them into the hood or incubator!!!! All steps should be performed using sterile technique!!!! If you don't know sterile technique, find someone who does to show you before attempting!!!!

1. Warm media to 37° C by placing in the water bath. This should take approximately 10-20 minutes.
2. Dry media bottle, spray with 70% ethanol and place in the hood.
3. Place approximately 5 mL of media into a 15mL centrifuge tube.
4. Remove stock of cell line from liquid nitrogen and place in 37° C water bath, watch carefully and do not allow water to touch cap/threads of tube.
5. Once thawed, remove from water bath, and dry. Spray liberally with 70% ethanol before bringing into hood.
6. Open cell stock and transfer content into tube of media.
7. Centrifuge cells at 500 rcf (g) for 5 minutes to pellet, aspirate supernatant.
8. Re-suspend pellet in complete media and transfer to flask.
9. For sensitive cells, change media once cells are adherent (overnight) to remove any residual DMSO.
10. You will mark the passage number on the flask as the same number as is on the tube.
11. **Don't forget to mark the removal of your stocks from the liquid nitrogen inventory!**

*RAW 264.7 cells and NIH 3T3 cells are not very sensitive to DMSO. In the case of these cells, place warmed media into the T75 flask and as soon as the cells are thawed you can place them into the flask. You can change the media once they are adherent, but this isn't necessary, they usually do just fine.

Freezing Cells for New Stocks

Components:

- Flask of cells at about 80% confluence
- Freezing solution: 90% FBS, 10% DMSO (should be in freezer)
- Freezing tubes (screw-on 2mL tubes, in drawers opposite hood)

All cell culture reagents and tools should be sterilized before placing them into the hood or incubator!!!! All steps should be performed using sterile technique!!!! If you don't know sterile technique, find someone who does to show you before attempting!!!!

1. Place FBS/DMSO solution in water bath to thaw. Vortex before use.
2. Remove cells from flask, count and spin down (500g for 5 minutes).
3. Decant supernatant and re-suspend cells in freezing solution, and aliquot into freezing tubes
4. Add at least 20% of your T75 flask to each freezer stock, as about half of them may die and 10% will be needed to repopulate the flask once thawed. You can make 3-5 vials from a single T75 flask depending how confluent your flask is and if they are primary cells, you will want to make only 3 vials, as more cells will likely die in the freezing process.
5. Label the cells with the passage number they will be once thawed and plated. For example if you just removed cells from the surface of a passage 3, and once replated will be a passage 4, you will label the freezer tube "passage 4".
6. Place freezing tubes in nunc rate freezer container, secure lid and leave overnight in -80° C freezer
7. Remove stocks from freezer, place in liquid nitrogen.
8. **Add your new stocks to the liquid nitrogen inventory.**